FAKULTÄT
FÜR !NFORMATIK

Faculty of Informatics

Model-driven Compensation of the Effects of Environmental Conditions on Quartz Oscillator based Clocks

DIPLOMARBEIT

zur Erlangung des akademischen Grades

Diplom-Ingenieur

im Rahmen des Studiums

Technische Informatik

eingereicht von

Nazir Alakhras BSc

Matrikelnummer 0225235

an der Fakultät für Informatik
der Technischen Universität Wien

Betreuung: Univ.Prof. Dipl.-Ing. Dr.rer.nat. Radu Grosu
Mitwirkung: Univ.Ass. Dipl.-Ing. Oliver Höftberger BSc
　　　　　　 Univ.Ass. Dipl.-Ing. Bernhard Frömel BSc

Wien, 29. November 2016　　　＿＿＿＿＿＿＿＿＿＿＿＿　　＿＿＿＿＿＿＿＿＿＿＿＿
　　　　　　　　　　　　　　　　　　Nazir Alakhras　　　　　　Radu Grosu

Technische Universität Wien
A-1040 Wien ▪ Karlsplatz 13 ▪ Tel. +43-1-58801-0 ▪ www.tuwien.ac.at

Model-driven Compensation of the Effects of Environmental Conditions on Quartz Oscillator based Clocks

DIPLOMA THESIS

submitted in partial fulfillment of the requirements for the degree of

Diplom-Ingenieur

in

Computer Engineering

by

Nazir Alakhras BSc

Registration Number 0225235

to the Faculty of Informatics
at the Vienna University of Technology

Advisor: Univ.Prof. Dipl.-Ing. Dr.rer.nat. Radu Grosu
Assistance: Univ.Ass. Dipl.-Ing. Oliver Höftberger BSc
                  Univ.Ass. Dipl.-Ing. Bernhard Frömel BSc

Vienna, 29th November, 2016   _____   _____
                                                            Nazir Alakhras   Radu Grosu

Erklärung zur Verfassung der Arbeit

Nazir Alakhras BSc
Einsiedeleigasse 9/4, 1130 Wien

Hiermit erkläre ich, dass ich diese Arbeit selbständig verfasst habe, dass ich die verwendeten Quellen und Hilfsmittel vollständig angegeben habe und dass ich die Stellen der Arbeit – einschließlich Tabellen, Karten und Abbildungen –, die anderen Werken oder dem Internet im Wortlaut oder dem Sinn nach entnommen sind, auf jeden Fall unter Angabe der Quelle als Entlehnung kenntlich gemacht habe.

Wien, 29. November 2016

_____
Nazir Alakhras

Acknowledgements

I would first like to thank my thesis advisor Radu Grosu, who gave me the opportunity to write my master thesis in this exciting field of research. I want to give thanks to the professor's assistants Oliver Höftberger and Bernhard Frömel. The door to their offices was always open whenever I ran into a trouble spot or had a question about my research or writing. They consistently allowed this paper to be my own work, but steered me in the right direction whenever they thought I needed it.

I also want to thank my wife. She helped me to manage and organize this thesis in addition to my job. The study was hard, so I am very glad that she has supported and encouraged me in frustrating moments to keep making progress.

Finally, my parents have been an inspiration throughout my life. They have always supported my dreams and aspirations. I would like to thank my entire family, especially my parents who always give me spiritual and moral support from my country Syria, because of you I am here.

<div align="right">

Nazir Alakhras
Vienna, November 2016

</div>

Kurzfassung

Quarzoszillatoren sind aufgrund der niedrigen Implementierungskosten und der akzeptablen Stabilität eine wichtige Frequenzquelle für die Uhren in Echtzeitsystemen. Da die Aufrechterhaltung einer globalen Zeit eine Voraussetzung für ein korrektes Verhalten von verteilten Echtzeitsystemen ist, werden die lokalen Uhren regelmäßig mit einer externen gemeinsamen Zeitreferenz synchronisiert, die größtmögliche Stabilität hat. Diese Lösung bietet eine genaue globale Zeit mit geringen Implementierungs- und Wartungskosten.

Wenn die externe Zeitreferenz nicht verfügbar ist, hängt die Länge der Zeitspanne, in der das System genügend genaue globale Zeit aufweist, von der Stabilität der Quarzoszillatoren in den jeweiligen lokalen Uhren ab. Die wichtigsten Faktoren, die Auswirkungen auf die Frequenzstabilität von Quarzoszillatoren haben, sind die Umgebungsbedingungen und die Quarzalterung. Obwohl verschiedene Ansätze existieren, um diese Auswirkungen auszugleichen, gibt es nur ein paar Ansätze, die mehrere Bedingungen berücksichtigen und noch weniger Ansätze sind erweiterbar hinsichtlich des Software- und Hardwaredesigns.

Das Ziel dieser Arbeit ist die Entwicklung und die Umsetzung eines quarzspezifischen Modells, das jene Frequenzabweichungen vorausbestimmt, welche durch die Auswirkungen der jetzigen Umgebungsbedingungen ausgelöst werden. Die berechnete Frequenzabweichung des Quarzes wird dazu verwendet, die Abweichung der Uhr zu korrigieren und somit die o.g. Zeitspanne zu verlängern. Die wichtigsten Anforderungen sind die Beherrschbarkeit der Systemkomplexität und die Erweiterbarkeit der Software und der Hardware. Dies wird durch die Entwicklung von zwei Modellen für zwei unterschiedliche Quarzoszillatoren demonstriert. Die Regressionsanalyse, als eine Form des maschinellen Lernens, wird zur Modellierung und zur Vorhersage des Quarzverhaltens eingesetzt.

Eine Verbesserung von einer Größenordnung für beide Quarzoszillatoren wird erreicht. Darüber hinaus berechnet das Modell regelmäßig einen Korrekturwert für die Abweichung der Systemuhr und erzeugt einen präzisen Puls pro Sekunde (PPS). Wenn die externe Zeitreferenz verfügbar ist, wird sie dazu verwendet, das Modell während der Betriebszeit zu trainieren. Der Quarzalterungseffekt und die mögliche Rechenungenauigkeit werden somit kompensiert. Dies führt zu einer zusätzlichen Verbesserung von einer Größenordnung für die Systemuhr.

Eine erweiterte Methode für die Identifikation und die Korrektur des Quarzalterungseffekts wird angegeben. Neben den Verbesserungen der Frequenzstabilität sind weitere Erweiterungen für den entwickelten Ansatz möglich, z.B. die Erkennung von manipulierten externen Synchronisationssignalen.

Abstract

Quartz oscillators have been established as the main frequency source for clocks in real-time systems due to their low implementation costs and acceptable stability. Since maintaining a global time is an indispensable presupposition for a correct behavior of distributed real-time systems, the local clocks are synchronized periodically with an external common reference time with the highest possible stability. This solution provides an accurate global time with lower implementation and maintenance costs.

When the external reference time is not available, the system holdover is determined by the frequency stability of the quartz oscillators of the local clocks. The main factors that have impacts on the frequency stability of quartz oscillators are the conditions of the enclosing environment and quartz aging. Although various approaches exist to compensate the effects of these factors and to extend the system holdover, there are few approaches which consider multiple conditions and even less ones are extensible regarding the software and hardware design.

The objective of this thesis is the design and implementation of a quartz specific model that predicts the frequency deviation caused by the effects of the current environmental conditions. The predicted deviation is used to correct the clock drift and hence to extend the system holdover. The main requirements are the manageable system complexity and the extensibility regarding the software and the hardware design. This is demonstrated by developing two compensation models for two different quartz oscillators using the regression analysis as machine learning technique to model the quartz behavior.

An improvement of one order of magnitude for both quartz oscillators is achieved. Furthermore, the model periodically predicts a correction value for the drift of the system clock and generates an accurate Pulse Per Second (PPS). The external reference time is used when it is available to train the model during the system operation. This compensates for quartz aging effects and calculation inaccuracies. As a result, an additional improvement of one order of magnitude for the system clock is achieved.

An enhanced technique for quartz aging identification and compensation is stated. Apart from the improvements in the frequency stability, further extensions for the developed approach are possible, e.g. the detection of manipulated external synchronization signals.
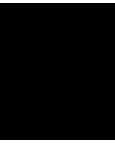
Contents

List of Algorithms

Introduction

This chapter introduces a model-driven approach to predict the frequency deviation of a Quartz Crystal Oscillator (XO). The predicted deviation is used to correct the drift of the system clock, which is in this case a Crystal Oscillator based Clock (XOC). The problem of the clock drift has impacts on the correct behavior of the system. Some examples are provided to outline the significance of this problem and the benefits of compensating the clock drift. A clear description and delimitation of the intended research design are provided afterwards. Finally, a short introduction to the chapters in this thesis is given.

1.1   Motivation

Nowadays, applications of real-time systems are ubiquitous in almost all infrastructures, such as control systems in power plants, multimedia systems and traffic control. As their name implies, real-time systems are information processing systems that are subject to the time constraints specified by the external world. The behavior of a real-time system is considered as correct when the logical result and its delivery time are both correct, i.e. a late or even an early response is also a wrong response [1]. The response time of a real-time system is not required to be as short as possible, but it should be predictable.

The clock in a real-time system is one of the important factors that determine the correctness of the system response, i.e. the logical result and its delivery time. A degradation in the stability of the system clock has serious impacts on the correct system response [2]. Digital clocks are realized by an oscillator and a counter that is incremented after every full oscillation. Since the economic success of a system also depends on its implementation and production costs, XOs have been established as the main frequency source for clocks in real-time systems. XOs are cheaper than other types of oscillators, such as cesium oscillators, but they are less accurate.

Two independent clocks will lose the synchronization exceeding any limit, even if both clocks are of same design and were once perfectly synchronized [3]. Maintaining an agreement on time, i.e. a common time, between independent clocks is hence an indispensable presupposition for a correct behavior of distributed real-time systems.

In a centralized real-time system, no clock synchronization is needed since one clock maintains the time within the system borders. The centralized approach is replaced evermore by the distributed one. Composability and scalability of the system architecture, dependability of its service and the simple physical installation are the main and most important arguments for a distributed approach of real-time systems, H. Kopetz [[4], Chapter 2].

To maintain a consistent common time, i.e. a global time, among the independent local XOCs of a distributed real-time system, the internal and the external clock synchronizations are applied. The internal synchronization aims to keep each local XOC in sync with other local XOCs, whereas the external approach maintains the global time by periodically synchronizing the local XOCs with an external reference time, such as the Pulse Per Second (PPS) from the Global Positioning System (GPS). A major reduction in the implementation overhead and lower maintenance costs are achievable using the external synchronization in comparison with the internal one. Additionally, externally synchronized XOCs are also internally synchronized, but the converse is not true [5].

The main drawback of this solution appears when the external reference time is no longer available. In this case, the local XOCs lose the synchronization and the communicating sub-systems will have different views on the global time maintained by the external reference time.

The stability of the XOs determines the time period the system can operate without the external reference time, i.e. its holdover. Correcting the drift of the XOCs increases the system holdover. This is of interest if the external reference time is temporarily not available, e.g. due to insufficient coverage of the GPS in mobile applications, or when the signal receiver is intentionally turned off to reduce the power consumption of the system.

The following example illustrates the importance of the global time in distributed real-time systems. The collision warning system as an example of a vehicular communication system uses the vehicle position and a timestamp to detect a possible collision between vehicles: If two vehicles have two clocks that do not run at the same rate, i.e. they have different views on the time, the two vehicles will not calculate the same distance between them. If the collision warning system fails, a loss of human life may be the result.

The deviation in the frequency of the XOs is mainly caused by mechanical imperfections during the quartz assembly, quartz aging and the effects of the environmental conditions, such as the temperature [6]. Studying the effects of several environmental conditions on the quartz provides the needed theoretical background to compensate those effects and correct the clock drift to maintain the global time in the absence of the

external reference time. Furthermore, the knowledge about the behavior of the quartz can compensate for the deviations caused by the mechanical imperfections and quartz aging.

Studying the quartz behavior and compensating the clock drift based on the gained knowledge increase the performance of XOs in several application fields. The benefits are visible when the system size and the power consumption are critical for the application, such as in mobile applications. Armored carriers in the military section deploy communication devices that should be operational, while on-the-move, in the extreme environments regarding the acceleration and vibration [7].
Similar challenges are faced in the aerospace applications. Radars determine, in a time duration of microseconds, the distance or velocity of objects by using radio waves. XO frequency deviation hence has critical impacts on the radar functionality since uncompensated deviations imply calculation errors [7].
An application field of XOs, which is of ever-increasing importance, is in the automotive domain in electric cars. The acoustical and electrical noise caused by electrical components in addition to the temperature variation, acceleration and vibrations represent a challenging environment for the XO [8] [9].
The performance improvement is also of interest when the frequency stability is mainly in focus, such as in applications that require synchronization in telecommunications. e.g. in wireless base stations. A model-driven approach that relies on the quartz behavior and on sensing the enclosing environment can replace the current solutions based on a relatively expensive rubidium oscillator or a power-consuming Oven Controlled Crystal Oscillator (OCXO) [10].

1.2   Objectives and Approach

This thesis works out a model-driven approach to correct the drift of a XOC caused by various environmental conditions. Not only the individual effects are important; the joint effects of the environmental conditions are, due to their physical dependency, of great interest. The main obstacle here is the fact, that the effects on the quartz frequency are in general non-linear and interdependent [11]. The developed model has to be able to deal with such interdependencies. The main requirements are the extensibility regarding the software and the hardware design and the manageable system complexity, which eases and supports the system extensibility.

The existing literature about the frequency deviation of XOs is studied and hereby the capabilities of the current approaches are analysed. A hardware setup consisting of a data logger, a set of sensors, a XO and a source of high quality external reference time is needed in order to perform the experiments and evaluate the results. Additionally, an isolation of the hardware setup in a sealed chamber is designated to accurately realize the variation of the environmental conditions and study their effects on the XO behavior. The methodological approach can be categorized in three main parts:

- **Data Collection**: The behavior of the XO is observed under the conditions of interest. To this end, the XO is exposed to these conditions and its frequency deviation is recorded. The experiment design has to guarantee that the individual and the joint effects of the environmental conditions are differentiable in the collected data.

- **Model Development**: Based on the gained knowledge about the XO behavior, a quartz specific compensation model is developed. In doing so, the model extensibility and its complexity are in focus. In order to guarantee the versatility of the approach, the model should not rely on any specific feature of the XO, such as the cut type. The implementation costs and the achieved improvement are determined by the chosen modeling technique.

- **Model Deployment**: The model periodically predicts a correction value for the counter of the XOC in order to generate an accurate time signal, that maintains the global time when the external reference time is unavailable. Furthermore, the system can use the external reference time when it is available to additionally train the compensation model during the system operation. This is done by constantly comparing the time signal from the external source with the generated time signal and using this knowledge to compensate for quartz aging effects and calculation inaccuracies.

There exist two approaches to correct the drift of a XOC. The proposed compensation system is based on the passive correction approach:

- **Active Correction**: The operating and the environmental conditions which have the highest impacts on the XO behavior, such as the temperature and the supply voltage, are adjusted during the operation time in order to control the quartz output frequency. The major frequency deviation caused by the variation of these conditions hence can be eliminated. High frequency stability is achievable by this approach, but it has high implementation costs due to the hardware design which comprises the enclosing chamber, its insulation and the heat and power supply control loops. Furthermore, this approach is infeasible when it comes to the acceleration, vibration and shock effects.

- **Passive Correction**: Based on a previous knowledge about the quartz behavior and on the measured environmental conditions, the deviation of the quartz is predicted and a correction value for the XOC counter is calculated, such that a time signal is generated when the XOC counter reaches a value that corresponds to a predefined period of time, e.g. the same period of the external time signal. The implementation costs are determined by the hardware (a set of sensors to measure the current environmental conditions) and the software (e.g., the memory consumption and the algorithm runtime) part.

4

1.3 Outline

Chapter 2 provides an overview on the basic concepts and the terminology used in the course of this thesis. The general requirements for an approach to compensate for the frequency deviation caused by environmental conditions and the current related work are the topics of Chapter 3.
Chapter 4 describes the methodological approach including the data collection, the model development and the model deployment part. The implementation of the proposed method is presented in Chapter 5, whereas Chapter 6 outlines the experiment results and provides an overview of the fulfillment of requirements by the implementation.
Chapter 7 concludes the thesis, summarizes the main results and suggests possible improvements.

CHAPTER 2

Basic Concepts

In this chapter the terminology that is used in the context of the thesis is introduced. The first section 2.1 introduces the concept of the Crystal Oscillator based Clock (XOC). The notions of a sensor and an actor are discussed in Section 2.2. Next section 2.3 deals with control theory and provides a basic background, that is necessary for a better understanding of the implemented control loops in the course of this thesis. The last section 2.4 introduces the used machine learning technique, the *Regression Analysis*.

2.1 Time in Distributed Systems

In order to introduce the XOCs, some fundamentals have to be discussed first, such as the notion of time, oscillators, and clocks. Further definitions are needed to illustrate the aim of this thesis, such as the accuracy and the precision of clocks and what approaches exist to have a balance between cost reduction, sufficiently achieved accuracy, and low maintenance costs of clocks. The concept of the Global Positioning System (GPS) is presented to provide a short introduction on one important application of it in the domain of clock synchronization. Afterwards, the XOC is discussed as a source of frequency, i.e. source of time, in computer systems.

2.1.1 Basic Concepts

In the Newtonian model, time is considered as an independent variable that is measured in seconds. The properties of a system can be described by combining the time with other physical fundamental quantities. For instance, the velocity of an object is the rate of change of its position in relation to the time.

7

The General Conference on Weights and Measures (CGPM) defines the physical second as the base unit of time as follows:

> **Second**: *An internationally standardized time measurement unit where the duration of a second is defined as 9 192 631 770 periods of oscillation of a specified transition of the Cesium atom 133.*[[12]]

The following concepts are treated by H. Kopetz in his book *Real-Time Systems* [4] and sharpened in the Conceptual Model of the project *Architecture for Multi-criticality Agile Dependable Evolutionary Open System-of-Systems* (AMADEOS) [13].

> **Timeline**: *A dense line denoting the independent progression of physical time from the past to the future..* [[13], p. 19].

> **Instant**: *A cut of the timeline.* [[13], p. 19].

> **Event**: *A happening at an instant.* [[13], p. 19].

The real time is thus the infinite set I of instants on the timeline. This set is an *ordered* set[[4], p.46]. If i_1 and i_2 are two instants in I, then either i_1 is before i_2, or i_2 is before i_1, or i_1 and i_2 are simultaneous, i.e. they represent the same cut on the timeline. Additionally, I is a *dense* set, i.e. there is always an instant i_3 between any two instants i_1 and i_2 on the timeline, if i_1 and i_2 are not simultaneous.

Based on the previous definitions, the *order* among events can be introduced:

> **Temporal Order**: *The order of the events on the timeline.*

> **Causal Order**: *The order that reflects the cause-effect relationships among the events.* [[13], p. 19].

In other words, the temporal order defines the conventional *before-after* relationship, whereas the causal order interprets the *after* as a consequence of the *before*. For instance, consider the events e_1 {*sense an overtemperature*} and e_2 {*turn on a ventilator*} in a cooling system. There are two possible temporal orders: e_1 before e_2 and e_2 before e_1. On the other hand, the only plausible causal order is e_1 before e_2. In the Newtonian model the causal order implies the temporal order.

The concept of instants and events allows to define the *interval* between events on the timeline and its *duration*.

> **Interval**: *The section of the timeline, that is bounded by two instants.* [[13], p. 19].

> **Duration**: *The length of a section of the timeline.* [[4], p.46].

The interval is fixed on the timeline between two instants, i.e. it represents the absolute position on the timeline, whereas the duration denotes the length of an interval and is expressed in seconds, or parts of a second.

To measure the progression of time in computer systems, digital clocks are used.

Oscillator: *An electronic device, that is realized by an electrical circuit, to generate a signal with a frequency, which is determined by the design and constants of the electrical circuit.*

Clock: *A device for measuring time, that consists of an oscillator and a counter. The counter is incremented on the event of a complete oscillation.* [[4], p.48].

Tick: *The event that increments the register is the tick of the clock.* [[13], p. 21].

Granularity: *The duration between two successive ticks of a clock is the granularity of the clock.* [[13], p. 21].

Timestamp: *The timestamp of an event is the state of a selected clock at the instant of event occurrence.* [[13], p. 21].

Observing two, or more, clocks at the same time introduces the term *clock drift*.

Clock Drift: *The drift of a real clock is a quality measure describing the frequency ratio between the real clock and the perfect clock.* [[13], p. 21].

Perfect clocks have no drift, whereas the drift of real clocks is determined by different factors, such as the specifications of its oscillator, the environmental conditions and the supply voltage of the circuit [14].

By assuming one clock as perfect and considering it as a reference clock, some notations can be given to express the clock drift of the other clock, the real one. The oscillators have a *nominal frequency*, that is determinant for each production series. The nominal frequency can be seen as the frequency of a perfect oscillator in some series. A real oscillator in this series is characterized by a frequency that is close to the nominal one with respect to some frequency tolerance at a given temperature. This is the *real frequency* of the oscillator. As an example consider an oscillator $\mathcal{O}$ of some manufacturer with a nominal frequency of 10MHz. If the frequency tolerance is given as $\pm$ 30ppm at 25 °C, a possible and acceptable real frequency for $\mathcal{O}$ hence lies in the range 9 999 700 Hz to 10 000 300 Hz.

The clock drift results in the deviation between the nominal and the real frequency of the oscillator.

Accuracy: *The maximum offset from the nominal frequency denotes the accuracy of the oscillator.*

Stability: *The variation of the measured frequencies about the real frequency is defined as the stability of the oscillator.*

Further classifications can be done by considering the mean and the variance of the measured real frequency of an oscillator. If the mean of the real frequency is close to the nominal one, the oscillator is said to be precise. The variance determines the accuracy of the oscillator, i.e. an accurate oscillator has a small variance. Figure 2.1 illustrates these terms on examples for a marksman, top, and for clocks, bottom.

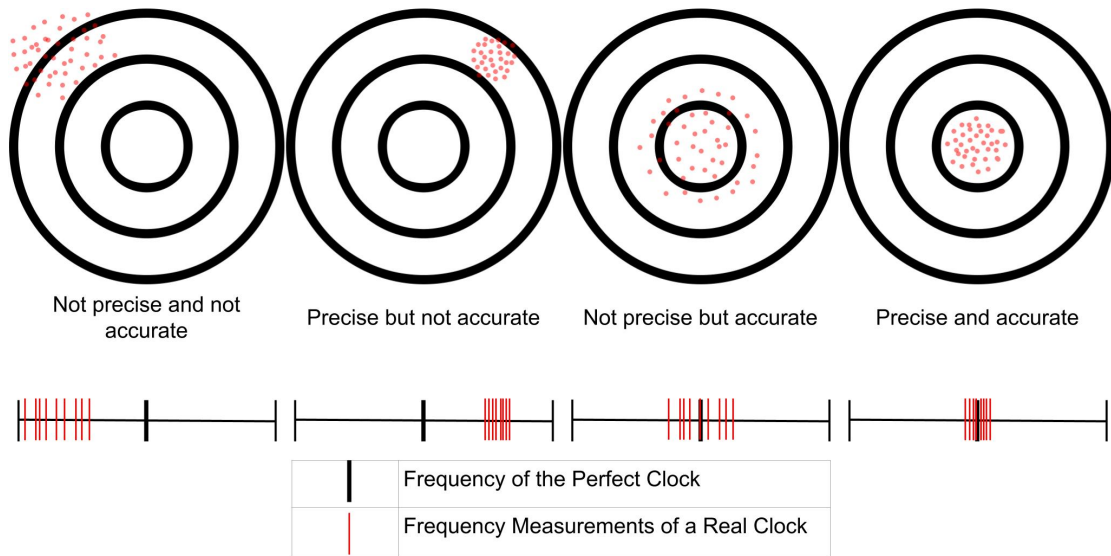|	Frequency of the Perfect Clock
	Frequency Measurements of a Real Clock

Figure 2.1: Accuracy and Precision. Source: Vig, John R. [15].

The name of real-time systems comes from the fact that such systems are subject to the real time behavior of the external world to which it is interfaced. This is of particular importance, e.g. for safety-critical systems. A distributed approach for the implementation of real-time systems has been pursued. H. Kopetz [[4], Chapter 2] presented a number of arguments in favor of a distributed approach. Composability, scalability and fault tolerance of real-time systems are the main and most important arguments.

In a distributed real-time system all nodes, or subsystems, should have the same view on a global time in order to guarantee a consistent system behavior. Otherwise, the temporal coordination and the temporally ordering of the observed events may fail. If two events have different timestamps on two different nodes, i.e. their temporal order is not consistent, it is not possible to reconstruct the causal order of the events. This is a crucial issue in many real-time systems, e.g. to resolve the cause of an alarm activation in a nuclear reactor [[4], Chapter 3].

To maintain a consistent view on time by the distributed clocks and to deal with the degradation of the oscillator precision, several synchronization approaches were developed and implemented. The approaches can be classified as internal or external clock synchronization [[4], Chapter 3].

***Internal Clock Synchronization**: The process of mutual synchronization of an ensemble of clocks in order to establish a global time with a bounded precision.* [[13], p. 22].

The internal clock synchronization approach ensures that the deployed clocks in the system agree on a common time. This time they agree on does not necessarily need to be correct for the external world, i.e. it is not in sync with an external standard of time. This is sufficient if the function of the system does not relay on that. Several variants are available to implement this approach, such as the central one, where the time comes from a master clock, and the distributed approach, where all of the local clocks have to participate in order to achieve the common time in the system.

***External Clock Synchronization**: The synchronization of a clock with an external time base such as the GPS.* [[13], p. 22].

The external clock synchronization approach syncs the local clocks with an external time source such as a time server connected to a GPS-receiver. The aim is to have a common time in the system, that is in sync with an external standard of time. The next subsection discusses the application of the GPS in the external clock synchronization.

In the context of the external clock synchronization, the holdover of a clock is defined as follows:

***Holdover**: The duration during which the local clock can maintain the required precision of the time without any input from the external time reference.* [[13], p. 23].

The aim of this thesis is to deal with this scenario, i.e. to extend the holdover of the system in the absence of the external time reference.

2.1.2 GPS Basics

The GPS was developed by the U.S. Department of Defense in the beginning of the 70s to provide an accurate positioning on the earth surface in any weather condition. The civilian application of this system ranges from marine navigation and surveying to automation of construction machinery, in addition to navigation systems.

In order to deliver its service, the GPS is divided into three subsystems[1]:

- **The Space Segment** consists of about 30 satellites orbiting the earth at some constellation. This ensures that at anytime and on any point on the earth surface, there are always at least 4 visible satellites to calculate the three dimensional coordinates and the time on that point. Each satellite is equipped with several accurate and precise atomic clocks, that are used to generate the broadcast signals.

---

[1] *The introduction to GPS* [16] provides an excellent reference about GPS for not GPS-experts.

The signals are used by the GPS-receiver to calculate its current position and time and to identify the sending satellites.

- **The Control Segment** updates the orbiting position of the satellites and calibrates and corrects their clocks. The clocks are corrected such that the Coordinated Universal Time (UTC) and the National Institute of Standards and Technology (NIST) time scale, are kept in agreement[2]. The control stations are distributed roughly on the earth equator.

- **The User Segment**: This segment refers to the GPS-receiver itself, that uses the signals from the satellites to determine its position. At this point the accuracy of the calculated position should be defined. The needed accuracy depends on the application field and on the GPS-receiver, not on the satellites. The GPS-receiver can reach an accuracy from $15m$ to $1cm$ or less.

To determine its current position, the GPS-receiver needs to measure the distance from each visible satellite to its position. This is done by applying the Newton's law of motion: *distance = velocity · time*, where the velocity is the speed of light and the time from the satellite to the GPS-receiver can be calculated by comparing the time of signal generation, which is coded in the signal, and the time of signal reception at the GPS-receiver. Intersecting the distances from three satellites delivers the position of the GPS-receiver on the earth surface. The fourth satellite is needed to verify the calculated position and to determine the current time.

This is the principle how positioning in the GPS works under the assumption of reception of perfect and error-free signals from the satellites. Some factors result in calculation errors and hence in a degradation in the accuracy of the position and time. For instance, ionospheric and atmospheric delays require further signal processing and error handling by the GPS-receiver and errors in the satellite clock should be detected and corrected by the control segment.

From the perspective of this thesis, the GPS is a potential source of accurate time. Hence, one important application of the GPS in the domain of clock synchronization is to make use of the accurate and precise clocks in the satellites as a time reference for the local clocks in distributed real-time systems.

> ***Global Positioning System Disciplined Oscillator (GPSDO)***: *An oscillator that synchronizes its time signals with the information received from a GPS-receiver.* [[13], p. 23].

The operation principle of GPSDOs is simple, see M. A. Lombardi [17]. Each GPSDO receives and encodes the signals from the satellites and corrects its frequency deviation based on the encoded data. A commercial GPS-receiver can track up to 12 satellites

---

[2]The NIST time scale data is updated monthly and can be downloaded from `http://tf.nist.gov/pubs/bulletin/timescaleindex.htm`.

12

and output a Pulse Per Second (PPS) signal synchronized to UTC. The system, that deploys the GPSDO, measures the difference between the PPS from the GPS-receiver and the frequency of the local clock. To simplify the design, the frequency of the local clock is divided to 1Hz, such that it also produces a local PPS. Afterwards, the GPSDO is corrected depending on the deviation between its PPS and the reference PPS. The accuracy of the GPSDOs depends on the quality of the oscillator, the GPS-receiver and the signals from the satellites.

2.1.3 Crystal Oscillators

The Quartz Crystal Oscillator (XO) is introduced as a technical implementation of oscillators in this subsection.

> **Quartz Crystal:** *A natural material that exhibits piezoelectricity, i.e. the ability to produce an electrical signal resulting from mechanical energy.*

This property of the quartz crystal can be used by a proper circuit design to generate electrical pulses with some frequency.

> **XO***: An oscillator, in which the frequency of oscillation is controlled by a piezo-electric crystal.* Graf, Rudolf F [[18], p.163].

Factors such as temperature fluctuations, vibration, noise in the electrical circuit, stress on the crystal and magnetic field affect the stability of the XO frequency. On the other hand, factors like temperature, crystal aging, ionizing radiation, atmospheric pressure, humidity, circuit electric current and retrace determine the frequency accuracy of the XO [6].

Real-time systems deploy XOCs as one of the important time sources. Compensating the effect of environmental conditions on the quartz frequency reduces the deviation between the frequencies of the distributed XOCs and contributes in maintaining the synchronicity for a longer period of time and hence extending the system holdover.

2.2 Sensors and Actors

This section provides an introduction to sensors and actuators, or actors. These two components are critical in the thesis for the following reasons:

- The sensors are used to collect information about the current environmental conditions in order to study their effects on the frequency of XOCs.

- The closed loop control systems, see Section 2.3, are implemented using sensors to read the current value of the controlled condition and actors to apply the steering value, that is calculated by the controller, see Figure 2.2.

R. H. Bishop et al. provide a fundamental introduction to sensors and actors in *The Mechatronics Handbook* [[19], Chapter 16-17].
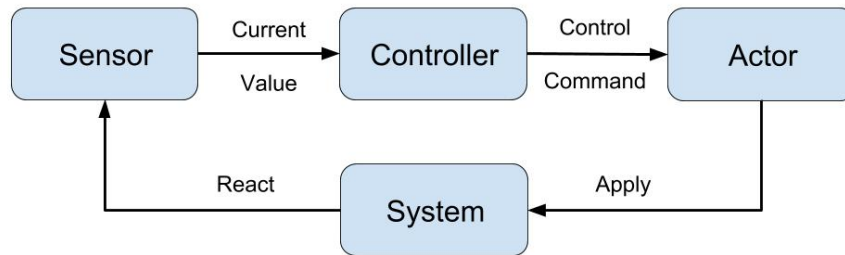
Figure 2.2: Application of Sensors and Actors in Control Systems

Sensor: A device that when exposed to a physical phenomenon (temperature, displacement, force, etc.) produces a proportional output signal (electrical, mechanical, magnetic, etc.). [[19], p. 327].

Sensors can be classified based on the following criteria:

- **Measurement Application**: The definition above refers to a *simple* sensor, when it performs a basic conversion to obtain the proportional output signal, that can be used directly by the processing unit. Apart from that, *smart* sensors also have their field of application, when the sensed data needs to be additionally stored and/or post processed before it can be used by the processing unit.

    Smart Sensor: A sensor equipped with additional signal processing units, such as filters and amplifiers.

- **Power Supply**: Depending on the power supply, sensors can be *passive* or *active*.

    *In **passive sensors**, the power required to produce the output is provided by the sensed physical phenomenon itself (such as a thermometer) whereas the **active sensors** require external power source (such as a strain gauge).* [[19], p. 329].

- **Output Signal**: An *analog* sensor outputs a continuous signal, that is proportional to the sensed parameter. Alternatively, a *digital* sensor produces a digital output, that is often obtained by an additional Analog to Digital Converter (ADC) on the sensor chip.

The control system calculates a steering value based on the sensed value and on the control algorithm. In order to control the environmental condition, actors are needed.

Actor: A component that accepts a control command (mostly in the form of an electrical signal) and produces a change in the physical system by generating force, motion, heat, flow, etc. [[19], p. 334].

Accordingly, actors can be classified as follows:

- **Energy Type**: Based on the applied energy, there are electrical, electromechanical, electromagnetic, hydraulic, or pneumatic actors.

- **Output Signal**: Similar to sensors, there exist digital (*binary*) and analog (*continuous*) actors. For instance, a relay with the two states *ON* and *OFF* is a binary actor and a stepper motor is a continuous one.

The classification criteria have to be considered as part of the system design. Table 2.1 provides additional criteria in order to select proper sensors and actors.

	Sensor	Actor
Range	Difference between max. & min. values	Range of motion
Resolution	Smallest change that can be sensed	Smallest possible increment of force
Accuracy	Difference between true & measured values	Linearity of the input-output function

Table 2.1: Sensors and Actors Selection Criteria

2.3 Controller Basics

This section provides a short introduction in the parts of control theory that are relevant for this thesis. S. Gerhard-Helge and W. Kastner discussed the basics of control theory in their book *Prozessautomatisierung* [[20], Chapter 6] as a part of automated systems. Figure 2.3 illustrates a classic block diagram of a system under control.
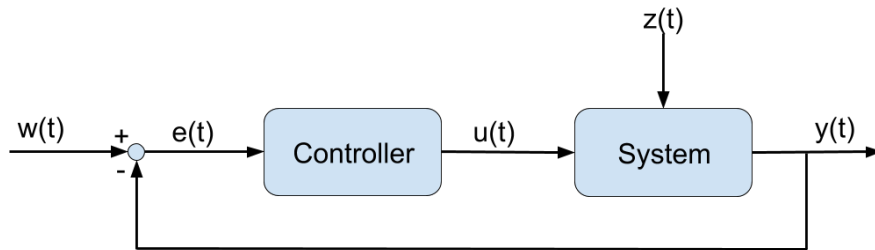

Figure 2.3: A Control Loop

- $w(t)$ is the setpoint of the controller, i.e. the desired value of the controlled variable.

- $y(t)$ is the measured, i.e. the real, value of the controlled variable.

- $e(t)$ is the error between the setpoint and the measured value, $e(t) = w(t) - y(t)$.

- $u(t)$ represents the steering value, that is calculated by the control algorithm depending on $e(t)$.

- $z(t)$ is the sum of disturbances on the system that causes the deviation error $e(t)$.

To control the value of some variable, the system should first be able to measure the actual value of it $y(t)$. From the difference between the actual value and the setpoint $e(t)$ the controller calculates a steering value $u(t)$ in order to keep $y(t)$ as close at possible to the setpoint $w(t)$. There exists plenty of algorithms to calculate $u(t)$. In the following, the PID- and the on-off-controller are presented.

2.3.1 PID-Controller

The PID-controller [[20], p.186] calculates $u(t)$ as the sum of three components: The P- (proportional), the I- (integral) and the D- (derivative) component. The mathematical expression is given by the Equation 2.1.

$$u(t) = \underbrace{K_P \cdot e(t)}_{\text{P-Component}} + \underbrace{K_I \int e(t) \cdot dt}_{\text{I-Component}} + \underbrace{K_D \cdot \frac{de(t)}{dt}}_{\text{D-Component}} \tag{2.1}$$

The P-component depends on the current value of $e(t)$ and is expressed by the proportional gain K_P. The controller multiplies $e(t)$ by K_P to get $u(t)$. Increasing K_P will increase the response of the controller, but if it is too large, the system will become unstable. The error $e(t)$ would never disappear when using only a P-controller. This can be reached by adding the I-component, that sums the errors over time. Hence, the response of the I-component is increasing over time unless $e(t)$ is zero and the tendency for oscillation is decreased. The D-component predicts the future by considering the rate of change of $e(t)$, i.e. of $u(t)$. The response of the D-component is proportional to the rate of change. This component is highly sensitive to the noise in the measurements.

The next step is to determine the values of the parameters K_P, K_I and K_D. This can be done by studying the step response of the system in the time domain or by the frequency response method in the frequency domain. Both are developed by John G. Ziegler and Nathaniel B. Nichols.

In general, the calculated values are not the optimal ones and they need to be tuned in order to have a better behavior. There exists some heuristics to do so, which are also known as the Ziegler-Nichols tuning method. Alternatively, software tools can be used to calculate and to tune the parameters of the PID-controller, such as the PID Control toolbox in MATLAB. To exemplify the response of a variable, that is controlled by a PID-controller, Figure 2.4 illustrates the behavior of the temperature in a heater.

2.3.2 On-Off-Controller

An On-off- or a two-point-controller [[20], p.190] can be used when the response of the system is extremely slow or when some deviation in the controlled value $y(t)$ can be tolerated without serious consequences. A typical example on such a controller is a thermostat. When the temperature goes below some threshold $w(t) - \Delta y$, the heater is
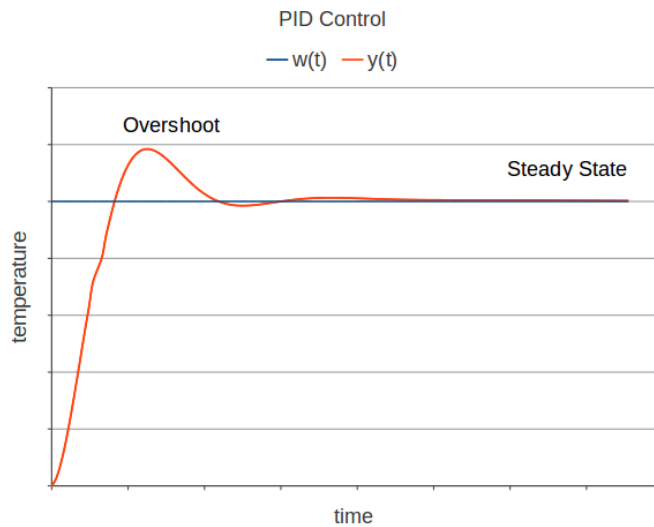
Figure 2.4: Temperature Control with a PID-Controller

switched on. When it reaches another threshold $w(t) + \Delta y$, the heater is switched off.

The difference $2 \cdot \Delta y$ between the upper and the lower thresholds is denoted as the *hysteresis* of the controller and it represents the tolerated deviation in the controlled variable. Figure 2.5 illustrates the behavior of the temperature under the on-off-control of a thermostat. The steering value $u(t)$ is depicted in the figure as a binary signal with two states: *ON* and *OFF*.

The hysteresis of the controller is a theoretical value. Due to the dynamics of real systems, a bigger hysteresis value has to be considered while developing the on-Off-controller. Figure 2.5 shows that the controlled temperature keeps increasing / decreasing after turning on / off the thermostat for a certain period of time.

2.4 Machine Learning

Machine Learning is one of the subfields of Artificial Intelligence (AI) that additionally comprises natural language processing, decisional algorithms, automated theorem provers, etc.

> ***AI****: (The automation of) activities that we associate with human thinking, activities such as decision-making, problem solving, learning, etc.* [21]

> ***Machine Learning****: A subfield of AI, that is concerned with discovering regularities and patterns in (big) data and building models for them.*

Regression Analysis, as a form of machine learning [22], is used to fit big data to a model that defines the dependent variable Y as a function of the independent variable X,
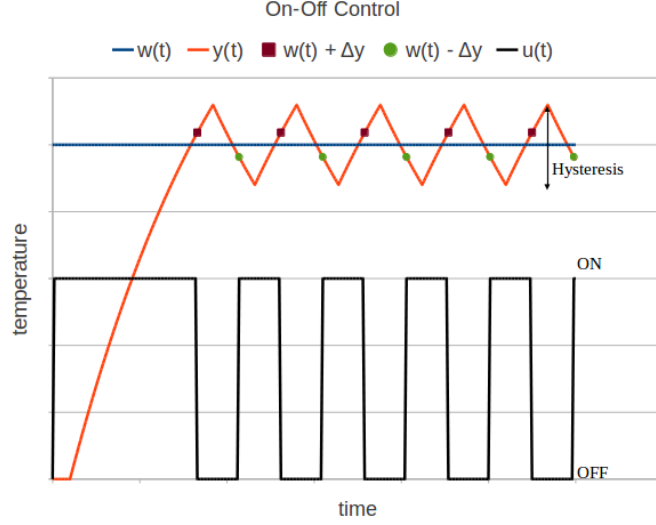
17

Figure 2.5: Temperature Control with an On-Off-Controller

i.e. $Y = f(X)$. X and Y can be simple variables or vectors of variables and the function $f(.)$ can be linear, polynomial, exponential, logarithmic, etc. In the context of this thesis, the term *big data* refers to the large volume of information, that describes the dependency of the frequency of a XOC on the environmental conditions. The output of the analysis is a model describing that dependency in form of polynomials. The dependent variable Y is the frequency of a XOC and X is a set of environmental conditions, see Equation 2.2. To simplify the equation, X and Y are considered as simple variables, i.e. as x and y.

$$y = f(x) = a_0 + a_1 \cdot x + a_2 \cdot x^2 + \cdots + a_n \cdot x^n = \sum_{i=0}^{n} a_i \cdot x^i \qquad (2.2)$$

The regression analysis of the data outputs the optimal parameters of the polynomial described in Equation 2.2. These are the order of the polynomial n and the polynomial coefficients a_i. This procedure is also called *curve fitting* [23]. One of the main optimality criteria for these parameters is the *chi-square* value as the sum of the squared error between the original and modeled calculated curves, see Equation 2.3. The lower the chi-square value, the better the model. Another criterion is the *coefficient of determination* $R^2 \in [0;1]$ between the original and the fitted data, see Equation 2.4. In this case the higher the value of R^2, the better the model.

$$\chi^2 = \sum_i \frac{(o_i - m_i)^2}{\sigma^2} \qquad (2.3)$$

$$R = \frac{\sum_i (m_i - \bar{m})(o_i - \bar{o})}{\sqrt{\sum_i (m_i - \bar{m})^2} \sqrt{\sum_i (o_i - \bar{o})^2}} \qquad (2.4)$$

18

Where o_i is the original value, $\bar{o}$ is the mean of original values, m_i is the calculated one from the model, $\bar{m}$ is the mean and σ^2 is the variance of the calculated values.

Depending on the analyzed data, different polynomials can be used as models, see Figure 2.6 and Figure 2.7 for linear and non-linear functions, respectively.
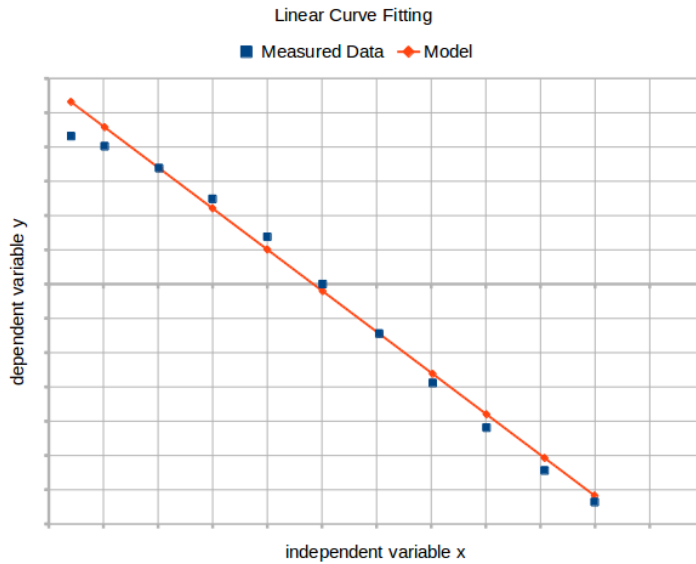

Figure 2.6: Linear Function as Model $\chi^2 = 8.6 \cdot 10^{-5}$ $R^2 = 0.99998$
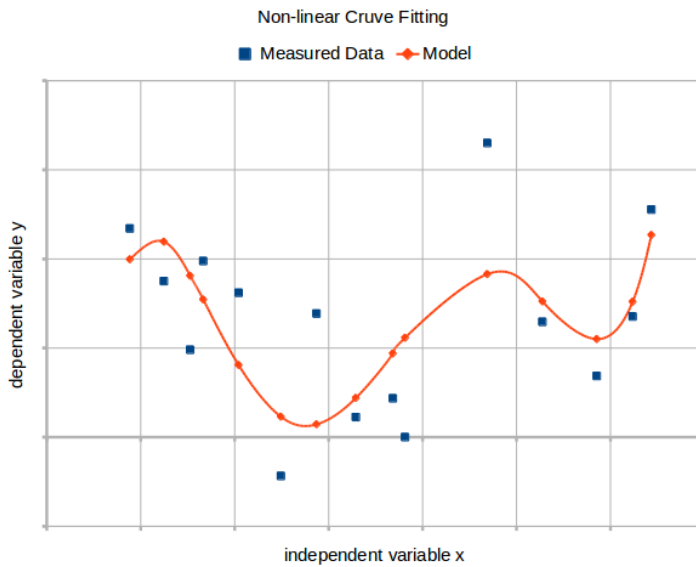

Figure 2.7: Non-linear Function as Model $\chi^2 = 6.77 \cdot 10^{-4}$ $R^2 = 0.89581$

CHAPTER 3

Requirements and Related Work

This chapter introduces the main requirements for an approach to compensate the effects of environmental conditions on a Crystal Oscillator based Clock (XOC). These requirements are essential to measure and to evaluate the quality of the compensation approaches, that are discussed afterwards. An overview of the fulfillment of the requirements by the discussed approaches is provided at the end of this chapter.

3.1 Requirements

The following requirements are introduced to provide quality criteria for the related work, as well as for the developed method. In the following, the extensibility of the system is measured by the required effort to implement the desired extension.

3.1.1 R1: Extensibility of the Hardware

A system to compensate the frequency deviation of a Quartz Crystal Oscillator (XO) has to be preferably designed to fit to the wide range of XOs in the sense that replacing the used XO requires to adapt the affected XO specific parts with no or a minimal impact to the existing system functions. Applying a parameterizable XO model implies that the model parameters are XO specific which eases the replacement of the XO.

The other hardware component that affects the compensation procedure is the sensor. Replacing the sensors has impacts on the quality of the collected data since different sensors collect and provide information in different ways, see Section 2.2 for the classification of sensors. For this reason, not only the XO specific model is affected by replacing the sensors, additional post processing of the collected data by the system may be required depending on the used sensor.

In general, deploying common used XOs and sensors increases the versatility of the approach and decreases the costs for the following production.

3.1.2   R2: Extensibility of the Software

The relevance of an environmental condition for the operation of the XOC is determined by the system field of operation. A well designed approach has to take future adaption into consideration. For instance, while a system to compensate the frequency deviation of a XO in a broadcasting tower has to mainly consider the effects of temperature, humidity and magnetic field, another system in a mobile application, such as in the automotive field, has to additionally take the acceleration into consideration. If the system approach is extensible, i.e. if its software is extensible, it can be deployed in both fields.

Adapting the compensation software is not required only as a consequence of changing the considered environmental conditions, but also due to increasing or shifting their operation ranges. A system that operates quite good in north Europe may need to be adapted concerning the operation range of the environmental temperature if it has to operate in central Africa, for instance.

Another aspect of the software extensibility is concerned about the ability of the system to correct itself while it is operational, i.e to learn from its inaccuracies. This is an important feature since the behavior of the XO changes by the progression of time due to quartz aging [24]. In this way, the system is able to improve its behavior.

A model-driven approach makes the first move towards an extensible software. Hence, using a XO specific model in the approach is essential to fulfill this requirement.

3.1.3   R3: Manageable System Complexity

A complex system is defined as follows:

> **Complex System:** *A system with numerous components and interconnections, interactions or interdependence that are difficult to describe, understand, predict, manage, design, and/or change* [25].

Hence, the main factors that increase the complexity of a compensation system are the number of the considered environmental conditions and the interdependencies between these conditions. Additionally, satisfying the previous requirements, *R1* and *R2*, necessitates the requirement of managing the increasing complexity.

A system that is able to deal with the high complexity should have a structural approach regarding the modeling technique of the individual and the joint effects of environmental conditions on the XO frequency. Another point that reduces the complexity is to consider dividing up the model into sub-models. This eases the implementation and adaptation of the approach. For instance, using a machine learning technique such

as the Artificial Neural Network (ANN) to compensate the effects of multiple factors is theoretically possible with a single ANN but its impractical due to the high learning and implementation complexity. Developing one ANN per factor and combining the individual outputs is a more realistic approach to be followed [26], a detailed discussion is provided in Subsection 3.2.2.

3.1.4 R4: Accuracy Improvement at Low Cost

The compensation approach must ensure that the improvement in the XO accuracy meets the requirements of the application field and fits to its constrains. The implementation cost can be described by the cost of the equipment, as well as by the operation costs such as the weight of the system and its energy and memory consumption.

The requirement on the system holdover determines the desired improvement since a higher XO accuracy implies a longer system holdover. For instance, the time offset of a quartz-based Global Positioning System Disciplined Oscillator (GPSDO) from the National Institute of Standards and Technology (NIST) time scale after one week of holdover is $82\mu s$ [17]. Hence, it can provide a holdover up to 2 hours if it shall not deviate by more than $1\mu s$ when the external time reference is not available.

The field of operation constrains the implementation of the approach and hence the reachable accuracy improvement. An Oven Controlled Crystal Oscillator (OCXO), for example, may be acceptable in a stationary cellular base station, but not in a mobile application such as in the aerospace, where the extra weight and energy consumption are of prime importance.

An approach that satisfies the previous requirement has an adjustable accuracy improvement that fits to the field of operation and to the cost of the implementation.

3.2 Related Work

The topic of sensitivities of XOs to the various environmental conditions has already been addressed by a wide variety of engineers and researchers. Questions were raised in literature about the the effects of individual conditions and how to compensate them [27] [28] [29]. The goal of these studies and the design of the approaches depend on the interested community. The methods used for measuring the environmental sensitivities of XOs and their limitations have been evaluated by the academic communities [30] [31] [32], whereas the industrial and military applications are concentrated on their specific application fields and on the most relevant environmental conditions in these fields, such as the sensitivity to acceleration in aerospace applications [33] or in highly dynamic environments as in helicopters and missiles [7].

Different compensation systems and their related design are covered in this section. Afterwards, a summary about the fulfillment of the presented requirements is given.

3.2.1 G-Compensated XO Technology

The impact of acceleration and vibration[1] on XOs has gained a significant importance in real-time systems due to the increasing need to mobile systems. The *G-Compensated XO* approach [7] is developed to defeat the degradation in the performance of XOs, that is subject to acceleration and vibration, e.g. in helicopters and military track vehicles. The main goal is to compensate the frequency deviation by a system design, that can be produced at reasonable cost.

A hard mounted Stress Compensated Crystal Oscillator (SCXO) is used in this approach, that represents a reliable frequency source in an acceleration-free environment. The SCXO has a frequency of 10MHz and its multiplied up to 200MHz in the application.

A 20Hz sinusoidal vibration with an amplitude of 4.5g and a typical aircraft random vibration with a frequency from 10Hz to 200Hz result in a performance degradation of almost $40dB$ in comparison to the original frequency deviation without the disturbing factors, i.e. a degradation by four orders of magnitude ($10^{\frac{40dB}{10}} = 10^4$). This has impacts on the system level performance.

The *G-Compensated XO* approach reaches an improvement between $45dB$ at 10Hz and $20dB$ at 200Hz, i.e. between four and two orders of magnitude, which reduces the overall deviation caused by the acceleration by an the order of 10^1 to 10^2 depending on the platform and application of the compensation system.

The compensation in the *G-Compensated XO* approach is performed as follows:

- **SCXO Design**: The cross-coupling between the three axes x, y and z is minimized by design and manufacture such that the acceleration in the direction of each axis is as independent as possible of the others.

- **Sensors**: They are mounted to each axis and respond to linear and oscillatory accelerations. By doing so, the amplitudes and the phase relationships of the sensed signals are adjusted by the compensation electronics, which leads to cancellation effects that compensates the sensed acceleration in total.

The approach is based on a custom hardware with low cross-coupling and low acceleration sensitivity and it is already used in the application field of interest. The compensation is performed by the electronics and not by a model of the XO, i.e. no software is involved in the system design. One environmental condition is considered and no future adaption is possible or foreseen. Furthermore, only linear and oscillatory accelerations are considered in this approach.

---

[1]In the following, vibration is considered as time-dependent acceleration.

3.2.2 Application of ANNs

The temperature is one of the important environmental conditions that affects the frequency of the XOs. J. Esterline [34] outlined the application of ANNs in compensating the effects of environmental temperature on the XO frequency. This approach is developed as a curve fitter to overcome the limitations of state of the art curve fitting, using a polynomial generator, regarding the broad industrial temperature range and the irresistible need to higher frequency stabilities. The compensation with curve fitting using a 5th order polynomial function generator reduces the frequency deviation of a Temperature Compensated Crystal Oscillator (TCXO) by an order of magnitude, i.e. a stability of $\pm 0.1 ppm$ is achievable. The ANN approach improves the original TCXO behavior by two orders of magnitude, where stabilities in the range of $\pm 0.01 ppm$ over the temperature range $-40\,^{\circ}\mathrm{C}$ to $+85\,^{\circ}\mathrm{C}$ are possible.

A TCXO is a XO with optimized behavior regarding the frequency deviation over temperature, i.e. a stability of $\pm 1 ppm$ is achievable with this type of XO. In this approach, an AT-cut TCXO with a frequency of 10MHz is used in the prototype testing. This cut is widely used where frequencies in the range 500kHz to +300MHz are required. Additionally, the TCXO has its own internal compensation circuit using a 5th order polynomial function generator.

A model of the neuron k is given in Figure 3.1, where the right model in the figure simplifies the left one. The inputs X_1 to X_n of the neuron are multiplied with their weights ω_{k1} to ω_{kn}. It is also possible to have a bias b_k with its own weight ω_{0b}. The sum of these products is the input of the *activation function* $\Phi(.)$, which maps the inputs of the neuron to a finite output value Y_k. In mathematical terms, Equation 3.1 and Equation 3.2 describe the functionality of the neuron[2]:

$$Z_k = (\sum_{i=1}^{n} \omega_{ki} \cdot X_i) + \omega_{0b} \cdot b_k \tag{3.1}$$

$$Y_k = \Phi(Z_k) = \frac{1}{1 + e^{-\alpha \cdot Z_k}} \tag{3.2}$$

Where ω controls the transition sharpness of the activation function, the bias b shifts the output to the left or to the right and α controls the slope of the output, see Figure 3.2.

---

[2]The unipolar sigmoid function is selected as activation function.
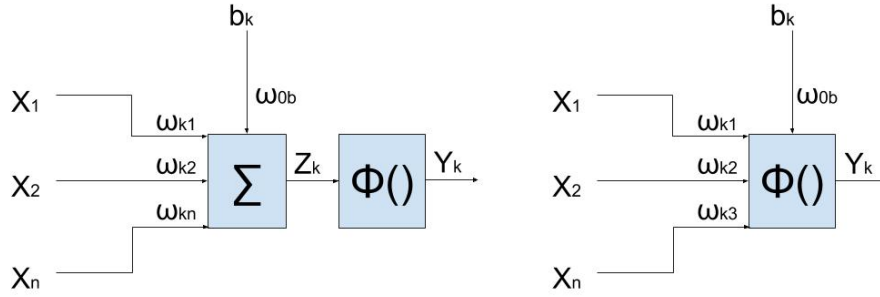
Figure 3.1: Model of the Neuron [34]

The ANN is formed out of the interconnections between different neurons. The function of the ANN is an outcome of the form of these interconnections, the choice of the activation function and the values of the input weights and biases. Figure 3.3 depicts the structure of the ANN that is used to compensate the deviation of the TCXO frequency. The single input X is a voltage that represents the current temperature and the output Y_{out} is the deviation of the TCXO in ppm, which is converted into a steering value to control the input voltage of the TCXO. The parameters of the model are calculated by a network training technique called *the least squares* [35].

Figure 3.3: ANN Structure for the Temperature Compensation [34]

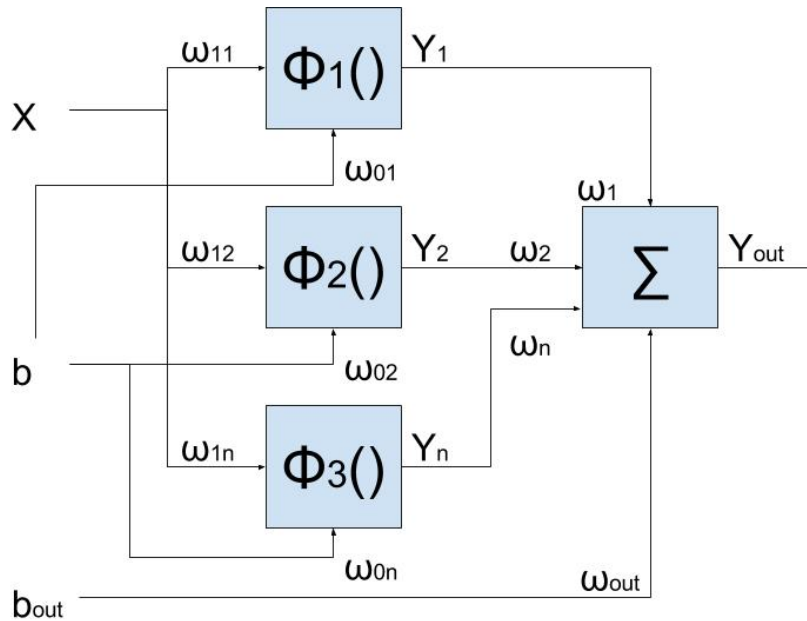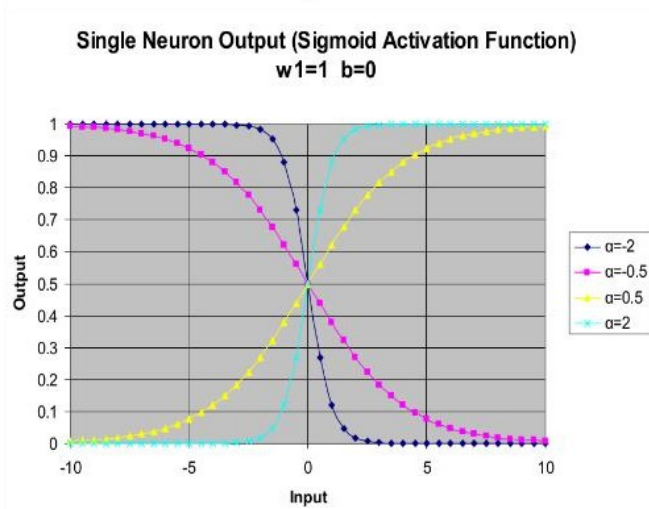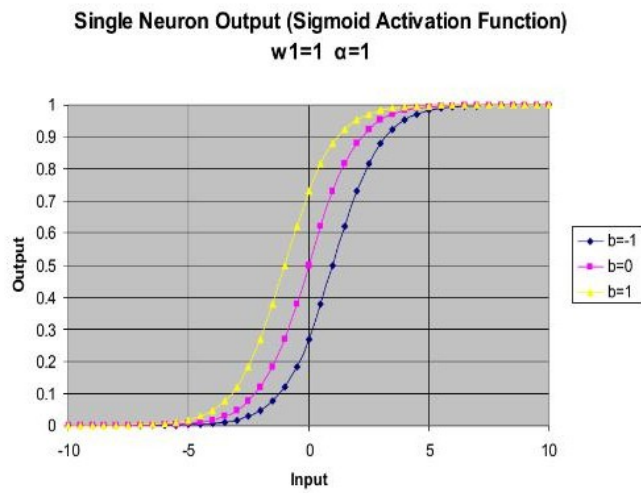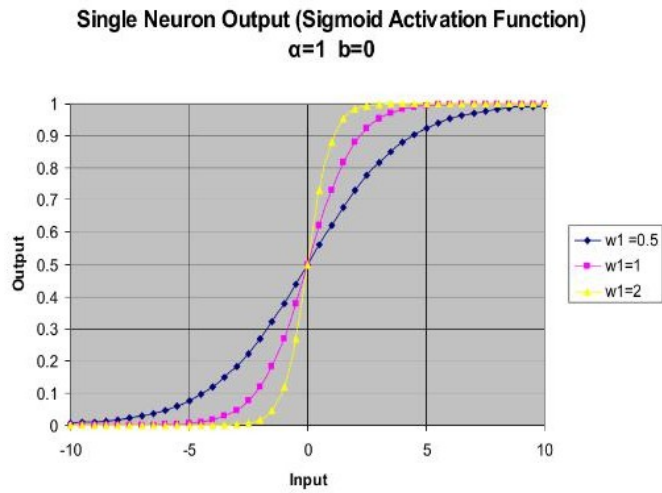Figure 3.2: Effects of the Parameters on the Output of the Neuron [34]

The compensation is done in the temperature range $-42\,^{\circ}\mathrm{C}$ to $+86\,^{\circ}\mathrm{C}$ by the following steps:

- The ANN was used as **primary compensation** for AT-cut XOs by turning off the internal compensation circuit of the TCXO. An improvement is achieved from a deviation of $\pm15.74ppm$ before to a deviation of $\pm0.035ppm$ after the primary compensation. The corresponding ANN has $n = 25$ neurons.

- Afterwards, the ANN was trained with the data set from the first compensation and the compensation is run again after turning on the TCXO internal compensation circuit, i.e. as **secondary compensation** for TCXOs. In this case, the deviation of $\pm0.102ppm$ before the secondary compensation is reduced to a deviation of $\pm0.005ppm$ using $n = 33$ neurons.

One side effect of deploying TCXOs with voltage control is the skewing of the frequency while its pulled away from the TCXO nominal frequency, i.e. the frequency it was compensated with. The so called *trim effect* becomes noticeable and not negligible anymore since some compensation methods achieve frequency versus temperature stabilities in the range of a $\pm0.01ppm$. To demonstrate the strengths of the ANN approach, J. Esterline [36] applied it to compensate the trim effect as it becomes noticeable after the ANN temperature compensation of the TCXO.

The activation function, given by Equation 3.2, is three dimensional in this case[3]. Furthermore, the structure of the ANN, depicted in Figure 3.3, should be adapted since the ANN have two inputs. The first input X_1 is the voltage that represents the current temperature and the second one X_2 is the applied TCXO control voltage, i.e. the output of the ANN used for temperature compensation which is the cause of the trim effect. This is the theoretical setup of the ANN, but it is impractical because of the high complexity of the resulting equations that have to be solved in order to obtain the parameters of the corresponding ANN. For this reason, two ANNs are implemented in parallel, one for each condition, and their outputs are summed together.

The compensation is done in the temperature range $-42\,^{\circ}\mathrm{C}$ to $+86\,^{\circ}\mathrm{C}$ as follows:

- First, the TCXO internal compensation circuit is turned on and the ANN of the temperature compensation is applied as secondary compensation. The frequency deviation resides in the range $\pm0.2ppm$ in the worst case when the difference between the nominal and the applied control voltage is at the maximum.

- The second ANN to compensate the trim effect is applied afterwards in parallel to the first ANN. The frequency deviation is reduced to $\pm0.0107ppm$ using $n = 10$ neurons for the second ANN.

---

[3]A three dimensional sigmoid sheet instead of the unipolar sigmoid function

The drawbacks of this approach are the calculations and the memory needed to compute and store the ANN parameters and the compensation values of the TCXO. Additionally, the rapidly increasing complexity with the increasing number of neurons represents a challenge that has to be managed. By applying this method on several environmental conditions a much higher complexity is expected because of the ANN multiple inputs and the selection of a proper activation function. Complex curves can be approximated but choosing the parameters of the activation function is not easy and requires deep understanding of the selected function and the curve to be modeled. Furthermore, no information about the required time to train the ANN was provided by the author.

3.2.3 Space XO

Because of the increasing importance of positioning systems, such as the Global Positioning System (GPS) or the Global Navigation Satellite System (GLONASS), the effects of atmospheric pressure and magnetic fields on the frequency of the XO is gaining more relevance. S. Galliou et al. [33] introduced a XO design, that is intended for space applications and considers the effects of environmental temperature, atmospheric pressure, magnetic field and vibrations on the XO frequency, see Figure 3.4.
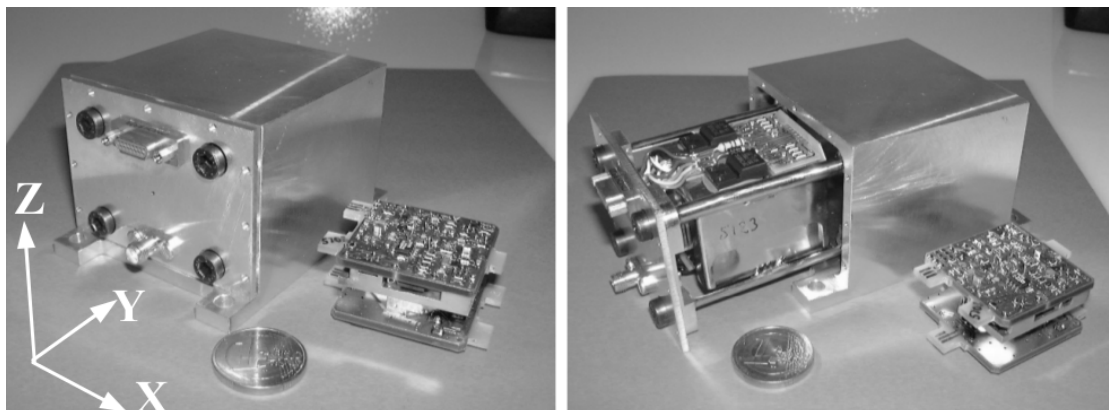
Figure 3.4: Space XO [33]

To fit to spacecraft applications, a SCXO with a frequency of 10MHz and a special configuration called *BVA* is used. This SCXO has improved aging characteristics and it is less sensitive to circuit disturbances, vibration and acceleration. The design of the used SCXO in this approach additionally ensures less sensitivity to temperature changes, by deploying the SCXO in a temperature controlled oven, and radiations.

The inner temperature in the oven is set to $82\,^{\circ}\text{C}$ and the design of the space oscillator provides a thermal path between the oven and the outer enclosure such that the temper-

ature fluctuations are eliminated. An experiment that lasted for 50 hours shows that, by varying the ambient temperature in the range $12\,°C$ to $30\,°C$ at atmospheric pressure and under vacuum, the observed frequency deviation resides in the range $\pm 0.00035 ppm$, or $\pm 0.35 ppb$ (part-per-billion or 10^{-9}).

The acceleration, shock and vibration resistance is mainly important to survive the launch process from the earth surface to the outer space by a spacecraft. For this purpose, random vibrations with a power spectral density of $0.05 g^2/\text{Hz}$ in the three dimensions were simulated. No particular compensation for these conditions were performed. The SCXO is, by selection, acceleration resistive. The SCXO exposed a frequency deviation of $\pm 0.5 ppb$, $\pm 0.25 ppb$ and $\pm 0.3 ppb$ on the x-, y- and z-axis, respectively.

The space oscillator is designed to be insensitive to the magnetic field by using *Mu-metal shells* as magnetic shielding. An experiment demonstrated the efficiency of such shielding by applying a magnetic field of ± 6Gauss on the three axes. A reduction in the frequency deviation from $\pm 1.5 ppb$ without to $0 ppb$ with the shielding is achieved.

The compensation of the effects of temperature, pressure and magnetic field is done by the design of the enclosure, whereas the selection of the XO cut and configuration eliminates the acceleration effects. The results of the experiments are in accordance with the intended behavior of a space oscillator.
No improvement in the power consumption in comparison to the state of the art space XOs was addressed. Furthermore, the complete system has a mass of $425 g$. A reduction in its mass is possible by modifying the outer enclosure, which could make the XO more vulnerable to temperature changes and magnetic field.

3.2.4   Temperature and Frequency Control

A widely used approach to obtain a stable XO frequency is to control some environmental conditions, such as the temperature. G. Swann et al. [37] presented a new architecture for precise temperature control and frequency stabilization of XOs. The XO frequency deviation is reduced by using an inner loop to *control* the temperature of the quartz, which resides in a chamber. Additionally, the XO is equipped with a control system for precise voltage tuning and hence to *stabilize* the XO frequency.

The temperature control is based on an analog temperature sensor and a *Zilog Z80* microprocessor that interfaces the sensor and controls the heater of the chamber as proportional controller in order to maintain the inner temperature as close as possible to a predefined setpoint. The XO resides in an insulated chamber that provides additional thermal stability.
To fine-tune the frequency of the XO, a frequency control system is designed and tested, which is composed of the XO, a voltage regulator and a tuning circuit that provides a frequency tuning voltage in the range $0V$ to $12V$.

The main focus of the approach was on the design, the implementation and the testing of the temperature and frequency control systems. The temperature experiments yield that the temperature error is less than $0.1\,^{\circ}$C. This reduces the temperature dependent frequency deviation to the minimum. Additionally, the XO frequency can be adjusted using the tuning circuit of the frequency control system. The frequency experiment exhibits that the frequency of the used XO is adjustable in the range ±55Hz around its frequency at the temperature setpoint with a granularity of 9.2Hz$/1V$.

This approach can achieve a very stable XO frequency. The temperature setpoint is adjustable depending on the test requirements and on the deployed XO, which makes this system applicable with any XO. On the other side, these are merely conclusions since no test results on a concrete XO were presented by the authors regarding the stability of its frequency.

3.2.5 Fulfillment of Requirements in Related Work

An approach that fulfills the defined requirements in Section 3.1 represents a paradigmatic approach, which is able to consider the wide range of XOs and sensors, deploys a XO specific compensation model with a manageable complexity, is able to learn and improve its behavior and fits to different application fields. None of the discussed approaches is able to fulfill the above mentioned requirements. Table 3.1 provides an overview of the requirements fulfillment in the related work.

The approaches that consider one environmental condition or one application field, such as the discussed ones in Subsection 3.2.1 and Subsection 3.2.3, deliver good results in their domain, but the extensibility of the hardware and/or the software is either not foreseen or not possible.
The ANN approach, see Subsection 3.2.2 overcomes this disadvantage but with high complexity due to the large number of interconnections in the ANN and the calculation overhead of the model parameters.
Many approaches control some environmental conditions in order to achieve better frequency stability, such as the discussed one in Subsection 3.2.4. They are undesirable in mobile applications because of the higher energy consumption and the extra weight compared to the other compensation approaches. Nevertheless, they are used due to the very stable XO frequency they can achieve.

	R1	R2	R3	R4
G-Compensated XO	**No**, custom SCXO: Hard mounted XO Acceleration sensors mounted to each axis	**No**, compensation by hardware design No software involved Adaption not possible	No software complexity No details regarding hardware complexity	Final product design Size $\leq 5in^3$
ANN Compensation	**Yes**, common XO and sensors possible A TCXO is used for prototype testing	**Yes**, parameterizable and extensible XO-model Adaption is possible	**No**, high complexity for one condition Rapidly increasing complexity to manage	Prototype design High impl. costs
Space XO	**No**, custom XO: BVA-SCXO Common sensors for testing purposes only	**No**, compensation by system design and selection of the XO Adaption not possible	No software complexity No details regarding hardware complexity	Final product design System weight 425g
Temperature & Frequency Control	Common used XO Custom oven design Custom temperature controller design	**No**, compensation by temperature and voltage control Adaption not possible	Manageable software complexity High hardware complexity	Prototype design High impl. costs

Table 3.1: Fulfillment of Requirements in Related Work

CHAPTER 4

Method

In order to compensate the effects of environmental conditions on a Crystal Oscillator based Clock (XOC), the behavior of the Quartz Crystal Oscillator (XO) has to be studied under these conditions. The observed behavior is evaluated and modeled afterwards. Based on the XO frequency deviation, that is predicted by the developed model, a correction value for the counter of the XOC is calculated. The XOC is corrected by adding/removing clock ticks to/from its counter. A time signal is generated when the clock counter is valid, i.e. when it reaches the correction value calculated by the model.

Section 4.1 provides a description of the compensation system and the XOC counter correction procedure. The following sections provide more details on the developed method. The first step is to analyze the XO frequency, see Section 4.2. This is done by performing experiments on the hardware including the XO and the sensors, that are needed to collect the data from the environment. The experiment design shall make sure that the individual and the joint effects of the environmental conditions are differentiable in the collected data. The evaluation of the collected data is the next step in the method, see Section 4.3. Relating the deviation in the XO frequency to the variation of individual or multiple environmental conditions is the goal of developing the compensation model. The model shall be able to predict the frequency deviation based on the evaluated data. The last step is to implement the model on the hardware target and to calculate the XOC counter correction value out of the predicted compensation values, see Section 4.4. A summary about the steps to be followed in order to develop and install the XO specific compensation model is presented in the last section 4.5.

4.1 Overview

The system is permanently exposed to and affected by the environmental conditions. Based on the current conditions, that are captured by the sensors, the deviation of the

XO frequency is predicted and a correction value for the XOC counter is calculated. If the external time reference is not available, the system generates the time signal out of the current XO frequency and its correction value. Otherwise, the external time reference is the source of the time signal and the system is able to improve its compensation model by applying an online learning technique, see Section 4.3. Figure 4.1 provides an overview of the system design.
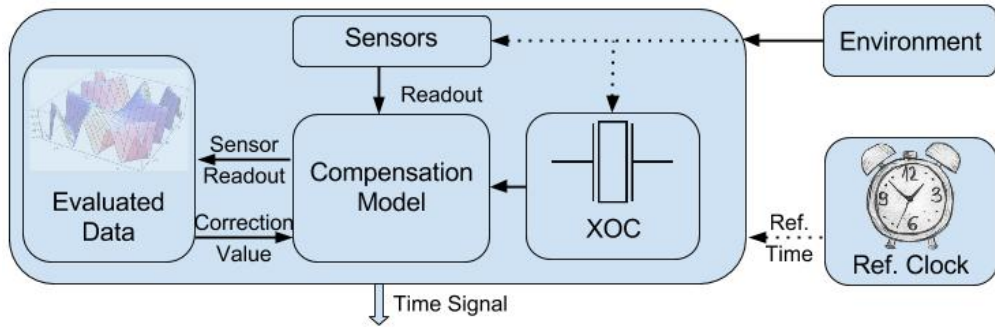
Figure 4.1: System Overview

Figure 4.2 illustrates how the correction of the XOC is performed. The idea is to calculate the ticks of the XOC, that are needed to complete some predefined duration and to output a pulse when this duration is reached. The deviation between that pulse, the red bar in Figure 4.2, and the pulse generated by a perfect clock with the same frequency, the black bar, is predicted by the model. Based on the predicted deviation, the system corrects the number of the ticks and outputs a pulse as accurately as possible. Its accuracy is measurable by defining a tolerance range for it. The pulse of the reference clock can be realized by an external time reference. For instance, defining the duration as one second allows the application of the Pulse Per Second (PPS) of the Global Positioning System (GPS) as the pulse of the reference clock.

🟩	Tolerance Range
	Pulse of a Perfect Clock
	Pulse of the Local Clock
↔	Frequency Correction Value

Figure 4.2: XOC Correction Procedure

4.2 Data Collection

The first step in the approach is to study the behavior of the XO under the influence of the environmental conditions. To this end, the XO is exposed to these conditions and the deviation of its frequency is measured in the data collection part. The values of the current conditions come from the sensors whereas the deviation of the frequency is calculated out of the number of XOC ticks per reference time unit, e.g. per PPS. Figure 4.3 illustrates the abstract hardware setup needed while collecting data.
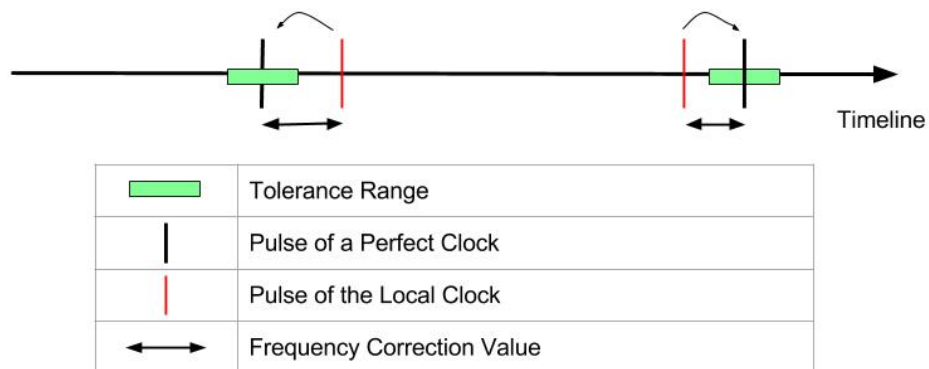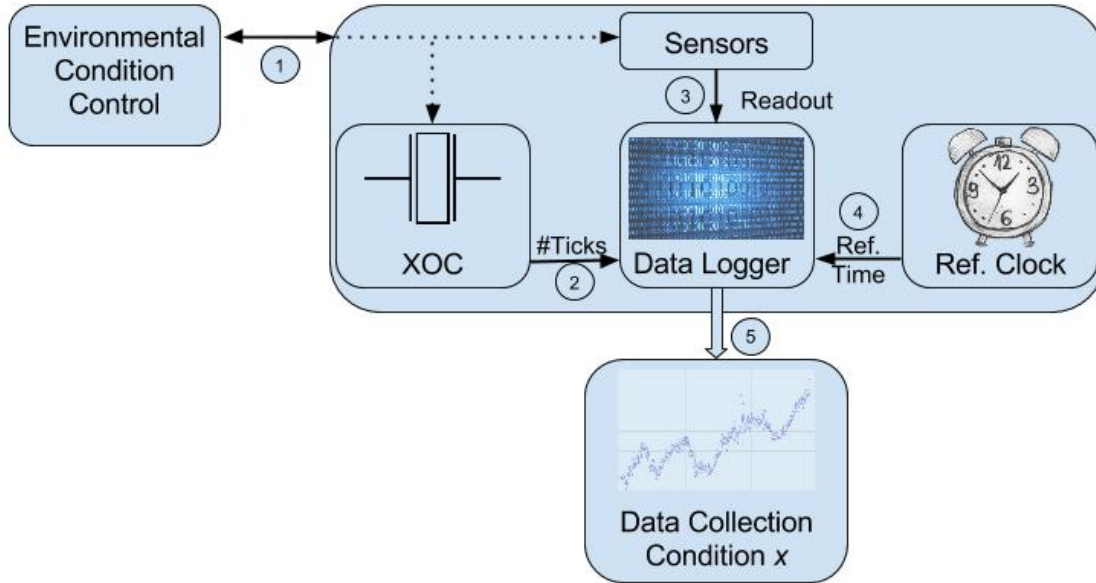

Figure 4.3: Hardware Setup of the Data Collection Part

4.2.1 Controlling the Environmental Conditions

In order to reveal the effects of environmental conditions on the XO frequency, the XO behavior should be studied while its exposed to these conditions. Therefore, the values of the environmental conditions are controlled in predefined operation ranges, cf. Label *1* in Figure 4.3. To study the effects of the condition in its operation range, a number of experiments at different setpoints is required. These setpoints have to cover the operation range of the environmental condition. The size of the individual operation ranges depends on the application field of the system. For example, a pressure operation range of $1000 \pm 70mbar$ corresponds to an altitude difference of $-400m$ below sea level to $+700m$ above sea level, respectively.

Furthermore, the way of controlling depends also on the environmental condition and on the used actuator. For instance, a PID-controller is suitable for the pressure control with an air pump, whereas an on-off controller is appropriate for the temperature control with a peltier element. Section 2.3 provides a short introduction in the involved control theory.

4.2.2   Quartz Frequency Measurement

In order to develop a precise model, the system has to be able to measure the real
frequency of the XO, see Label *2* in Figure 4.3 and Section 2.1.1. The real frequency is
calculated out of the counted quartz oscillations, i.e. the ticks of the XOC, in the time
interval, which is determined by the reference clock. For example, receiving a reference
time with a frequency of 1Hz implies that the real frequency is equal to the number of
the counted oscillations in the reference time interval of 1*s*.

4.2.3   Sensor Readout

One of the most important steps in the data collection part is to retrieve an accurate
value of the studied environmental conditions, which will be attached by the data logger
to the measured frequency, cf. Label *3* in Figure 4.3. This pair of values represents the
effect of the environmental condition on the XO frequency at the measurement time
instant. The set of the collected pairs represent the big data, that describes the effects of
the studied conditions on the XOC.

Retrieving an accurate value out of the sensor readout is a critical factor for the
evaluation of the data in the model development part, see Section 4.3, and for the
precision of the compensation value in the model deployment part, see Section 4.4. For
this reason, the sensor readout has to be preprocessed before it can be taken on by the
compensation model. The preprocessing depends on the studied environmental condition
and on the deployed sensor. The following points illustrate the importance of this step.

The measured temperature or humidity values are not exactly the same values the
XO is exposed to. The XO lies usually in a sealed up housing. This implies that the real
variation in the temperature or humidity value does not instantly follow the measured one.
To be able to consider this fact in the method, the readout of a temperature or a humidity
sensor needs additional filtering to dampen the measured variations. Interpreting the
measured variations as noise, that has to be flattened to obtain smoother stepping in
the measured values, demands the application of data smoothing techniques. There
exists a wide range of techniques, see [38], [39] and [40]. Hence, the application of a cer-
tain smoothing technique is implementation specific and depends on the observed readout.

The same technique can be used for another problem. Analog sensors transform the
sensed value into a voltage or a current, which might include imprecisions. Hence, the
readout of an analog sensor requires an additional processing or filtering to flatten the
fluctuations in the measured values. Interpreting the outliers of the analog sensor readout
as noise allows to apply a data smoothing technique. To exclude this kind of imprecision,
digital sensors post process the analog sensor readout before delivering it as a digital
value. Section 2.2 provides a discussion about sensor types.

Another important issue is the dependency of sensors on some environmental conditions. The developed compensation model has to be aware of such dependencies. This is illustrated by bringing up the temperature dependency of pressure sensors. H. Dudaicevs et al. [41] discussed this problem on an analog pressure sensor. The observed measurement error after two experiments with a temperature difference of $+100\,°C$ amounts to a maximum of $\pm200ppm$. It has to be kept in mind that the discussed absolute pressure sensor was developed specially for the measurements in the automotive domain to have a low temperature dependency. The temperature operation range in this domain is from $-40\,°C$ to $+125\,°C$. This result implies that general purpose sensors may have a bigger measurement error. Nevertheless, high measurement errors are related to the wide temperature range where extreme values cause higher errors.

4.2.4   Reference Time

In order to calculate the real XO frequency out of the counted oscillations, a reference clock is required, cf. Label *4* in Figure 4.3. The reference clock should provide a very accurate timing signal. This can be reached by using an atomic clock or a GPS-receiver. Most commercial GPS-receivers provide a PPS, see Section 2.1.2, with a jitter less than $50ns$, i.e. a frequency tolerance less than $0.05ppm$. This PPS represents the most accurate time reference that can be reached with commonly available hardware.

4.2.5   Output Data

The system measures the XO frequency and attaches it to the value of the environmental conditions at every time pulse from the reference clock, cf. Label *5* in Figure 4.3. This set of values represents the captured knowledge about the XO behavior in the presence of the conditions at the measurement time instance.

To keep the compensation algorithm general and independent from the deployed XO, the frequency deviation is used instead of measured frequency. It will be treated as an absolute value in *ppm* and not as a relative one in Hz. For instance, consider a frequency measurement of 16 002Hz of a XO with a nominal frequency of 16kHz. It exhibits a relative deviation of 2Hz from the nominal frequency and an absolute deviation of 125*ppm*, that is used in the model instead of the 2Hz.

The outcome of each experiment is a sequence of tuples ⟨*frequency deviation, sensor readouts*⟩. The set of sequences, as an outcome of the complete experiments of some environmental condition, forms a compensation model for that particular condition. The compensation models of the individual environmental conditions represent the bricks to build the XO specific compensation model, cf. the following section.

4.3 The Compensation Model

This part is concerned with the evaluation of the collected data. The output of the previous step contains the dependency of the XO frequency on the studied environmental conditions. This dependency is represented as a set of sequences of pairs of values. The developed compensation model is implemented afterwards on the hardware. Few points have to be considered while analyzing the raw data in order to develop the compensation model.

There exists no precise physical model of the quartz and the dependency of the sensors on the environmental conditions additionally falsifies the physical model. For this reason, the method applies a machine learning technique to develop a compensation model, which functions as an implicit quartz model. The selection of the machine learning technique influences the computational cost of the system. Techniques such as neural networks with an online calculation of the compensation values have higher computational cost than linear regression with an offline calculation, see Section 4.4.2. The selection of the machine learning technique is one of the decisions to be taken during the implementation phase. A reasoned selection allows this approach to fit in the main application fields of distributed real-time systems regarding the computational cost and the resource consumption.

The temperature is considered as one of the most important conditions when studying the effects of environmental conditions on XOCs. Most manufacturers of XOs provide the frequency deviation of their product in relation to the temperature. This is done by stating the maximum deviation or by describing the behavior of the frequency in the temperature operation range. Small variations in the temperature have clearly visible effects on the short-term frequency stability, i.e. it is observable in seconds to minutes. Additionally, the temperature has effects on the long-term frequency stability and the aging phenomenon [24].

The output of the first part does not necessarily reflect the dependency of the XO frequency on the studied environmental condition only. Potential dependencies between different conditions have to be kept in mind. The joint effect of two or more environmental conditions can not be completely separated unless these conditions are statistically independent. At this point, its important to outline the non linear interdependence between temperature, humidity and air pressure [11].

In the compensation model, this joint effect is not covered by trying to completely separate the individual effects, but by considering it in the compensation in spite of the mathematical or physical relation behind it. During the data collection part, the values of all other environmental conditions are kept constant while studying the effect of a certain condition. Subsection 5.3.1 provides some examples from the data collection part.

4.3.1 Offline Learning

The offline learning refers to the process of the evaluation of the collected data and the development of the compensation model. The purpose of the model is to relate the variation of the environmental conditions to the variation of the XO frequency. Hence, the compensation model is the mathematical representation of the XO dependency on the environmental conditions. The compensation model is built up from the collected data in the previous part, see Figure 4.4.
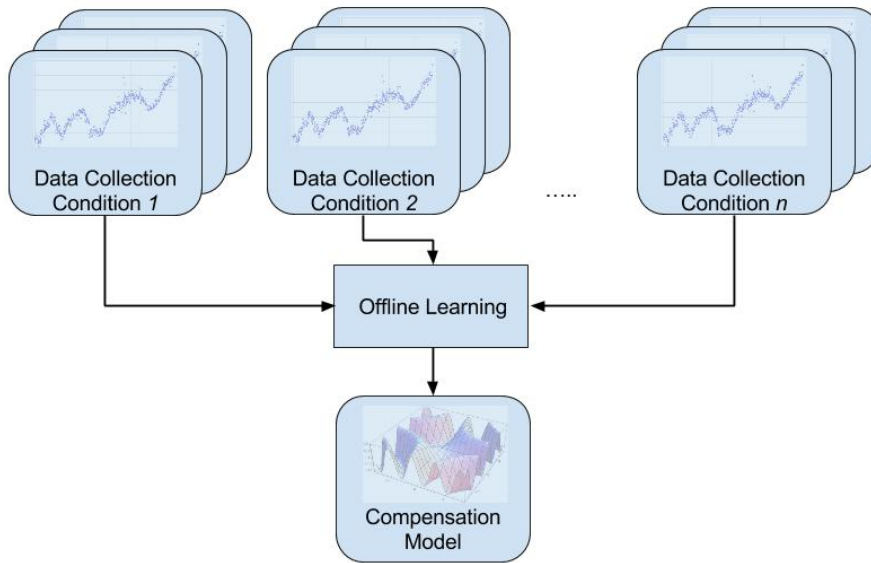
Figure 4.4: Building The Compensation Model

In the first step, the aim is to build a mathematical model based on already observed behavior. After that, the model is used to predict the XO behavior. When both steps are successfully complete, it can be said that a model is found for the system. The compensation model depends on the used modeling technique, which, in turn, depends on the observations made in the data collection part.

Data-fitting techniques, such as linear and nonlinear regression, are appropriate if direct dependencies were observable, i.e. when changing the value of the environmental condition causes a significant and reproducible variation in the XO frequency. Section 2.4 introduces the regression analysis as a form of machine learning. In this case, the dependencies are given in form of mathematical functions and the compensation model has to solve the individual functions and to combine the solutions to obtain a correction value for the XOC counter. In the simplest case, when considering only one environmental condition x, the compensation model has to solve the function $y = f(x)$, where y is the frequency deviation caused by x.

If no obvious dependencies could be established, dynamic models are more appropriate because they allow the model to consider the past behavior in the current and future prediction. An example for modeling techniques that produce dynamic models are neural networks and system identification. Lennart Ljung [42] introduced the theory behind the system identification. This technique is more sophisticated and requires ideally a specific data collection part, the *identification experiment*. The special design of the experiment is destined to differentiate between models of the *model structure*, the set of candidate models. The last step is to determine the *best* model candidate in the model structure, which will be the compensation model.

Motivated by the computation art of the human brain, S. Haykin [35] provided an excellent reference to neural networks. A neural network is a "*machine that is designed to model the way in which the brain performs a particular task or function of interest*". The Artificial Neural Network (ANN) technique was already applied by J. Esterline [34] to compensate the effects of the environmental temperature on XOs, see Subsection 3.2.2. The model here is composed of a number of processing units, the neurons. No explicit equation is needed to solve the problem. The model, the ANN, should learn from the collected data before it can output the anticipated deviation correction.

The choice of which model is to be used depends on many factors, such as the number of environmental conditions, the observations during the data collection part and the complexity of the model or the hardware target itself. The modeling technique that can be used in this approach is not limited to the introduced ones in this discussion.

4.3.2 Online Learning

The time signal is generated simply from the accurate reference clock if it is available. The aim of online learning is to use the reference time for correcting the model when the differences between the generated and the reference time signal become significant over a period of time.

Consider the case where at every time instant from the reference clock a time gap of $t \pm \delta t$ between the reference time and the calculated time occurs. The system can recognize this when it happens often enough and apply it as an additional correction value to improve the correction of the XOC counter. This difference t between the calculated time and the reference time represents an additional knowledge about the frequency deviation of the XO. For instance, a difference of $t = 0.01 \mu s$ every PPS leads to a deviation of $1ms$ between the local and the reference time signal in 27.7 hours.

The first cause of the time difference t are imprecisions in the model compensation values. This can be improved by averaging the value of t over time and considering it in the calculation of the XOC counter correction value. The other cause is the alteration of the XO behavior. This is known as *quartz aging*, which is of great interest for the long-term application of XOs and hence for the application of this method in turn. Wang

et al. [43] studied and listed two aging models to predict the frequency deviation of XOs, the *Arrhenius* and the *Mattuschka* models. Although it is difficult to have a general rule for predicting the behavior of the quartz [24], some basic mathematical concepts are introduced, which ease the extension of the compensation model by recognizing and correcting the aging phenomenon.

This is illustrated by the following example: Consider the effects of the aging phenomenon on the temperature-frequency dependency curve. In particular on XOs that have a temperature-frequency dependency curve that can be effectively modeled by a quadratic function, i.e. a parabola:

$$f(x) = a * (x - h)^2 + k \qquad (4.1)$$

where x is the current temperature in $^\circ$C, $f(x)$ is the frequency deviation in *ppm* and h and k represent the coordinations (h, k) of the vertex.

To compensate the aging phenomenon the system needs to recognize how this affects the dependency of the quartz. For this reason, the plane is divided into four quadrants. This requires a though-out choice of the dividing lines. In the following, the theory will be demonstrated by choosing the lines going through the vertex and through the focus of the parabola. Figure 4.5 illustrates a possibility to do this:

- The vertex line is defined by the equation $x = h$.

- The focus line is defined by the equation $f(x) = p$.

- Both lines form the four quadrants represented by the set of points X_i, X_l, X_k and X_j, respectively.

Furthermore, let d represent the difference between the calculated frequency and the frequency determined by the reference time at some time instant of the reference clock. Consider the following definitions:

- $d_{x_i}, d_{x_l}, d_{x_k}$ and d_{x_j} represent the difference described above for individual points in the plane according to their positions in the defined quadrants. Each point corresponds to a pair $(^\circ C, ppm)$ at some time instant of the reference clock.

- $d_{\overline{x}_i}, d_{\overline{x}_l}, d_{\overline{x}_k}$ and $d_{\overline{x}_j}$ represent the averaged respective difference over a period of time.
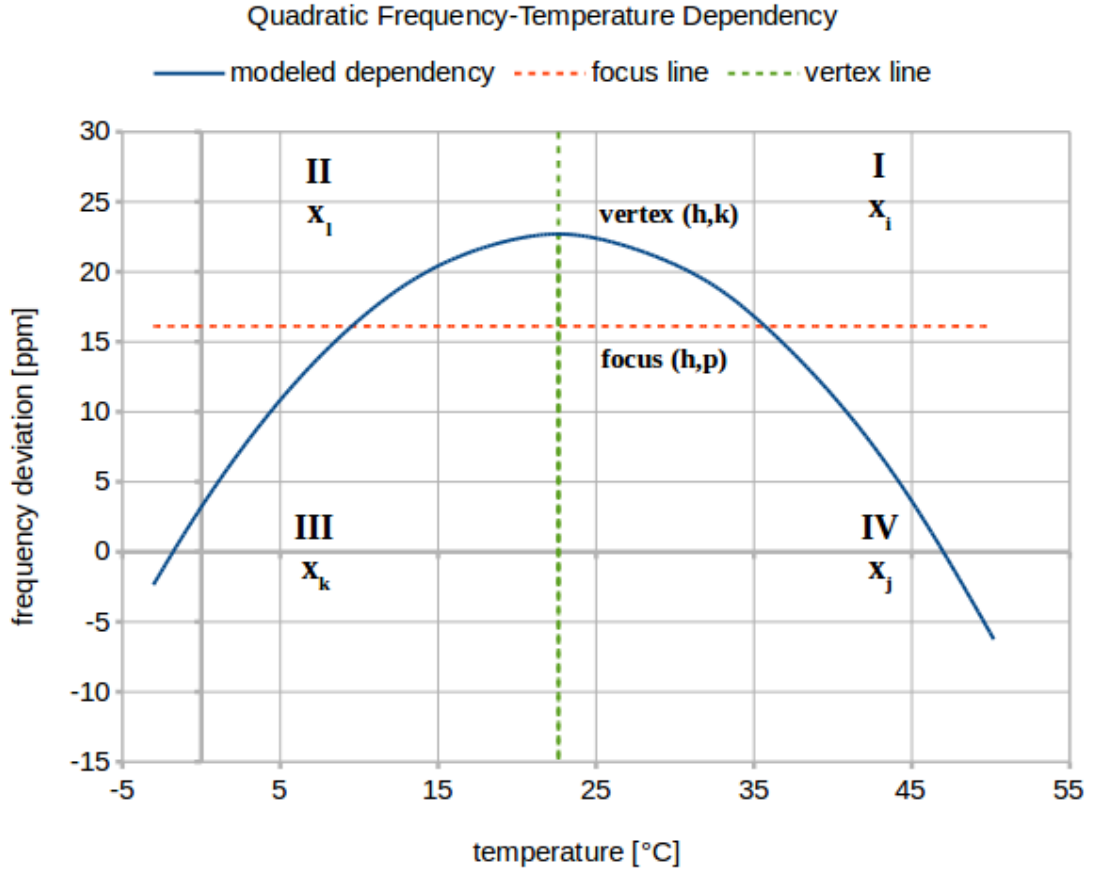
Figure 4.5: Basic Concepts to Detect the Quartz Aging

Regarding the introduced basic concepts the system can differentiate the following cases based on its observations over a period of time [1]:

1. **Horizontal Shifting**: The following condition 4.2 implies that the modeled dependency has to be shifted horizontally:

$$d_{\bar{x}_l} + d_{\bar{x}_k} = -(d_{\bar{x}_i} + d_{\bar{x}_j})$$ (4.2)

   The direction of the shifting operation is given by the following conditions:

$$d_{\bar{x}_l} + d_{\bar{x}_k} > 0 \quad (4.3) \qquad\qquad d_{\bar{x}_l} + d_{\bar{x}_k} < 0 \quad (4.4)$$

   Left shifting, i.e. decreasing h, is given by Condition 4.3 whereas right shifting, i.e. increasing h, is given by Condition 4.4. Figure 4.6 illustrates the horizontal shifting, in red, of the modeled dependency.

---

[1]The four quadrants are also shifted in the horizontal and vertical shifting cases. Only the original quadrants are depicted in the figures to keep them simple.
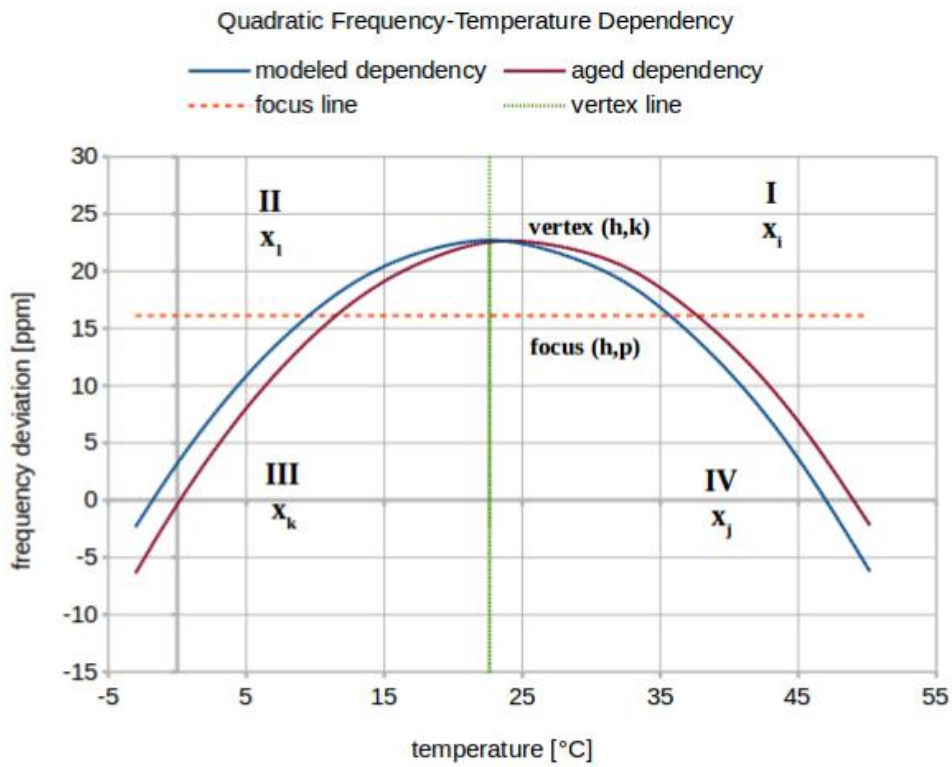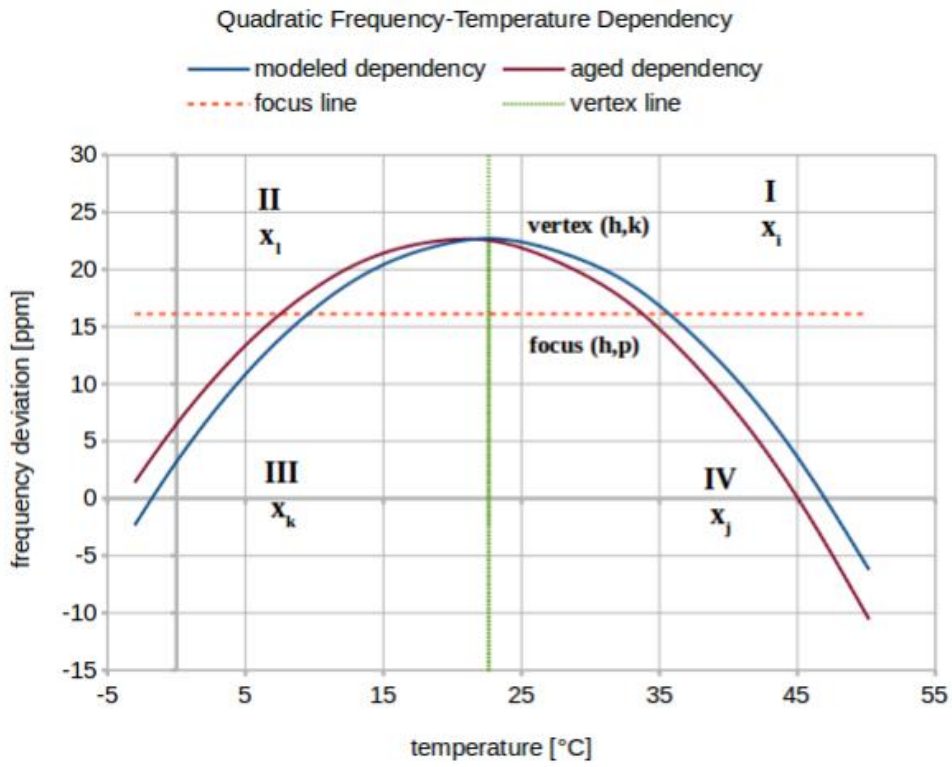
Figure 4.6: Horizontal Shifting

2. **Vertical Shifting**: The following condition 4.5 implies that the modeled dependency has to be shifted vertically:

$$d_{\overline{x}_l} = d_{\overline{x}_k} = d_{\overline{x}_i} = d_{\overline{x}_j} \tag{4.5}$$

The direction of the shifting operation is given by the following conditions:

$$d_{\overline{x}_l} > 0 \tag{4.6} \qquad\qquad d_{\overline{x}_l} < 0 \tag{4.7}$$

Shifting up the modeled dependency, i.e. increasing k, is given by Condition 4.6 whereas shifting it down, i.e. decreasing k, is given by Condition 4.7.

3. **Degree of Opening**: The following conditions 4.8 imply that the parabola has to become broader, i.e. increase a where a is in range -1 to $+1$:

$$d_{\overline{x}_k} = d_{\overline{x}_j}, \; d_{\overline{x}_k} > 0 \text{ and } d_{\overline{x}_k} + d_{\overline{x}_j} \gg d_{\overline{x}_l} + d_{\overline{x}_i} \tag{4.8}$$

If the parabola has to become steep, i.e. decrease a where $a < -1$ or $a > 1$, the following conditions 4.9 will be true:

$$d_{\overline{x}_k} = d_{\overline{x}_j}, \; d_{\overline{x}_k} < 0 \text{ and } d_{\overline{x}_k} + d_{\overline{x}_j} \ll d_{\overline{x}_l} + d_{\overline{x}_i} \tag{4.9}$$

4.4 Model Deployment

After evaluating the collected data, the developed compensation model is installed on the system in order to compensate the effects of the studied environmental conditions. Figure 4.7 illustrates the abstract hardware setup needed while running the system and the model [2].

Figure 4.7: Hardware Setup of the Model Deployment Part

---

[2]Figure 4.7 is the same figure introduced in the overview section with additional labels, cf. Figure 4.1.

4.4.1 Sensor Readout

The current values of the measurable environmental conditions are used as an input for the compensation model, cf. Label *1* and Label *2* in Figure 4.7. A precise value is important as in the data collection part. The same considerations are also applicable in this part, see Section 4.2.3.

4.4.2 Calculating the Correction Value

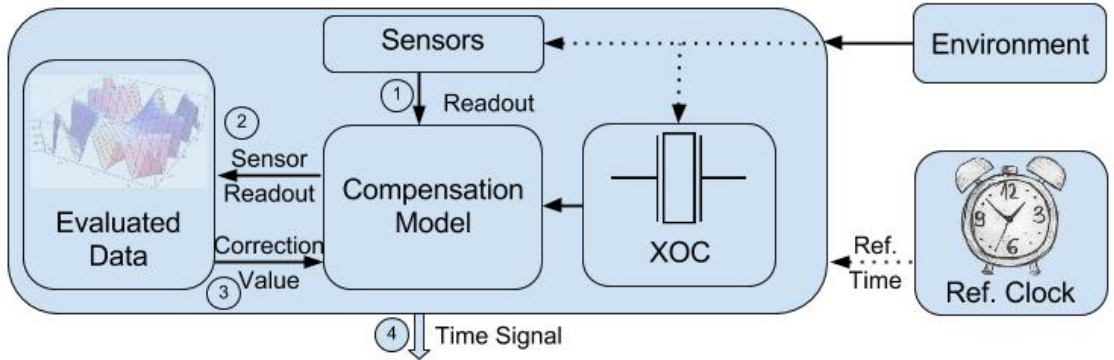The compensation model, that is developed in the second part, see Section 4.3, calculates a correction value for the XOC counter depending on the collected data in the first part, see Section 4.2. The output of the individual compensation models is a compensation value in *ppm* for the effect of the respective environmental condition. The correction value of the XOC counter is calculated by considering the compensation values of the individual environmental conditions, cf. Label *3* in Figure 4.7. The system, depending on the nominal frequency of the XO, converts it to a correction value in Hz. For instance, a compensation model output of 150*ppm* for a XO with a nominal frequency of 16kHz at some time instance corresponds to a XOC counter correction value of 2.4Hz.

The model calculates for each environmental condition and for each value in the respective operation range a compensation value in *ppm*. According to the number of studied conditions, the chosen model representation and the complexity of the developed model, two possibilities can be differentiated to realize the calculation of the compensation values:

- **Offline Calculation**: The continuous calculation is sampled and an interpolation technique is applied. This approach requires low computational power but it has a high memory consumption.

- **Online Calculation**: The calculation is implemented on the target hardware as is. This implies less memory consumption but a higher computational power in comparison with the previous approach.

4.4.3 Time Signal Generation

The compensation model is developed based on the observations in the data collection part in the presence of the reference time. It predicts the frequency deviation caused by the environmental conditions and corrects the XOC counter, cf. Label *4* in Figure 4.7. The XOC counter correction value is calculated by combining the compensation values of the individual environmental conditions.

In the model deployment part, the system operates without the need to the reference time and generates its own time signal as an outcome of the XOC counter correction. One of the possibilities is to output a time signal with a frequency of 1Hz, i.e. a PPS. If the reference time is not available, the system generates the time signal based on the

described method. Otherwise, if it is available, the time signal of the system is simply determined by the reference time. The model runs all the time in both cases. The system can improve the precision of the compensation model by implementing an online learning technique, see Section 4.3.2.

4.5 Compensation Algorithm

This section summarizes the abstract steps needed to perform the compensation. The structuring of the developed method is followed to group the steps.

4.5.1 Data Collection

1. Determine the operation range of the environmental condition and its coverage set: The environmental condition describes a physical property of the system and it is hence continuous. This continuous range is covered by a finite set of values, the *coverage set*. For instance, an operation range of $1000 \pm 70 mbar$ for air pressure can be covered by the set: $x_n = x_{n-1} + 20$, where $x_0 = 930, n = \{1, 2, .., 7\}$.

2. Each value of the coverage set will function as a setpoint for the corresponding control loop for a period of time. This period depends on the environmental condition itself. For instance, the temperature value has to stabilize before obtaining correct data for the current setpoint, see Subsection 5.2.2.1, whereas the effect of acceleration or vibration can be instantly observed.

3. The data is collected for each environmental condition and for each value in its coverage set.

4. Additionally, data is collected while tracing the continuous operation range from its minimum to its maximum, and vice versa. This data can contain additional information for the compensation model or can be used to test the model in its development phase, i.e. as verification data.

4.5.2 The Compensation Model

1. Combining the different runs of data collection for each environmental condition results in a compensation model for each condition.

2. Based on the observations made during the first part, an appropriate modeling technique is chosen.

3. The XO specific compensation model is developed based on the set of the compensation models of the studied environmental conditions.

4. The model is tested on the verification data and refined, if needed. Afterwards, the model is ready to be implemented on the target hardware.

4.5.3 Model Deployment

1. Based on the chosen modeling technique, an online and an offline calculation are possible. The implementation is hardware specific.

2. After testing the model implementation on the target, initial tests are needed to obtain feedback about the behavior of the model. The test can be also similar to the experiments in the data collection part.

3. The feedback from the initial tests is used to enhance the model. An online learning technique can be implemented afterwards to improve the model precision.

The replacement of the XO or the consideration of more than one XO at the same time is possible with minimal effort, cf. Requirement *R1* in Subsection 3.1.1. Furthermore, the method deals with more than one environmental condition. Extending the model, i.e. adding, removing or updating one or more environmental condition, affects only the respective data collection part, cf. Requirement *R2* in Subsection 3.1.2.
The complexity of studying the joint effect of environmental conditions grows with the number of the considered conditions. The modular structure of the method qualifies it to deal with that complexity. The designer is free to outline or to ignore various dependencies in the implementation phase, cf. Requirement *R3* in Subsection 3.1.3.

The output of the described method above is a system performing the compensation steps and generating a time signal in the absence of the reference time. Additionally, the system is able to learn and to enhance its performance by applying one of the discussed techniques in Subsection 4.3.2.

CHAPTER 5

Implementation

In this chapter, the developed method in Chapter 4 is followed to implement the compensation algorithm for a Crystal Oscillator based Clock (XOC). The aim is to study the effects of the following conditions on the behavior of the Quartz Crystal Oscillator (XO): Temperature, humidity, acceleration and air pressure. The first section describes in detail the used hardware setup. Afterwards, the implementation of the developed method is introduced. The same structuring of the previous chapter in the three main parts is followed.

5.1 Hardware Setup

A custom hardware reduces the versatility of the method and increases the costs for the following production. For this reason, commonly used hardware was in focus, cf. Requirement *R1* in Subsection 3.1.1. This requirement is valid for the hardware setup that implements the compensation algorithm, i.e. for the processing unit, on which the algorithm runs, and the sensors. On the contrary, the processing unit that controls the environmental conditions with the aid of its own sensors and actuators should have the best possible technology in order to obtain precise parameters for the compensation model.

As proposed in the data collection part, see Section 4.2, there are two tasks to be supported by the hardware design:

- **Main Task:** Collect data, implement the model and run the compensation algorithm. This represents the *Final Product* of the implemented method. Section 5.1.1 introduces the hardware setup for this task.

- **Subsidiary Task:** Control the environmental conditions. This is necessary in the development phase to study the behavior of the XO under the effects of the environmental conditions in order to obtain the parameters of the compensation model. Section 5.1.2 introduces the hardware setup for this task.

5.1.1 The Main Controller

This section proposes the hardware setup, that is needed to implement the main task. i.e the CPU and its sensors.

5.1.1.1 The CPU

Conventional microcontrollers are deployed as control and processing units. Microcontrollers are designed to be applied in embedded systems, such as in the automotive control systems or in medical devices.

The micorcontroller that performs the main task is referred to as the *main controller*. Beside being a commonly used micorcontroller, the main controller has to have at least one external XO. The following XO characteristics should be available: The nominal frequency, the temperature operation range and the frequency tolerance at some temperature and in the specified operation range. The latter is a first indication on the extent of the XO frequency deviation in the temperature operation range. Additionally, it may give a rough idea about the behavior of the XO depending on its unit. For instance, a value with the physical unit $[ppm/\,^{\circ}\mathrm{C}\,^2]$ implies a quadratic deviation of frequency in relation to temperature variation.

The main controller has to have enough peripherals to connect the sensors and the communication modules. Preferably, it contains most of this on one Printed Circuit Board (PCB). As a consequence, a flight controller is deployed. Flight controllers have a compact PCB design with a 16- or 32-bit chip. Additionally, they have enough connectors for the sensors and actuators that are needed for their operation such as an accelerometer, a thermometer and a pressure sensor.

The Smart Autopilot (SmartAP) 2.0 [44] depicted in Figure 5.1 satisfies the above-mentioned requirements. It has the following relevant specifications:

- **XO:** There are two external XOs on the PCB. The Low Speed External Quartz (LSEQ) *KX-38* [45] and the High Speed External Quartz (HSEQ) *KX-KT* [46] with the following characteristics:

	LSEQ	HSEQ
Nominal frequency	32.768kHz	8MHz
Temperature operation range $[\,^{\circ}\mathrm{C}\,]$	-20 to $+70$	-40 to $+85$
Frequency tolerance at 25 $^{\circ}$C $[ppm]$	±20	±10 to ±50
Frequency tolerance in the operation range	$-0.042\ [ppm/\,^{\circ}\mathrm{C}\,^2]$	±25 to $\pm100\ [ppm]$

Table 5.1: LSEQ and HSEQ Specifications

- **Chip:** *ARM Cortex M4* microcontroller with a floating point unit (FPU) [47].

50

- **On-Chip Sensors:** An Inertial Measurement Unit (IMU) [48] and a pressure sensor [49].

- **Additional Extension Connectors:** The connectors are used to integrate a temperature and humidity sensor, a wireless communication module and the Global Positioning System (GPS) receiver.
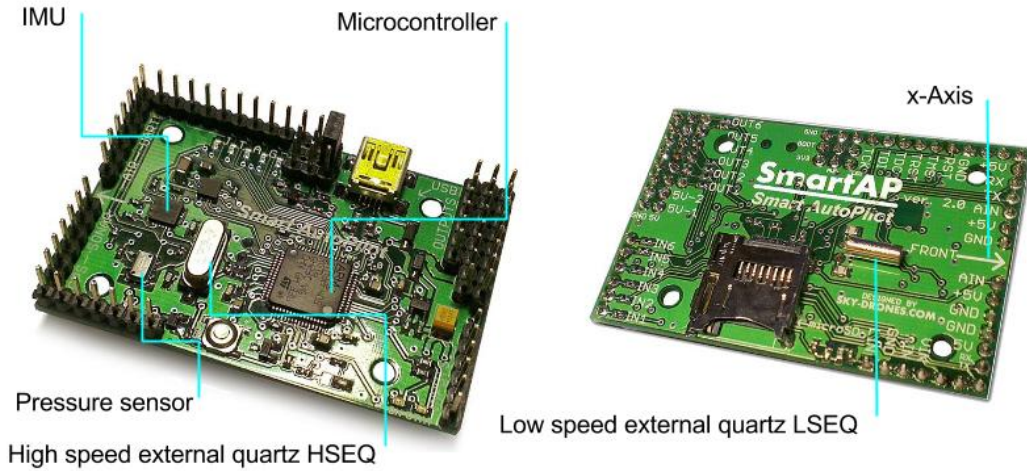
Figure 5.1: The SmartAP 2.0

In order to demonstrate the fulfillment of Requirement *R1*, see Subsection 3.1.1, the method is applied on the two XOs of the main controller. The following differences can be observed beforehand from the specifications in Table 5.1:

- **Real Frequency:** The LSEQ has a frequency tolerance of $\pm 20ppm$ at $25\,^{\circ}\mathrm{C}$. Hence, its real frequency resides in the range 32.768kHz ± 0.65536Hz. The HSEQ has a higher frequency tolerance. Its real frequency lies in the range 8MHz ± 400Hz. Higher deviations in the frequency of the HSEQ are expected to be observed in the experiment phase.

- **Temperature Dependency:** The LSEQ temperature dependency is expressed in $[ppm/\,^{\circ}\mathrm{C}^{2}]$. Hence, the deviation of the LSEQ frequency is quadratic in relation to the temperature variation. On the other hand, the specification of the HSEQ gives no information about its behavior in the temperature operation range.

The system clock of the main controller is configured by default to be based on the HSEQ. The main controller has a Phase Lock Loop (PLL) that generates a signal with 84MHz frequency as system frequency out of the HSEQ frequency. To measure the frequency of the HSEQ a timer on the main controller is configured, that has the same frequency of the system clock. The timer value, i.e. the number of ticks that the timer has counted, corresponds to the number of the HSEQ oscillations and indicates its real

frequency. On each timing signal from the reference clock the timer value is captured and reset. For instance, if the timing signal has a frequency of 1Hz, the HSEQ real frequency is equal to the timer value.

The consequence of using the internal PLL on the measurement comes up when the timer delivers a value of approx. $84 \cdot 10^6$ ticks instead of $8 \cdot 10^6$. The PLL will not affect the accuracy of the frequency measurement. The design of the PLL and the fact that the PLL is locked to the input of the HSEQ strengthen this assumption. From now on, the nominal frequency of the HSEQ refers to 84MHz and not 8MHz.

The measurement of the LSEQ frequency is done by configuring another timer to count the oscillations of the LSEQ in the period time of the reference time signal. The main controller was equipped with the LSEQ as a clock source for the Real-Time Clock (RTC). Hence, the real frequency is measured directly without any components in between such as a PLL.

The main controller needs the reference clock mainly for the time signal generation in the data collection part and for implementing an online learning technique in the model deployment part. For this purpose, a GPS-receiver [50] is used as a reference clock. The sole requirement on the GPS-receiver is to provide the Pulse Per Second (PPS) in form of pulses to an external pin. By doing this, the main controller can react directly to the time pulse as an external interrupt without the need to retrieve and decode the GPS-messages over a serial interface. Therefore, the main controller reacts faster since it is interested solely in the PPS and not in the current time, position or number of seen satellites.

The main controller and its additional hardware are deployed in a sealed chamber to perform the experiments. The sensed and calculated data are transmitted to a computer where the data analysis and the model development are done. Therefore, the connection between the computer and the main controller is realized by a bluetooth-transceiver [51], that transmits the data wirelessly in real-time to another bluetooth-transceiver [52] on the computer side.

5.1.1.2 Sensors

The main controller is shipped with the following sensors: An IMU, a magnetometer and a digital pressure sensor. It is expanded by a temperature and a humidity sensor. Table 5.2 lists the used sensors.

5.1.2 Experiments Chamber

The hardware setup, that is required to perform the experiments and to realize the variation of the environmental conditions, is introduced in this section. This includes the CPU with its sensors and actuators and the chamber itself.

5.1.2.1 The CPU

The subsidiary task, i.e. implementing the control loops of the environmental conditions, is performed by the *external controller*. The label *external* reflects the fact that this microcontroller is not involved in implementing and running the compensation model.

The application of this microcontroller allows to specify and follow curves of the different environmental conditions and a combination of them, i.e. a set point for the control loops which is variable in value and time.

The main requirement on the external controller is to have enough free connectors to interface the sensors and actuators needed for the control loops. There exists a plenty of development boards that satisfy this requirement. The STM32 Nucleo development board [53] depicted in Figure 5.2 is shipped with a chip [54] of the same family of the main controller chip and is deployed as the external controller in order to reduce the programming effort.
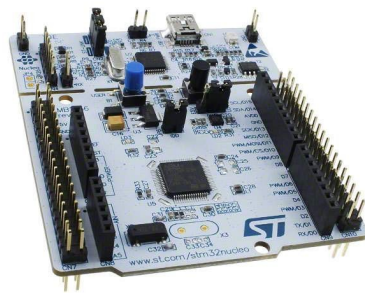
Figure 5.2: The STM32 Nucleo Development Board

5.1.2.2 Sensors

The external controller is equipped with another set of sensors to implement the individual control loops. Table 5.2 lists the used sensors:

	Used by	Sensor Type and Interface
Temperature and Humidity Sensor [55]	*M, E*	Digital, I^2C-alike interface
Pressure Sensor [49]	*M*	Digital, I^2C-interface
Accelerometer [48]	*M*	Digital, I^2C-interface
Pressure Sensor [56]	*E*	Analog, *ADC*-interface

Table 5.2: Sensors used by the Main Controller, *M*, and the External Controller, *E*

5.1.2.3   Actuators

Since the task of the external controller is to implement the control loops to simulate the variation of the environmental conditions, all actuators are connected to it. In the following the deployed hardware is introduced.

Temperature

To cover the largest possible temperature range, the environment of the main controller and its hardware is heated and cooled. This is done by deploying a Thermoelectric Cooler (TEC) [57]. Based on the direction of the current, the TEC heats one side of it and cools the other one. This effect is known as the *Peltier Effect*, which is named after the physicist *Jean Peltier*. An operation range of $-10\,°C$ to $+60\,°C$ is achievable inside the experiments chamber depending on the room temperature outside the chamber.

Humidity

A desktop humidifier is deployed in order to increase the humidity. Connecting the humidifier to the external controller allows to control the duration and the intensity of the released moisture. This setup permits to control the humidity in the increasing direction only, i.e. from the current room relative humidity up to approximately 100%. Nevertheless, the desktop humidifier is used because no obvious effect was expected on the XO frequency in both directions. Keeping the simple design and avoiding high setup costs are additional reasons for this design decision.

Acceleration

To simulate the acceleration effect on the XO, the main controller and its hardware are placed on a round plastic plate. The plate has a hole in the middle, which fits to mount the shaft of a stepper motor. The stepper motor operates as follows: The position of the shaft is controlled by a sequence of pulses. The rotation frequency of the shaft is hence given by the frequency of pulse generation, that is controlled by the external controller.

This constellation allows to save an accelerometer on the external controller, cf. Table 5.2. The reason behind that is the synchronicity of stepper motors, which makes it possible to use an open loop control system without a feedback to the controller. In this case, the weight load on the plate should fit to the rotor inertia.
To maintain the simplicity of the software design and to obtain a subtler rotation, a motor driver is deployed between the external controller and the stepper motor [58].

As depicted on Figure 5.1, the direction of the arrow is defined as the direction of the x-axis. Changing the direction of the acceleration may result in a different frequency deviation. The acceleration effect is studied in both directions by changing the placement of the PCB on the plastic plate.

Pressure

Sealing the chamber airtight makes pressure experiments possible. The external controller

is interfacing an air pump, which is airtight attached with two tubes to the chamber. The air pump has two culverts for overpressure- and vacuum-directions. This setup allows the simulation of pressure variation in the range $1000 \pm 150 mbar$.

5.1.2.4   The Chamber

The design of the chamber depicted in Figure 5.3 should allow to perform experiments on the environmental conditions. Hence, it should be temperature- and air-proof at least in the respective operation range. To performe the acceleration experiments, it is necessary to equip the main controller and its hardware with a battery as a power source since no fixed connection is possible during the rotation of the plate. The GPS-receiver is located outside the chamber where a better signal reception is guaranteed. Therefore, a sliding contact is needed to enable the main controller to obtain the PPS from the GPS-receiver.

Figure 5.4 and Figure 5.5 illustrate the setup of the hardware. The main controller has an extension board, the *M-extension board*, where the additional hardware is located. The temperature and humidity sensor, the bluetooth module and the connectors to the GPS-receiver are placed on the M-extension board. On the other hand, the external controller has two such boards, the *E-extension boards*. The first one is inside the chamber where the temperature and humidity sensor is placed on. The second one is outside the chamber where the pressure sensor, the actuators and the auxiliary circuits are located.

This hardware setup makes it possible to simulate individual or joint variations of the temperature, humidity, acceleration and pressure in the respective operation range. The frequency deviation of the two external XOs of the main controller is measured and related to the current environmental conditions. Finally, the pinout of the hardware setup, i.e. the main controller, the external controller and their hardware are depicted in Figure A.1 and Figure A.2.
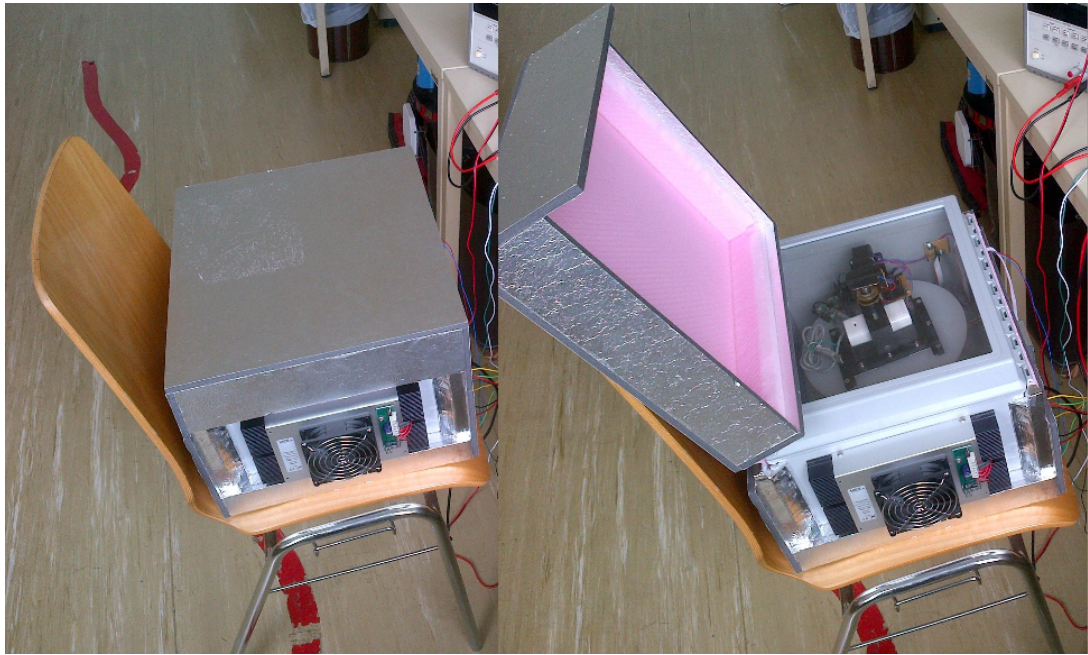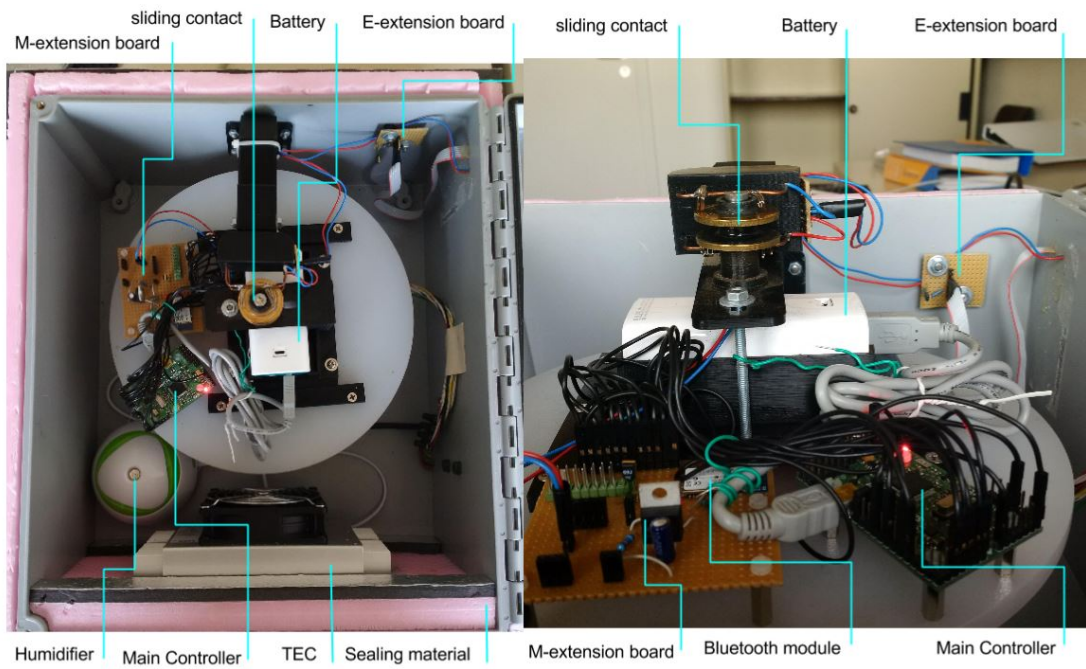
Figure 5.3: The Experiments Chamber

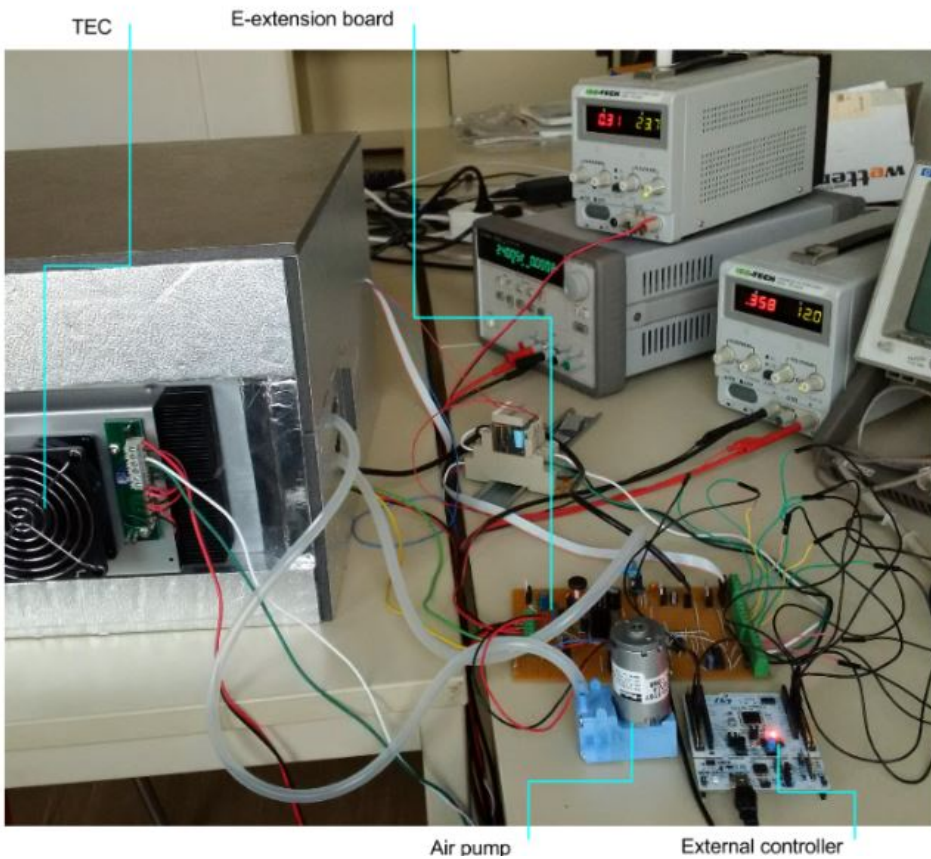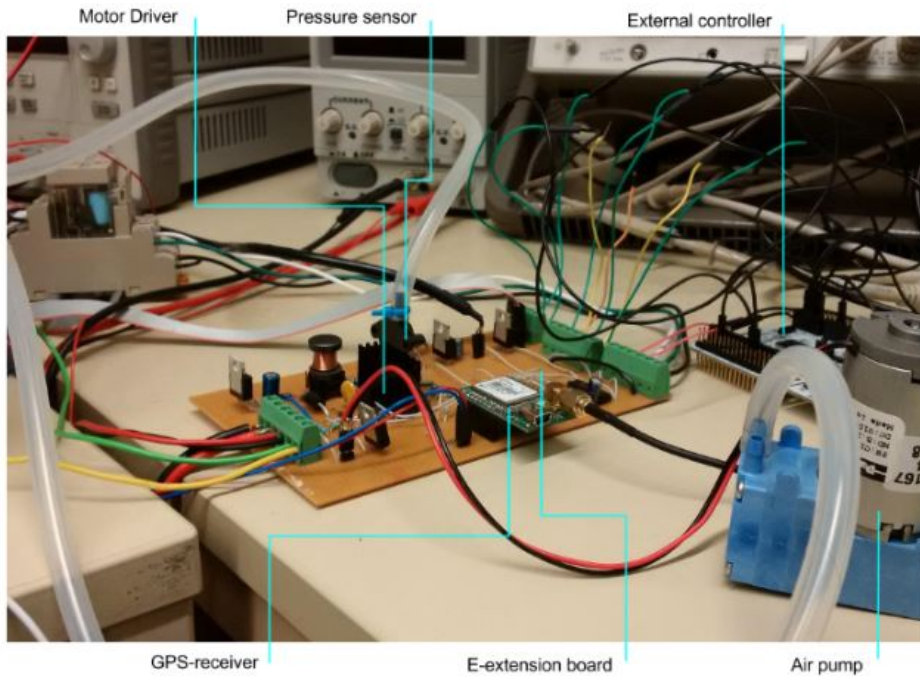Figure 5.4: Hardware Setup of the Main Controller

Figure 5.5: Hardware Setup of the External Controller

5.2   Data Collection

The data collection part is the most critical part in this approach. The efficiency of the compensation model relies on the accuracy of the collected data, no matter which modeling technique was chosen. In the course of this section, the processing of the sensor readout by the main controller is introduced first, as this belongs to the main task. The implementation of the control loops by the external controller is introduced afterwards as a part of the experiments chamber.

5.2.1   Main Task

In this section the processing of the sensor readout is discussed. First, the focus will be on the main controller. It performs the processing in order to obtain more accurate values of the environmental conditions. This is critical in the data collection part and while developing and testing the XO compensation model. Nevertheless, the external controller also processes the readout from its sensors. This is introduced at the end of this section.

5.2.1.1   Processing the Temperature Readout

The temperature and humidity sensor is not placed on the same PCB where the two XOs are. Despite the fact that the chamber is designed to be airtight and temperature proof in the respective operation range, the measured temperature and humidity do not exactly meet the ones of the XOs. The solution is to implement a software filter to smoothen those variations in the measurements which are faster than the possible reaction time of the quartz. This filter is deployed while evaluating the readout in the data collection part and while passing the value of the environmental condition to the compensation model to calculate the compensation value of the XO frequency deviation. Algorithm 5.1 illustrates the implementation of the temperature filter.

The algorithm is executed periodically every 1s and it implements a low-pass filter for the temperature values. Two constants determine to what extent the current quartz temperature is influenced by its current ambient temperature and its own temperature from the previous algorithm run. For instance, the equation:

$$\text{quartz temperature} \; = \; 0.9 \cdot \text{ambient temperature} \, + $$
$$0.1 \cdot \text{previous quartz temperature}$$

indicates that the current quartz temperature is influenced to 90% by the current ambient temperature and to 10% by the quartz temperature from the previous calculation. Decrementing the first and incrementing the second constant apply a stronger smoothing on the measured temperature. The two constants are required to sum up to 1, i.e. 100%. The algorithm also differentiates between two pairs of constants based on R, the temperature rate of change. A fast rate of change reduces the effect of the current ambient temperature and hence applies a stronger smoothing than a slow one. The values

58

of the calculation constants in Table 5.3 are determined experimentally based on the observations during the data collection part. This is done by applying the temperature compensation model using the filtered values and by comparing the compensation results of different pairs of constants with the compensation values using the unfiltered sensor readout.

The temperature filter is developed on the computer and applied on the collected data. It is implemented afterwards on the main controller, such that no offline processing of the data in the model deployment part is needed.

R [°C]	C_1	C_2	C_3	C_4
0.02	0.95	0.05	0.9	0.1

Table 5.3: Constants of the Temperature Filter

Algorithm 5.1: Temperature Filter

   Data: current temperature ct

   Result: calculate the quartz temperature qt

1 **Function** *temperatureFilter(ct)*

      /* local variables to be memorized */

2   qt: quartz temperature;

3   pqt: previous quartz temperature;

4   pt: previous temperature;

5   **if** *first run* **then**

6   assign the value of ct to qt, pqt and pt;

7   **else**

8   change rate $= |ct - pt|$;

9   **if** *change rate is not bigger than R* **then**

10            $qt = C_1 \cdot pqt + C_2 \cdot ct$;

11   **else**

12            $qt = C_3 \cdot pqt + C_4 \cdot ct$;

13     $pt = ct$;

14     $pqt = qt$;

15   **return** qt

16 **End**

5.2.1.2 Processing the Humidity Readout

The same procedure is followed while filtering the humidity value, see Algorithm 5.2. The humidity sensor delivers a temperature compensated relative humidity. The interesting physical quantity is the actual amount of water vapor in the air, i.e. the absolute humidity. For this reason, the sensor readout is converted from relative humidity in [%] to absolute humidity in [g/m^3]. The calculation is based on the application note provided by the

sensor manufacturer [59]. This is done by solving the following equation:

$$\underbrace{H_A}_{\text{absolute humidity}[g/m^3]} = C_4 \cdot \alpha \cdot \underbrace{H_R \cdot 10^{-2}}_{\text{relative humidity}[\%]} \cdot \overbrace{\exp\left((\beta * t)(\gamma + t)^{-1}\right)}^{\text{saturated vapor pressure}} \cdot (\underbrace{C_3 + t}_{\text{absolute temperature}[K]})^{-1}$$

The algorithm is executed every 1s and it filters the relative humidity from the sensor in the same way the temperature filter does. The rate of change is not considered by the algorithm because it is always slow in comparison with the temperature rate of change. The constants C_1 and C_2 of the filter are determined experimentally. The absolute humidity is calculated afterwards by solving the previous equation with the filtered relative humidity. The constants of the conversion equation are given in Table 1 on page 1 in the application note and in Table 5.4.

The humidity filtering and conversion are developed first on the computer, applied then on the collected data and implemented afterwards on the main controller.

C_1	C_2	C_3 [°C]	C_4	α[hPa]	β	γ [°C]
0.2	0.8	273.15	216.7	6.112	17.62	243.12

Table 5.4: Constants of the Humidity Filter

Algorithm 5.2: Humidity Filter

Data: current relative humidity crh and quartz temperature qt
Result: calculate the quartz absolute humidity qah

1 **Function** *humidityFilter(crh, qt)*
       /* local variables */
2   *pqrh*: previous quartz relative humidity to be memorized;
3   *qah*: quartz absolute humidity;
4   *qrh*: quartz relative humidity;
5   t_K: temperature in Kelvin [K];
6   *svp*: saturated vapor pressure;
       /* filter calculation */
7     $qrh = C_1 \cdot pqrh + C_2 \cdot crh$;
       /* absolute humidity calculation */
8     $t_K = qt + C_3$;
9     $svp = \alpha \cdot \exp\left((\beta \cdot t)(\gamma + t)^{-1}\right)$;
10     $qah = C_4 \cdot qrh[\%] \cdot svp \cdot t_K^{-1}$;
11     $pqrh = qrh$;
12   **return** qah
13 **End**

5.2.1.3   Processing the Pressure Readout

The external controller performs a readout processing for the pressure sensor. This is not done by the main controller because the digital pressure sensor performs a post processing of the measured value before delivering it to the main controller. The external controller is equipped with an analog pressure sensor, which delivers an analog voltage to the Analog to Digital Converter (ADC) of the external controller. It converts this voltage to a pressure value in accordance with the sensor data sheet.

The voltage output of the pressure sensor is noise sensitive due to the nature of the output signal. As a consequence, a big number of outliers in the sensor readout is observed in comparison to the digital sensor attached to the main controller. On the other hand, the measurement of the pressure is much faster on the analog sensor. It takes approx. $2\mu s$ to retrieve and convert one voltage measurement. To benefit from the fast A/D conversion, a filter is implemented to average the value of the last 500 measurements. Figure 5.6 and Figure 5.7 illustrate the difference between averaging 2 and 500 values while trying to maintain a pressure setpoint of $1040mbar$. The second figure shows that a hysteresis tolerance of $5mbar$ is reasonable for the control loop.
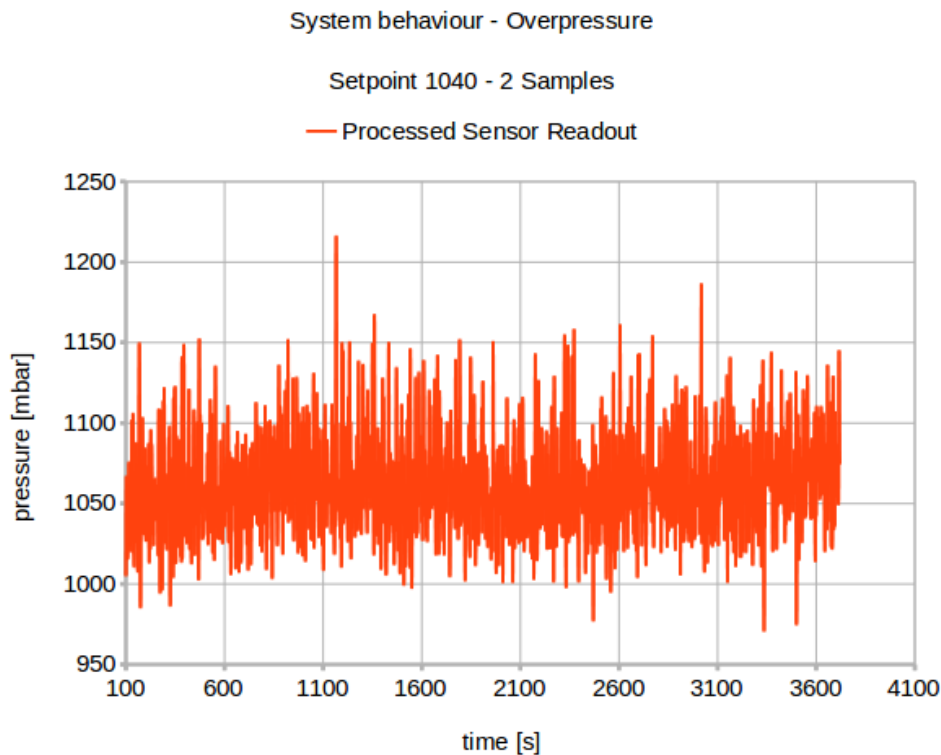
Figure 5.6: Readout Processing with 2 Samples
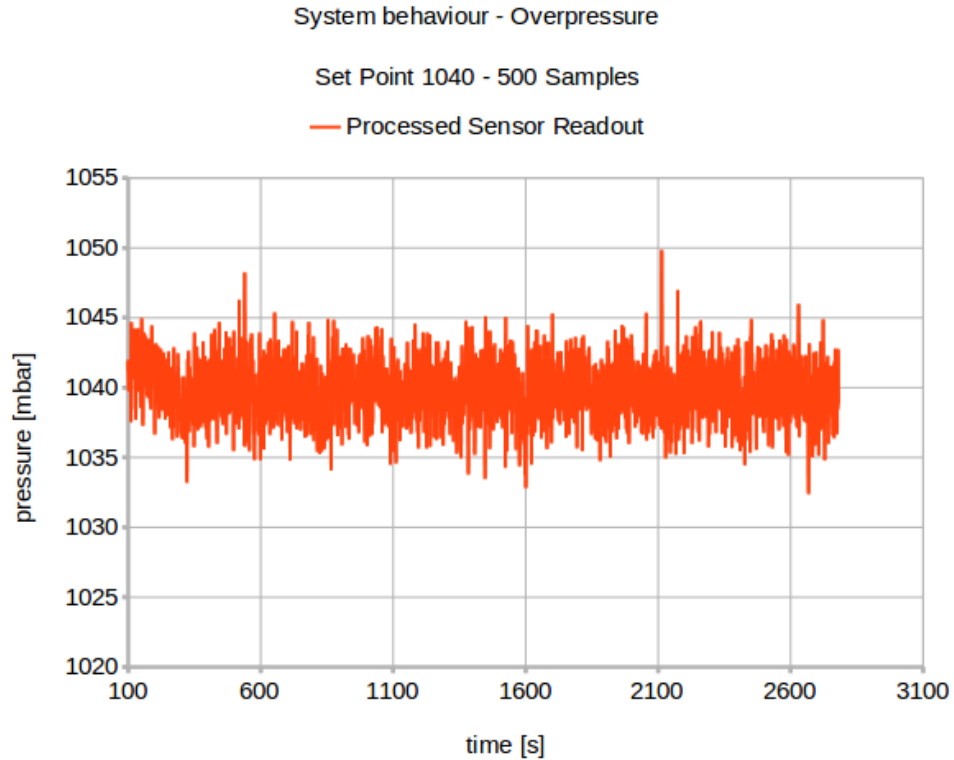
Figure 5.7: Readout Processing with 500 Samples

5.2.2 Subsidiary Task

The hardware setup including the deployed sensors and actuators was presented in Section 5.1. In this part, the control loops are described in details. For each environmental condition a control loop is developed. The following subsections outline the implementation.

5.2.2.1 Temperature Control

The TEC is placed in the chamber in such a way that one side is facing the interior of the chamber and the other side the exterior of it. By doing so, the peltier effect can be used to control the temperature. To have a better temperature distribution inside the box and to conduct away the heat at the outside, two ventilators are placed on both sides. They are always turned on when the TEC is operational.

The temperature distribution inside the chamber is not homogeneous in spite of the ventilators. To make sure that all the mechanical and electronic parts in the chamber have reached approximately the same temperature, a time period after the setpoint is reached has to be considered as stabilizing time for the temperature. Temperature fluctuations lead to variations in the XO frequency, which reduces the precision of the

collected data. For this reason, the stabilizing time is important for the XO frequency before collecting data.

The thermoelectric cooler is interfaced by two inputs: A control signal and an on-off-switch. The control signal determines the direction of the current, i.e. the cold and the hot side of the TEC. A simple two-point-controller with a hysteresis tolerance of $\pm\,0.1\,°\text{C}$ is implemented, see Algorithm 5.3. Two operation modes are distinguishable, which are chosen depending on the desired setpoint and the ambient temperature: Heating and cooling mode. The mode switching is possible via the controller but the two modes are introduced in order to prevent the controller from continuously switching between cooling and heating around the desired temperature setpoint.

The algorithm is executed periodically with a frequency of 1Hz. Based on the operation mode, thats is given by the control signal, and on the algebraic sign of the error between the current temperature and the setpoint, the TEC is either turned on or off using the on-off-switch. For instance, a negative error in the heating mode indicates that the current temperature is below the setpoint and it turns on the TEC. On the other hand, a positive error will cause the TEC to be switched off.

Algorithm 5.3: Temperature Control Loop

    Data: mode: heating or cooling, setpoint and current temperature.
    Result: update the control signal and the on-off-switch of the TEC.

1 **Function** *temperatureControl(mode, setpoint, current temperature)*
      /* local variables */
2   error = current temperature - setpoint;
3   **if** *mode is heating* **then**
4   **if** *error is negative and outside the tolerance range* **then**
5   turn on the TEC in heating mode;
6   **else**
7   turn off the TEC;
8   **else if** *mode is cooling* **then**
9   **if** *error is positive and outside the tolerance range* **then**
10   turn on the TEC in cooling mode,
11   **else**
12   turn off the TEC;
13 **End**

5.2.2.2 Humidity Control

The design of the desktop humidifier and the physical characteristics of the humidity make it hard to use a two-point- or a PID-controller. A finite state machine FSM is developed to control the relative humidity in the chamber, see Algorithm 5.4.

The following observations justify the implementation of the FSM: The environment responds at different rates to the moisture released by the humidifier depending on the current relative humidity. Figure 5.8 illustrates the step response of the humidifier, i.e. the reaction of the air inside the chamber on the turned on humidifier. A fast rise below 60% and a very slow rise above 90% are observed. This is considered when calculating *time_to_off*. The relative humidity reacts in general non-linear and mostly quadratic to the on-time of the humidifier. It remains almost constant when the humidifier is turned on for some time and rises later at some rate depending on the current relative humidity in the chamber. This is considered when calculating *time_to_wait*. When this time elapses the algorithm starts over. The duration of these two timeouts are determined experimentally. They are characteristic for the used chamber and humidifier.

The algorithm is executed periodically with a frequency of 1Hz. The algorithm remains in the *IDLE*-state as long as the current humidity is lower than the setpoint with respect to some hysteresis tolerance. When this changes, the parameter *time_to_off* is calculated based on the error between the current humidity and the setpoint and the humidifier is turned on, i.e. the *ON*-state. The *time_to_off* parameter is decremented in each execution while the algorithm in the *ON*-state. When it becomes zero, the humidifier is turned off, i.e. the *OFF*-state, and the *time_to_wait* parameter is calculated based on the current humidity. The algorithm jumps to the *WAITING*-state for a time period corresponding to *time_to_wait* and starts over afterwards in the *IDLE*-state.
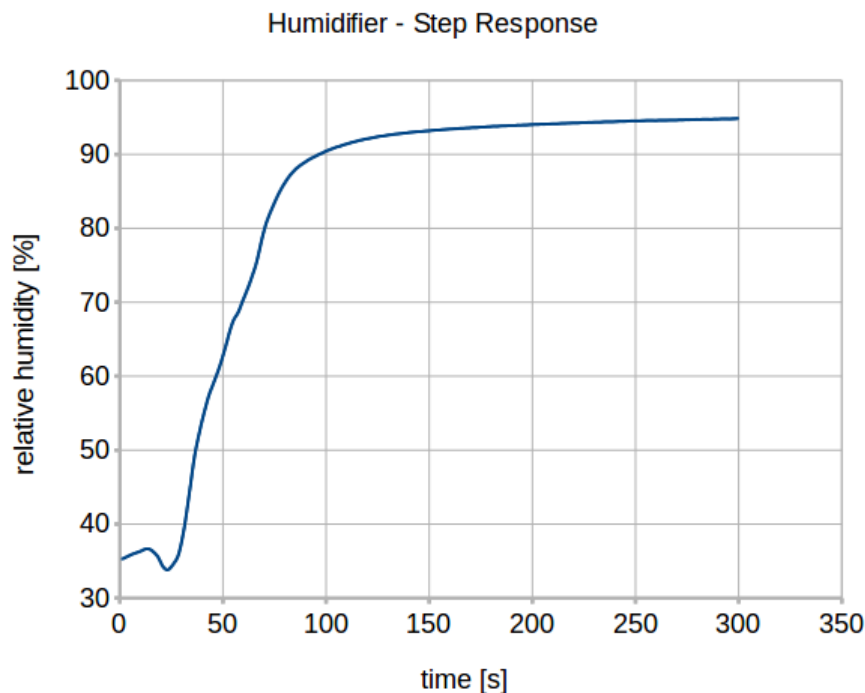

Figure 5.8: Humidifier Step Response

64

Algorithm 5.4: Humidity Control Loop

Data: state: current FSM state, setpoint and current humidity.
Result: update the FSM state and the time variables.

1 Function *humidityControl(state, setpoint, current humidity)*
2   **if** *state is IDLE* **then**
3   error = current humidity - setpoint;
4   **if** *error is negative and outside the tolerance range* **then**
5   update *time_to_off* based on the error and current humidity;
6   state = ON;
7   **else if** *state is ON* **then**
8   turn on the humidifier;
9   decrement *time_to_off*;
10   **if** *time_to_off is zero* **then**
11   state = OFF;
12   **else if** *state is OFF* **then**
13   turn off the humidifier;
14   update *time_to_wait* based on current humidity;
15   state = WAITING;
16   **else if** *state is WAITING* **then**
17   decrement *time_to_wait*;
18   **if** *time_to_wait is zero* **then**
19   state = IDLE;
20 End

5.2.2.3 Acceleration Control

Deploying a stepper motor and the respective motor driver in the acceleration control eases the software implementation of the control loop, see Algorithm 5.5. The acceleration is simulated by rotating the shaft of the motor. The plastic plate with the main controller and its hardware rotates with the same frequency. Hence, the XO is exposed to the acceleration that is evoked by the shaft rotation. The studied acceleration condition is the so called gravitational acceleration (g-acceleration) that is measurable by the accelerometer. Figure 5.9 illustrates the relation between the shaft rotation frequency and the acceleration, that is used to develop the acceleration control loop.

    The controller outputs 2 signals with a known pattern in a defined frequency to rotate the shaft of the motor as given by the frequency setpoint. Consider the two signals S_1 and S_2 and let the values 1 and 0 refer to the signal state *high* and *low*, respectively. The pattern is defined as follows: $(S_1, S_2) = ((1,0),(1,1),(0,1),(0,0))$. As specified by the motor manufacturer, the shaft is rotated 7.2° when generating this pattern. A full rotation of 360° hence corresponds to 50 successive patterns. Therefore, the rotation frequency is determined by the frequency of generating these successive patterns. The control signals S_1 and S_2 are generated as two Pulse Width Modulated (PWM)
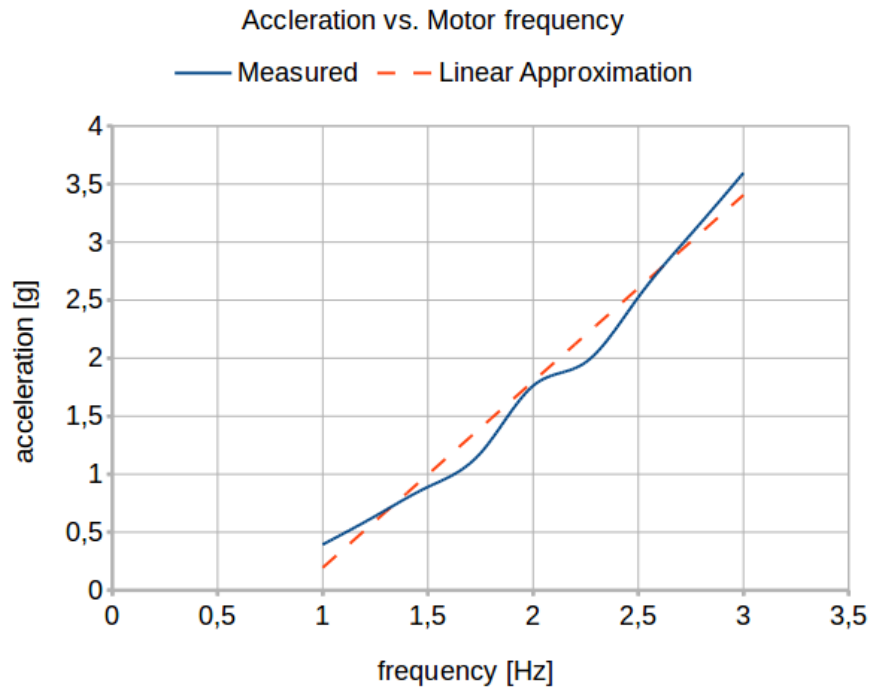
Figure 5.9: The Acceleration/Rotation-Relation

signals with 50% duty cycle. By shifting S_2 with 90° phase, the desired pattern is achieved.

The control algorithm is executed periodically with a frequency of 1Hz. The frequency setpoint is not set from the beginning since the weight load of the plate prevents the motor shaft from rotating instantaneously with the given frequency. For this reason, the algorithm sets the minimal frequency value and increments it in each execution until the given frequency is reached. The parameter *motor_step_size* is the increasing step size and is chosen to be 0.05Hz. Additionally, the motor needs some time to stabilize with the new setpoint, the parameter *motor_steady_time* determines this. If the frequency setpoint is increased in each execution, the plate begins to oscillate due to the inhomogeneous distribution of the load on it. The steady time is set experimentally to 10s. The effect of acceleration on the XO frequency is expected to be instantaneously observable, and hence, no stabilizing time has to be considered. The experiment duration is shorter than the other experiments.

5.2.2.4 Pressure Control

To control the pressure in the specified operation range, two operation modes are required: Overpressure and vacuum. The air pump has one culvert for each mode and it is hence not possible to switch the modes automatically. A PID-controller is developed by studying the step response of the air pump in both modes. From the step response the initial values

---

Algorithm 5.5: Motor Control Loop

Data: setpoint: frequency of the motor shaft
Result: frequency of the control signals S_1 and S_2

1 Function *motorControl(setpoint)*

2   error = current frequency - setpoint;

3   **if** *(error is positive) and (motor_steady_time is reached)* **then**

4   decrement current frequency by *motor_step_size*;

5   reset *motor_steady_time*;

6   **else if** *(error is negative) and (motor_steady_time is reached)* **then**

7   increment current frequency by *motor_step_size*;

8   reset *motor_steady_time*;

9   decrement *motor_steady_time*;

      /* 50 sequential patterns to perform one rotation */

10   frequency of pattern generation is 50 · current frequency;

11   generate the PWM signals;

12 End

---

of the controller constants are calculated. These values represent a rough estimation, which needs an adaption. This is done empirically after running the software on the target to match the optimal behavior, see Table 5.5.

-	K_P	K_I	K_D
Initial value	1.452	0.13	0.0575
Tuned value	0.726	0.0726	0.001

Table 5.5: Constants of the Pressure PID-Controller

The PID-controller is not implemented from the scratch. The CMSIS DSP software library[1] provides a set of functions that implements the PID-controller. Algorithm 5.6 uses the function *arm_pid_f32()* to obtain the correction value based on the current error and on the constants of the controller. Section 2.3 provides an overview on the PID-controllers.

The algorithm is called periodically every 1s to calculate the correction value using the function above. Based on the operation mode and on the error between the current pressure and the setpoint, the correction value is passed to the air pump as a duty cycle of a PWM signal or the air pump is turned off completely. For instance, a positive error in the vacuum mode indicates that the current pressure is higher than the setpoint and the air pump is powered with the calculated duty cycle. On the other hand, the algorithm reacts on a negative error in the same operation mode by turning off the air pump. Additionally, a pressure tolerance of 5*mbar* is considered in the calculation as

---

[1]A suite of common signal processing functions for use on Cortex-M processor based devices.

discussed in Subsection 5.2.1.3.

Algorithm 5.6: Pressure Control Loop

    Data: mode: overpressure or vacuum, setpoint and current pressure.
    Result: calculate the correction value and pass it to the air pump.

1 **Function** *pressureControl(mode, setpoint, current pressure)*
       /* local variables */
2   error = current pressure - setpoint;
3   PID-correction $= arm\_pid\_f32(error, PID\text{-}constants)$;
4   **if** *mode is overpressure* **then**
5   **if** *error is negative and outside the tolerance range* **then**
6   power air pump with the PID-correction as duty cycle of PWM signal;
7   **else**
8   turn off air pump;
9   **else if** *mode is vacuum* **then**
10   **if** *error is positive and outside the tolerance range* **then**
11   power air pump with the PID-correction as duty cycle of PWM signal;
12   **else**
13   turn off air pump;
14 **End**

5.2.2.5   Overview on the Control Loops

Table 5.6 provides an overview of the main characteristics of the developed control loops. The step size value is the recommended value to calculate the coverage set of the operation range in this implementation. For instance, a step size of $5\,^{\circ}\mathrm{C}$ for the temperature requires to perform 15 experiments with a temperature set point increasing by $5\,^{\circ}\mathrm{C}$ in each experiment to cover the operation range. The step size is required only during the data collection part and it is estimated as a reasonable compromise to cover the operation range with a finite set of points without a big loss in data accuracy.

Environmental Condition	Controller Type	Operation Range	Step Size
Temperature [$^{\circ}$C]	Two-point	-10 to +60	5
Relative Humidity [%]	FSM	current to 100	15
Acceleration [Hz]	Open-loop	0.5 to 4.5	0.25
Pressure [*mbar*]	PID	840 to 1200	20

Table 5.6: Characteristics of the Control Loops

5.3   The Compensation Model

The challenge of developing the compensation model is to evaluate the collected data in the previous part to acquire as much knowledge about the XO behavior as possible.

This knowledge is based on the set of measurements of environmental conditions and the related XO frequency deviations. The meaning of the collected data is discussed first in Subsection 5.3.1 by providing examples from the experiments. The chosen offline learning technique is proposed afterwards in Subsection 5.3.2. The implemented online learning technique is outlined in Subsection 5.4.2.2.

5.3.1 Interdependencies of Environmental Conditions

As stated in Section 4.3, the temperature is the most important environment condition in this approach. In the used hardware setup, the maximum deviation in the whole temperature operation range is given for both XOs, whereas the behavior of the LSEQ deviation is specified to be quadratic in relation to the temperature.

The temperature effect is clearly visible while studying the other conditions. This is due to the joint effect with other environmental conditions and due to the temperature dependency of the used sensors. For instance, performing the same acceleration experiment, i.e. same setpoint and duration, at two different room temperatures yields different results. Therefore, the experiments on the environmental conditions are performed under additional temperature control.

For instance, collecting data while studying the acceleration condition is repeated at different temperature setpoints. By doing this, a well-defined temperature dependency in addition to the dependency on the acceleration is achieved. This means, that the output of the experiments, except the temperature experiment, is not a function in two, but in three dimensions: The frequency deviation, the current condition and the temperature values. Studying the acceleration effect is easier in this case by compensating the temperature effect first, see Figure 5.10. The left diagram depicts the repeatedly collected data at different temperature setpoints. The right diagram represents the same data after compensating the temperature effect.
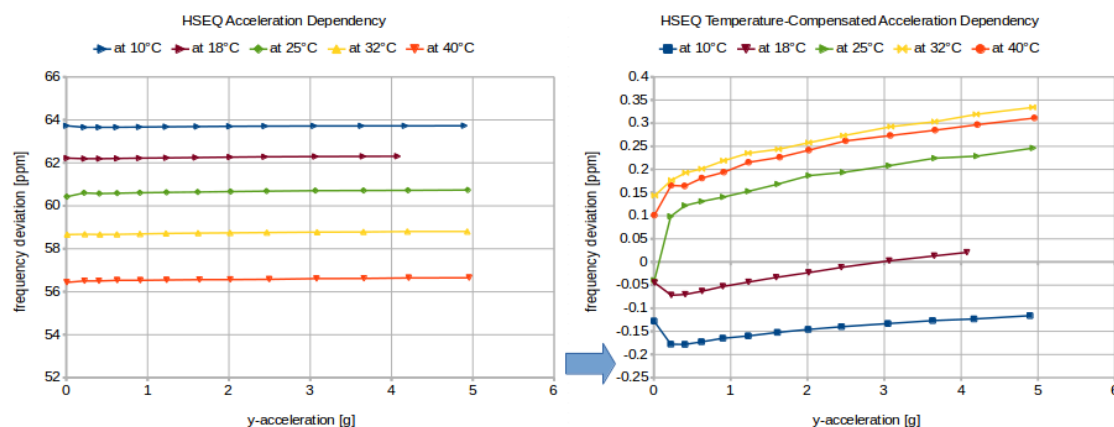
Figure 5.10: The Temperature Effect in the HSEQ y-Acceleration Experiment

Another example from the data collection part clarifies the way, how the joint effect of multiple environmental conditions is handled. During the pressure experiments, the measured HSEQ frequencies at extreme temperature and pressure values were not always distributed around the same value. The diagram in Figure 5.11 shows the distribution at 25 °C of measured frequency deviations at three different pressure setpoints: Atmospheric, minimum and maximum pressure. The distributions from the three experiments are overlapped. The figure shows the case where the frequency of the HSEQ is not much affected by the pressure variation in this operation range.

Figure 5.12 illustrates the distribution of the three pressure setpoints at 10 °C and 40 °C. The distributions are not overlapped anymore. It seems now that the HSEQ is affected the most at the maximum pressure.
The underlying cause is not obvious: The extreme temperature values may intensify the effect of the pressure on the frequency, i.e. the joint effect of both conditions could be visible here. The temperature dependency of the pressure sensor or of the measurement equipment in general can also be the cause of the phenomenon, or a combination of both. The compensation model is aware about the distribution of the frequency deviation in the discussed case and it delivers a value to compensate this deviation in spite of the underlying cause.
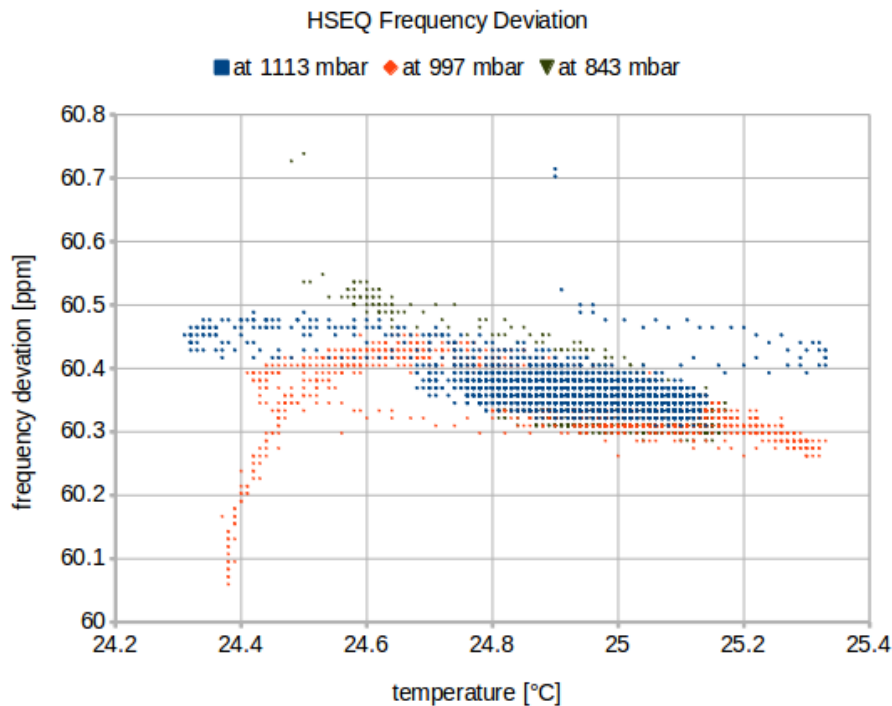
Figure 5.11: Distribution of the HSEQ Deviation at 25 °C
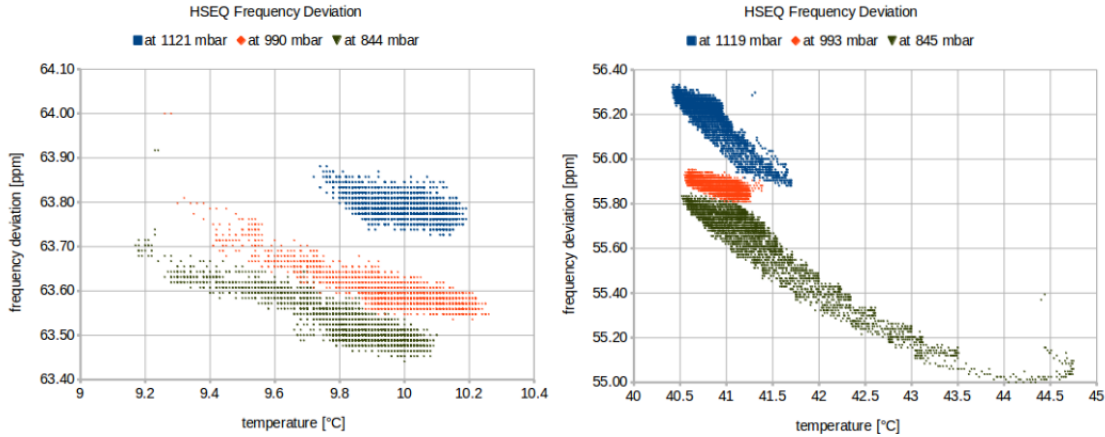
Figure 5.12: Distribution of the HSEQ Deviation at $10\,^\circ$C and $40\,^\circ$C

5.3.2 Building the Model

Once the experiments are done and the measured data is available, the XO compensation model can be built. In this subsection the regression analysis as modeling technique is introduced. For each condition a model is built to compensate its effect on the XO frequency. The main controller corrects the XO frequency based on the individual compensation values. The set of the compensation models of all environmental conditions represents *the* XO compensation model.

As stated before in Section 4.3.1, choosing a modeling technique depends on many factors. The number of environmental conditions, the observed dependencies between the conditions during the experiments and the model complexity are the main ones.

Based on the measured dependency between the XO frequency and the environmental condition, the regression analysis is applied to calculate the optimal function that models this dependency. This can be done in the whole operation range by one function or piece- or interval-wise by two or more functions. The type and the degree of the mathematical functions, e.g. a linear or quadratic or of higher order polynomial, are determined by the collected data, Subsection 5.3.2.1 provides two examples from the temperature experiments.

The previous subsection 5.3.1 discussed the problem of the interdependencies between the environmental conditions. To solve this problem, the approach while developing the compensation model is introduced as follows:

- The sensor measurements of the available sensors are collected all the time, e.g. while studying the effects of the acceleration, the data from the other sensors is also collected. By doing so, all possible interdependencies between the environmental conditions can be analyzed when the data collection part is done.

71

- The first step is to develop a compensation function for the temperature effect. This function is applied on the collected data of the other environmental conditions in order to compensate the temperature effect. The individual compensation functions are developed afterwards using the temperature compensated data.

- The next step is the humidity compensation. These two conditions, temperature and humidity, are affecting the XO all the time, quite contrary to the acceleration, where its effect is present only when the physical acceleration is available. Additionally, the XO is more sensitive to the higher rate of change of these two conditions in comparison with the pressure.

- Afterwards, the compensation functions of the other conditions are developed.

- To achieve a well-defined temperature dependency, the data collection is repeated for different temperature setpoints that cover the temperature operation range. The data collection part is repeated for the temperature values 10, 18, 25, 32 and 40 °C. By using interpolation and extrapolation techniques, these values can equally cover a temperature operation range of 0 °C to 50 °C.

5.3.2.1   Compensation Model for the Temperature

The quadratic dependency of the LSEQ and the linear dependency of the HSEQ on the temperature suggest to model the collected data by a quadratic and a linear function, respectively. Based on the measured frequency deviation at the temperature setpoints, which are given by the coverage set, an optimal function has to be found that models the behavior of the XO at different temperatures. Figure 5.13 from the temperature data collection part depicts the frequency deviation of the LSEQ and HSEQ and suggest possible compensation functions.
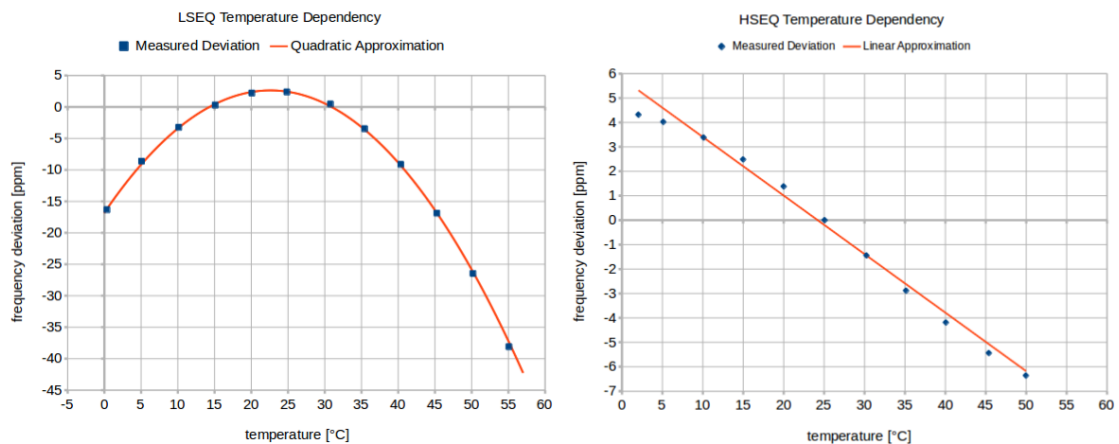
Figure 5.13: LSEQ and HSEQ Temperature Dependency
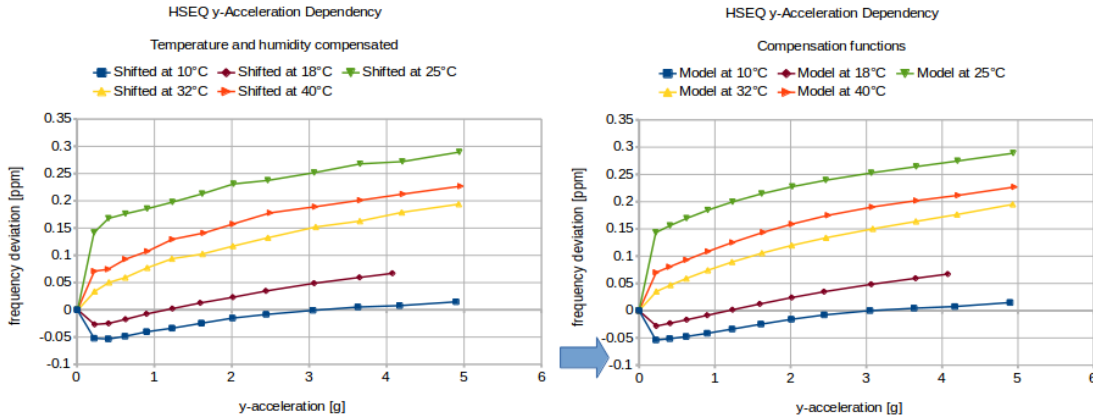
Figure 5.14: HSEQ *y*-Acceleration Dependency

5.3.2.2 Compensation Model for the other Conditions

Performing the data collection repeatedly for different temperature setpoints results in a three dimensional compensation function with three axes: The value for the studied condition, the temperature and the frequency deviation. Figure 5.10 illustrated this approach on the acceleration condition. Further steps are shown by Figure 5.14. The temperature and the humidity effects are compensated and the datasets are shifted in the left diagram to meet the assumption: "*Zero deviation at zero acceleration*". The compensated temperature and humidity effects strengthen this assumption. The right diagram shows the compensation function at the different temperature values after applying a curve fitting algorithm to model the XO dependency.

5.4 Model Deployment

The main challenges in the model deployment part are mainly the following: The implementation of the compensation model on the main controller and the calculation of the compensation values and the XOC counter correction value. The compensation value is delivered by a compensation model in *ppm*, that is related to the sensor readout of a specific environmental condition. The compensation value is a real number in mathematical terms, i.e. its an element from $\mathbb{R}$ with an integer part and a possible decimal part. The XOC counter correction value is an integer, that is calculated by the compensation model from the individual compensation values. Due to the conversion from real to an integer numbers, possible remainders have to be considered. This is done by summing the remainder in each execution until the sum overflows and results in an integer. For instance, the following consecutive outcomes from the calculation 12.34Hz, 12.71Hz and 13.1Hz result in the consecutive XOC counter correction values 12Hz with the remainder 0.34, 13Hz with the remainder 0.05Hz and 13Hz with the remainder 0.15Hz.

5.4.1 XOC Counter Correction

Before presenting the implementation of the algorithm to calculate the compensation values and the XOC counter correction value, the implementation of the compensation models on the main controller is proposed. As discussed in Subsection 4.4.2, the offline calculation is chosen in this thesis to obtain the compensation values from the compensation functions as follows:

- The temperature compensation function is sampled in the temperature operation range. The result is stored on the main controller as one dimensional array. The compensation value is obtained by linear interpolation or extrapolation.

- The compensation function of the other environmental conditions is sampled in the operation ranges of the temperature and of the condition. The result is stored as a two dimensional array. In this case a two dimensional interpolation or extrapolation has to be performed: First in the environmental condition and then in the temperature dimension.

- The sampling step size depends on the compensation functions. Smaller sampling step size is required by higher order functions, whereas the step size can be increased without higher loss of precision for linear functions.

The set of sampled data is stored as arrays in the C-programming language. Figures 5.15 and 5.17 depict the sampling results of the HSEQ temperature compensation function in Figure 5.13 and the HSEQ y-acceleration compensation function in Figure 5.14, respectively. The temperature array is two dimensional to simplify the implementation of the C-compensation function. The output of the compensation algorithm for each condition is a compensation value in ppm. The sum of all compensation values is converted to a XOC counter correction value in Hz depending on the nominal frequency of the studied XO. For instance, a compensation value of $30ppm$ corresponds to 0.983Hz for the LSEQ and 240Hz for the HSEQ.

In the following, the XOC counter correction procedure is illustrated by two examples from the HSEQ temperature and y-acceleration compensation functions.

```
static const float temp_function_HSEQ[T_ROW_SIZE_HSE][T_COL_SIZE_HSE] = {
  4.512014,  4.416012,  4.320010,  4.224008,  4.128006,  4.032004,  3.907635,  3.779330,  3.651025,  3.522720,
  /* 0°C       1°C        2°C        3°C        4°C        5°C        6°C        7°C        8°C        9°C    */
  3.394415,  3.216900,  3.033485,  2.850070,  2.666655,  2.483096,  2.262776,  2.042456,  1.822136,  1.601816,
  /* 10°C      11°C       12°C       13°C       14°C       15°C       16°C       17°C       18°C       19°C   */
  1.381496,  1.109919,  0.837743,  0.565567,  0.293391,  0.021215, -0.257901, -0.537584, -0.817267, -1.096950,
  /* 20°C      21°C       22°C       23°C       24°C       25°C       26°C       27°C       28°C       29°C   */
 -1.376633, -1.667059, -1.961040, -2.255021, -2.549002, -2.842983, -3.111850, -3.376290, -3.640730, -3.905170,
  /* 30°C      31°C       32°C       33°C       34°C       35°C       36°C       37°C       38°C       39°C   */
 -4.169610, -4.407211, -4.642652, -4.878093, -5.113534, -5.348975, -5.563366, -5.764251, -5.965136, -6.166021,
  /* 40°C      41°C       42°C       43°C       44°C       45°C       46°C       47°C       48°C       49°C   */
 -6.366906};
  /* 50°C */
```

Figure 5.15: HSEQ Sampled Temperature Compensation Model

74

The current quartz temperature qt is calculated and filtered as described in Subsection 5.2.1. It represents, in addition to the sampled temperature compensation function, the input of the interpolation algorithm, see Algorithm 5.7. The interpolation is done in a segment of the compensation function, which is given by two pairs of values representing the coordinates of the known lower and higher points (x_1, y_1) and (x_2, y_2), see Figure 5.16. x_i denotes the value of the environmental condition and y_i the respective compensation value. For $qt = 26.5\,°C$, the segment is determined by the following values: $(26, -0.257901)$, $(27, -0.537584)$. The length of the segment is given by the step size of the sampled compensation function, that is equal to $1\,°C$ in the function depicted in Figure 5.15.

The linear interpolation is done by calculating the parameters of the straight line going through (x_1, y_1) and (x_2, y_2). This is done based on the so called *slope-intercept*-equation $y = m \cdot x + d$, where m is the slope of the line and d is the y-coordinate of the intersection between the line and the y-axis. The final temperature compensation value $c_f = -0.397743ppm$ at $qt = 26.5\,°C$ is the result of the calculation $c_f = m \cdot qt + d$, that is done by executing Algorithm 5.7 $c_f = linearInterpolation(qt, x_1, x_2, y_1, y_2)$.
This compensation value and the HSEQ nominal frequency of 84MHz result in a XOC counter correction value of -33Hz with a remainder of -0.41Hz for the temperature effect.
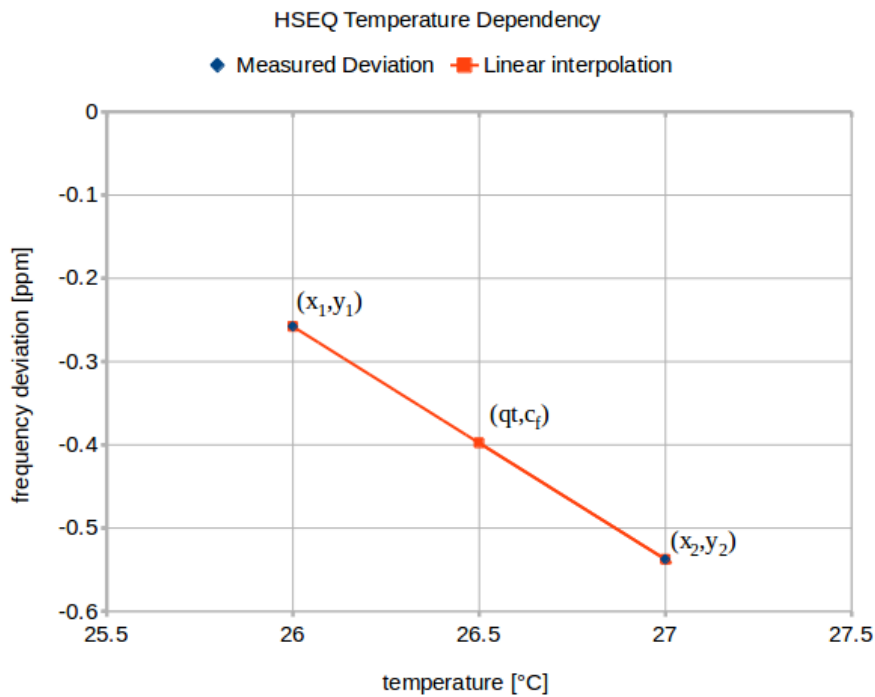

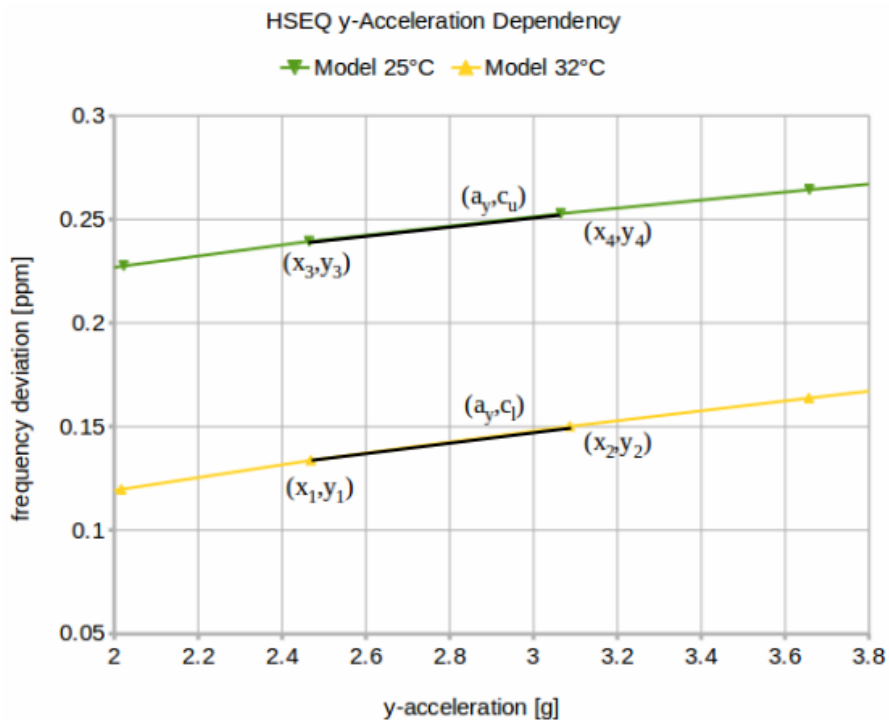Figure 5.16: Interpolating the HSEQ Temperature Compensation Value

```
static const float accel_y_function_HSEQ[AY_ROW_SIZE_HSE][AY_COL_SIZE_HSE]={

  {/*»    »       »         »        »           »           Sampled Compensation Function at 10°C»    »        »        »         »        */
    0.000000,  -0.023029, -0.046058, -0.053038, -0.051604, -0.049974, -0.048175, -0.046232, -0.044168, -0.042006, -0.039767,
   -0.037472, -0.035138, -0.032784, -0.030427, -0.028081, -0.025761, -0.023480, -0.021250, -0.019081, -0.016983,
   -0.014964, -0.013031, -0.011190, -0.009446, -0.007802, -0.006260, -0.004822, -0.003487, -0.002255, -0.001122,
   -0.000086,  0.000859,  0.001719,  0.002500,  0.003212,  0.003863,  0.004465,  0.005029,  0.005569,  0.006099,
    0.006633,  0.007190,  0.007787,  0.008442,  0.009177,  0.010012,  0.010970,  0.012076,  0.013353,  0.014828
  },
  {/*»    »       »         »        »           »           Sampled Compensation Function at 18°C»    »        »        »         »        */
    0.000000, -0.009582, -0.019164, -0.027706, -0.025447,-0.023136,-0.020780,-0.018388,-0.015965,-0.013519,-0.011055,
   -0.008580, -0.006100,-0.003619,-0.001143,0.001323,0.003775,0.006209,0.008621,0.011007,0.013364,
    0.015690,0.017980,0.020235,0.022450,0.024625,0.026757,0.028847,0.030893,0.032895,0.034852,
    0.036765,0.038633,0.040459,0.042242,0.043985,0.045688,0.047355,0.048986,0.050585,0.052154,
    0.053697,0.055217,0.056719,0.058205,0.059681,0.061150,0.062620,0.064093,0.065577,0.067077
  },
  {/*»    »       »         »        »           »           Sampled Compensation Function at 25°C»    »        »        »         »        */
    0.000000,0.063335,0.126671,0.148573,0.155144,0.161402,0.167358,0.173027,0.178421,0.183554,0.188438,
    0.193085,0.197507,0.201716,0.205723,0.209539,0.213176,0.216643,0.219951,0.223111,0.226131,
    0.229021,0.231791,0.234450,0.237005,0.239466,0.241840,0.244136,0.246360,0.248520,0.250623,
    0.252676,0.254685,0.256656,0.258595,0.260508,0.262399,0.264275,0.266139,0.267997,0.269851,
    0.271707,0.273568,0.275437,0.277318,0.279212,0.281123,0.283053,0.285004,0.286977,0.288975
  },
  {/*»    »       »         »        »           »           Sampled Compensation Function at 32°C»    »        »        »         »        */
    0.000000,0.014459,0.028918,0.039467,0.045587,0.051491,0.057183,0.062671,0.067961,0.073059,0.077971,
    0.082704,0.087264,0.091658,0.095891,0.099971,0.103903,0.107694,0.111350,0.114877,0.118283,
    0.121572,0.124752,0.127829,0.130809,0.133699,0.136504,0.139231,0.141887,0.144478,0.147011,
    0.149490,0.151924,0.154318,0.156678,0.159011,0.161324,0.163622,0.165912,0.168200,0.170493,
    0.172796,0.175117,0.177462,0.179836,0.182247,0.184700,0.187203,0.189760,0.192380,0.195067
  },
  {/*»    »       »         »        »           »           Sampled Compensation Function at 40°C»    »        »        »         »        */
    0.000000,0.031096,0.062191,0.074287,0.080059,0.085762,0.091386,0.096921,0.102358,0.107688,0.112905,
    0.118001,0.122971,0.127807,0.132507,0.137065,0.141478,0.145744,0.149860,0.153826,0.157640,
    0.161302,0.164814,0.168176,0.171391,0.174463,0.177393,0.180187,0.182849,0.185386,0.187803,
    0.190107,0.192307,0.194410,0.196426,0.198365,0.200237,0.202053,0.203825,0.205566,0.207289,
    0.209008,0.210738,0.212494,0.214292,0.216150,0.218084,0.220112,0.222254,0.224530,0.226958
  }
};
```

Figure 5.17: HSEQ Sampled y-Acceleration Compensation Model

The calculation of the compensation value of multidimensional compensation functions is more tricky. This is illustrated by an example from the HSEQ y-acceleration compensation function, see Figure 5.14. The input of the algorithm to calculate the compensation value for the acceleration in the y-direction a_y at the quartz temperature qt is the current value of these conditions in addition to their sampled compensation functions as depicted in Figure 5.17. Let $qt = 26.5\,°C$ and $a_y = 3g$.

The first step is to calculate two compensation values, c_l and c_u[2], by linear interpolation from the *nearest* known compensation functions. The current quartz temperature qt determines the two acceleration compensation functions that will be used in the calculation. For $qt = 26.5\,°C$, the linear interpolation is performed in the known compensation functions at $25\,°C$ and $32\,°C$. Similar to the previous case, c_l and c_u are calculated by Algorithm 5.7 as follows $c_l = linearInterpolation(a_y, x_1, x_2, y_1, y_2)$ and $c_u = linearInterpolation(a_y, x_3, x_4, y_3, y_4)$, see Figure 5.18. The algorithm calculates the following values: $c_l = 0.148012ppm$ and $c_u = 0.251389ppm$.

---

[2]The subscripts l and u refer to lower and upper, respectively

Figure 5.18: Interpolating the HSEQ y-Acceleration Compensation Value

The next step is to calculate the final compensation value c_f from c_l and c_u. This is done based on the distance of qt to the temperature values, at which the lower and upper compensation functions are developed. This distance determines how much the final compensation value c_f is influenced by c_l and c_u. For $qt = 26.5\,°C$, c_f has to be influenced more by c_l since qt is closer to $25\,°C$ than $32\,°C$. In particular, c_f is calculated to 78.57% from c_l and to 21.43% from c_u, i.e. $c_f = 0.7857 \cdot c_l + 0.2143 \cdot c_u = 0.17ppm$. This compensation value and the HSEQ nominal frequency of 84MHz result in a XOC counter correction value of 14Hz with a remainder of 0.29Hz for the y-acceleration effect.

The behavior of the compensation algorithm for some environmental condition is given by its sampled compensation function, that is determined by the following parameters:

- **Number of Rows**: The number of repeated experiments for an environmental condition at the different temperature setpoints.

- **Number of Columns**: The count of sampled data, that is also related to the operation range and to the sampling step size.

- **Data**: The stored data is given by the dependency of the XO on the environmental condition.

Algorithm 5.7: Linear Interpolation

Data: x the x-coordinates of the interpolated point.
x_1 the x-coordinates of the first known point.
x_2 the x-coordinates of the second known point.
y_1 the y-coordinates of the first known point.
y_2 the y-coordinates of the second known point.
Result: calculate the y-value between known lower and upper x,y-pairs

1 Function *linearInterpolation(x, x_1, x_2, y_1, y_2)*
```
/* local variables */
```
2 m: the slope of the line between (x_1, y_1) and (x_2, y_2)
3 d: the y-coordinate of the intersection between the line and the y-axis
```
/* perform calculation */
```
4 $m = (y_2 - y_1)/(x_2 - x_1)$;
5 $d = y_1 - m * x_1$;
6 $y = (m * x) + d$;
7   **return** y
8 End

5.4.2 Time Signal Generation

The output of the previous step is used to correct the frequency of the XO. Two operation modes are distinguishable depending on the application purpose of the system.

5.4.2.1 Open Loop

The open loop system in Figure 5.19 is designed to reflect the results of the study on the effects of environmental conditions. It is triggered by the GPS_PPS. At each time instant, that is carried out by the GPS_PPS, the system collects data from its sensors and calculates the compensation and correction values for both XOs. The data from the sensors and the calculated data are transmitted to the computer via the bluetooth module.

The open loop mode was first implemented to visualize the results of the performed experiments. Furthermore, the system can be deployed as a calculation unit for the purpose of drift compensation for more than one XOC. While the main controller in the closed loop mode generates a PPS by compensating the effects on one XO only, the main controller in the open loop mode can implement n models for n XOs, e.g. the LSEQ and the HSEQ, and provide different systems with the counter correction value for each XOC.

5.4.2.2 Closed Loop

The system in the closed loop mode is an autonomous system, that generates its own time signal. The system corrects the frequency of the HSEQ and generates its own PPS,
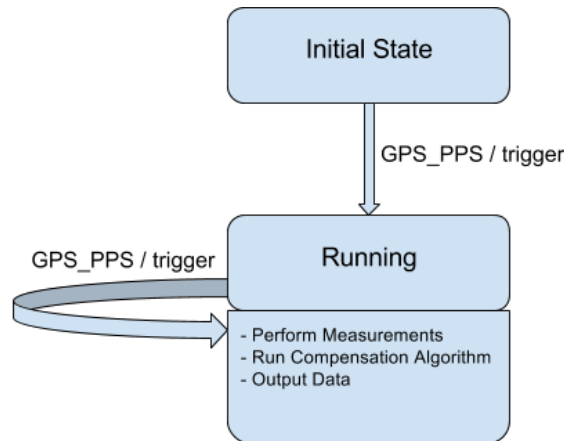
Figure 5.19: Open Loop Mode

the SYS_PPS. The system clock of the main controller is based on the HSEQ, therefore it is used in the closed loop design. The LSEQ can be used in this design by configuring the main controller to use the LSEQ as the base for the system clock instead of the HSEQ. Figure 5.20 illustrates the closed loop design.
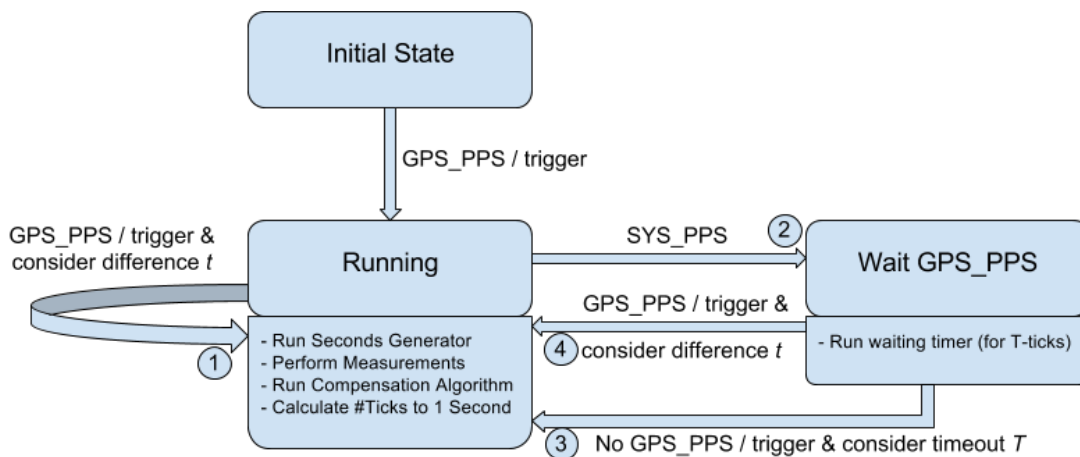

Figure 5.20: Closed Loop Mode

The *Seconds Generator* is a timer that has the same frequency as the HSEQ, i.e. the time period of one tick of the seconds generator is equal to the time needed for one oscillation of the HSEQ. The consequence of this configuration is the following: The XOC counter correction value, that is calculated by the compensation algorithm is added to the HSEQ nominal frequency and set as top counter value of the seconds generator. This is also the reason why the XOC counter correction value has to be an integer.

The first trigger is carried out by the GPS_PPS. The seconds generator is initially configured to count as many oscillations as the nominal frequency of the HSEQ. The XOC counter correction value is calculated based on the measured environmental conditions and the corrected frequency replaces the initial top counter value of the seconds generator.

The following cases have to be distinguished in accordance with Figure 4.2[3]:

- A GPS_PPS arrives before the SYS_PPS: The corrected XO frequency is higher than it should be, cf. Transition 1 in Figure 5.20. The system starts over. The time difference t between the two pulses is considered as long-term correction value as discussed in Subsection 4.3.2.

- The seconds generator outputs the SYS_PPS before the next GPS_PPS: The corrected XO frequency is *maybe* lower than it should be, cf. Transition 2 in Figure 5.20: Another timer, the *Waiting Timer*, is armed to implement a timeout T. This timeout is necessary as a jitter tolerance and as a detection of the availability of the GPS_PPS.

    - If the timeout elapses, the system infers that the GPS_PPS is not available and it operates autonomously, cf. Transition 3 in Figure 5.20.

    - Otherwise, if the system receives a GPS_PPS before the timeout elapses then the corrected XO frequency is indeed lower than it should be, cf. Transition 4 in Figure 5.20. The time difference t between the two pulses is also considered as long-term correction value similar to system behavior in Transition 1.

t is averaged over time and considered as additional XOC counter correction value to improve the compensation accuracy. This additional correction value c_A is initially set to zero and updated on each GPS_PPS by applying an averaging filter, similar to the temperature and humidity filtering. In particular, c_A is calculated from the previous correction value c_{Ap} and the current time difference t by the equation:

$$c_A = C_1 \cdot t + C_2 \cdot c_{Ap}$$

Where C_1 and C_2 are the filter constants. This is done in the presence of the reference time. When no reference time is detected, c_A retains its value from the last GPS_PPS occurrence.

The timeout T of the waiting timer is the time difference, that the system tolerates between the SYS_PPS and GPS_PPS. See Subsection 6.3.3 for the concrete calculation of c_A and T.

---

[3]The system assumes that the GPS_PPS is not manipulated.

In this chapter the implementation of the developed method is proposed. The idea behind this implementation is to demonstrate the ability of using the developed method mainly in the application field of distributed real-time systems. Two models were developed for the available two XOs, which demonstrates the fulfillment of Requirement *R1* in Subsection 3.1.1.

One of the main challenges is to use an appropriate modeling technique for the purpose of offline learning. The direct dependencies, that were observed during the development of the compensation functions, are behind the decision to choose a simple modeling technique such as the regression analysis rather than more sophisticated ones. The offline preparation and calculation of the compensation functions are preferred in order to have a simple software implementation, that is easier to adapt and test. The online learning compensates for aging effects of the XO, cf. requirements *R2* in Subsection 3.1.2 and *R3* in Subsection 3.1.3.

The computational cost of the offline calculation is lower in comparison with the online calculation. This implies a lower power consumption, cf. requirements *R4* in Subsection 3.1.4. The experiments, the results of the proposed implementation and a detailed discussion of the fulfillment of the requirements in Section 3.1 will be the scope of the next chapter.

Experiments and Results

The aim of this thesis is to develop a cost-efficient procedure to compensate for the deviation of the Quartz Crystal Oscillator (XO) frequency in the absence of the reference time. The implementation of the developed method was proposed in Chapter 5. The implementation of a compensation algorithm was introduced, that relies on the XO specific compensation model. In this chapter the results of the method implementation are presented: First, the experiments and the individual compensation models, see Section 6.1, then the modeled and sampled dependencies are presented, see Section 6.2. Afterwards, the results of the model deployment on the main controller are introduced, see Section 6.3. To conclude this chapter, Section 6.4 provides an overview on the fulfillment of the requirements defined in Section 3.1.

In accordance with the abstract steps to realize the compensation algorithm, see Section 4.5, the following approach is developed when studying and integrating the environmental conditions in the compensation algorithm:

- The initial experiments to spot the dependencies are characterized by the operation range and the respective coverage set of each environmental condition. The experiments are done under additional temperature control as stated in Subsection 5.3.2 to achieve a well-defined temperature dependency. Table 6.1 states the characteristics of the performed experiments[1].

- Additional experiments are performed by tracing the operation range from its minimum to its maximum and vice versa in order to collect validation data to test the compensation models before implementing them on the main controller.

---

[1]Different values compared to the specified ones in Table 5.6 are due to setup specific restrictions. The step size values are given in terms of the control loops implemented by the external controller. Measured values by the main controller may vary.

- When the collecting of data is done, the sensor readout is post-processed. This comprises the temperature filtering, the humidity filtering and the conversion from relative to absolute humidity.

- The resulting dependencies in form of two or three dimensional functions are modeled and sampled.

- Offline tests are performed on the compensation models before implementing them on the main controller. The tests are done by applying the compensation models on validation data that is not considered while building the model.

- The implementation of the compensation model on the main controller is done afterwards. This comprises storing the sampled compensation function and adding its specific parameters, such as the number of repeated experiments at the different temperature setpoints and the sampling step size, cf. Figure 5.15 and Figure 5.17.

- Initial tests that are concerned with individual environmental conditions are performed online. Afterwards, a number of tests on the joint effect of all integrated environmental conditions are performed on the system in the open and closed loop operation modes.

Env. Cond.	Operation Range	Step Size	Duration $[min]$	Stabilizing Time $[min]$
Temperature	$0\,°C$ to $+50\,°C$	$5\,°C$	60	30
Humidity	current to $\approx 100\%$	15%	60	30
Acceleration	0.5 to 4.5Hz	0.25Hz	6	-
Pressure	840 to $1120\,mbar$	$20\,mbar$	60	30

Table 6.1: Characteristics of the Experiments of the Data Collection Part

6.1 Data Collection

The experiments on the environmental conditions, the filtering of sensor readout and preparing the data for further processing are discussed in this part. The output of each experiment is a sequence of tuples:

$\langle$ *timestamp*; *temperature* $[°C]$; *relative humidity* $[\%]$; *x-acceleration* $[g]$

y-acceleration $[g]$; *pressure* $[mbar]$; *HSEQ frequency* $[Hz]$; *LSEQ frequency* $[Hz]\rangle$

The number of tuples per experiments is calculated as follows: One tuple per Pulse Per Second (PPS) from the Global Positioning System (GPS) receiver, i.e. per second, multiplied by the duration of the experiment in seconds, e.g. a temperature experiment produces at least 3600 tuples and an acceleration experiment at least 360 tuples.
For each experiment the values are averaged over the number of tuples. For instance, after a pressure experiment the temperature, humidity, pressure and frequencies are

averaged to denote the experiment result. In the following figures, each point in the diagrams corresponds to an output of one experiment.

6.1.1 Temperature Experiments

The experiments are performed in the temperature operation range with a duration of $60min$ each. The setpoint of the temperature control loop was increased by $5\,°C$ in each experiment starting from $0\,°C$, cf. Table 6.1. The temperature filter, that was introduced in Section 5.2.1, is applied on the measured temperature values afterwards.
Figure 6.1 illustrates the result of the temperature experiments. An example for the temperature experiment output at $35\,°C$ is given in Table 6.2.
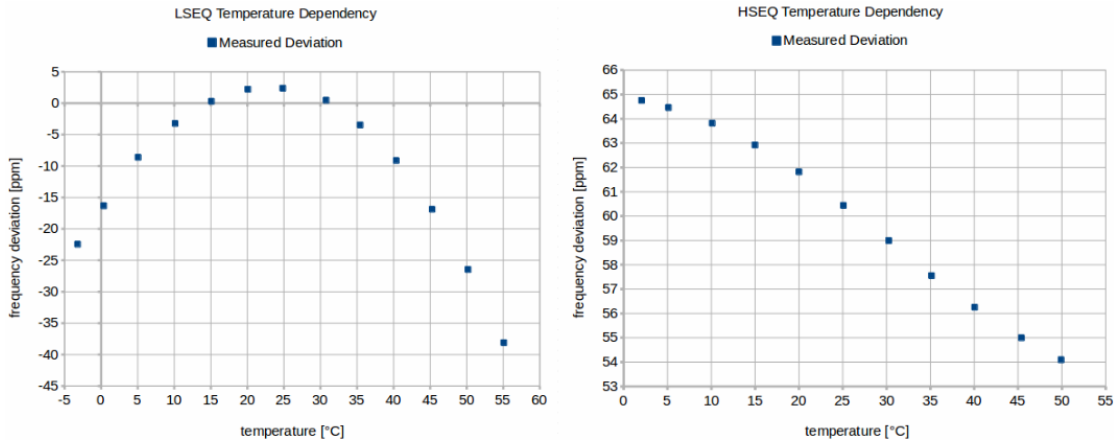
Figure 6.1: LSEQ and HSEQ Temperature Dependency

	LSEQ Frequency	HSEQ Frequency	Temperature	Quartz Temperature
Average	32767.8862 [Hz]	84004834.2832 [Hz]	35.1435 [°C]	35.1492 [°C]
Variance	0.1 [Hz^2]	9.49 [Hz^2]	0.02 [°C ^{2}]	0.01 [°C ^{2}]

Table 6.2: LSEQ and HSEQ Temperature Experiment Result at $35\,°C$

The result of the temperature experiment are in accordance with the specifications of the LSEQ in the temperature operation range. The HSEQ exhibits a linear dependency whereas the LSEQ a quadratic one. The deviation of the HSEQ frequency is high in comparison with the LSEQ frequency.

6.1.2 Humidity Experiments

The humidity experiments are performed starting from the current room humidity to approx. 100% relative humidity and repeated for the several temperature setpoints. Afterwards, the filtering and the conversion to the absolute humidity in $[g/m^3]$ are done. The result of the experiments is given in Figure 6.2.
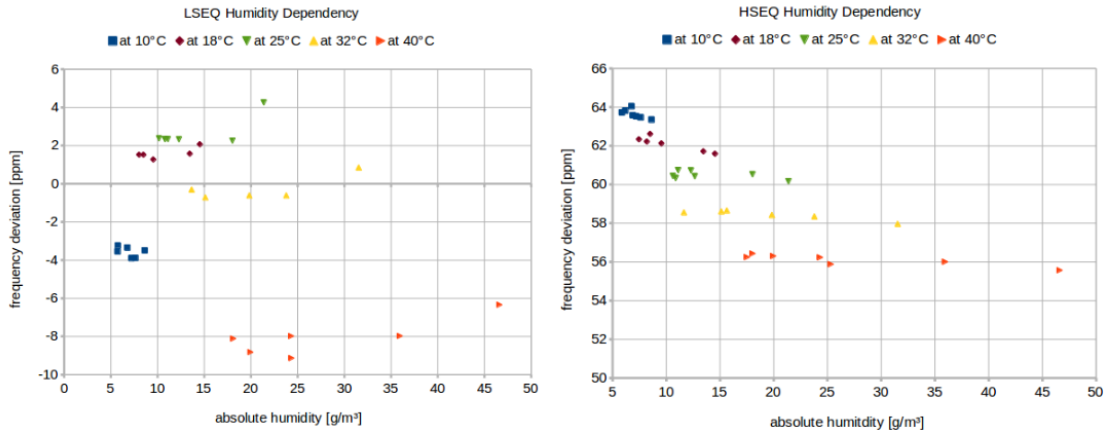
Figure 6.2: LSEQ and HSEQ Humidity Dependency

6.1.3 Acceleration Experiments

The LSEQ and the HSEQ are placed orthogonally on the Printed Circuit Board (PCB), cf. Figure 5.1. This allows to observe the frequency deviation in the x-direction of one XO and in the y-direction of the other one in the same experiment. First, the PCB is placed on the plastic plate such that the g-acceleration is at the maximum in the x-direction and zero in the y-direction. After the set of experiments in this placement was done, the PCB is rotated on the plate by $90°$ to have the maximum g-acceleration in the y-direction, cf. Figure 6.3 and Figure 6.4 for the LSEQ and HSEQ experiments output, respectively. To differentiate between the two acceleration experiments, the direction is added as a prefix, e.g. the y-experiment or the x-acceleration.
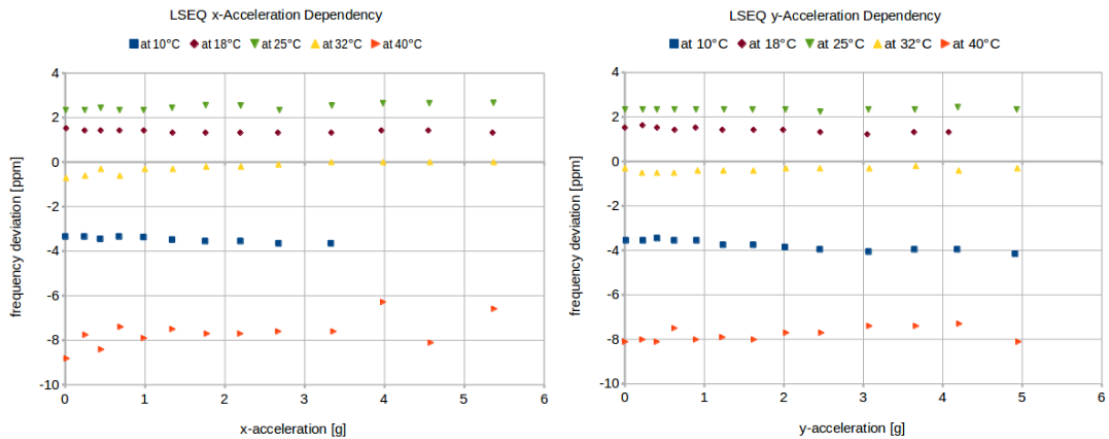
Figure 6.3: LSEQ Acceleration Dependency
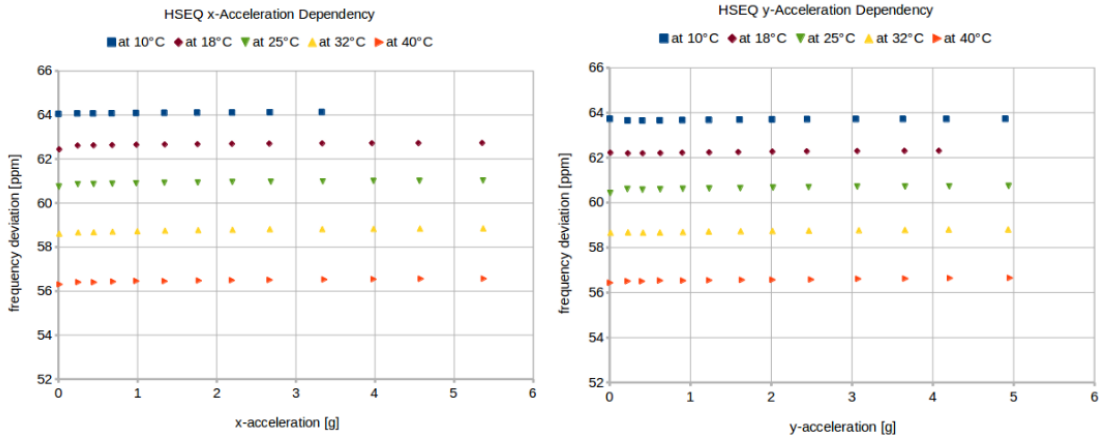
Figure 6.4: HSEQ Acceleration Dependency

6.1.4 Pressure Experiments

Compared to the other environmental conditions, the XOs do not respond to the pressure variations in the respective operation range. The result of the experiment design is depicted in Figure 6.5. The left diagram shows the *no* response of the LSEQ to pressure variations at 25 °C. The frequency deviation in this experiment is equal to the observed deviation at the same temperature setpoint without the pressure variation, which is aligned to the secondary y-axis in the left diagram. The right diagram illustrates the result of the experiments on the HSEQ.
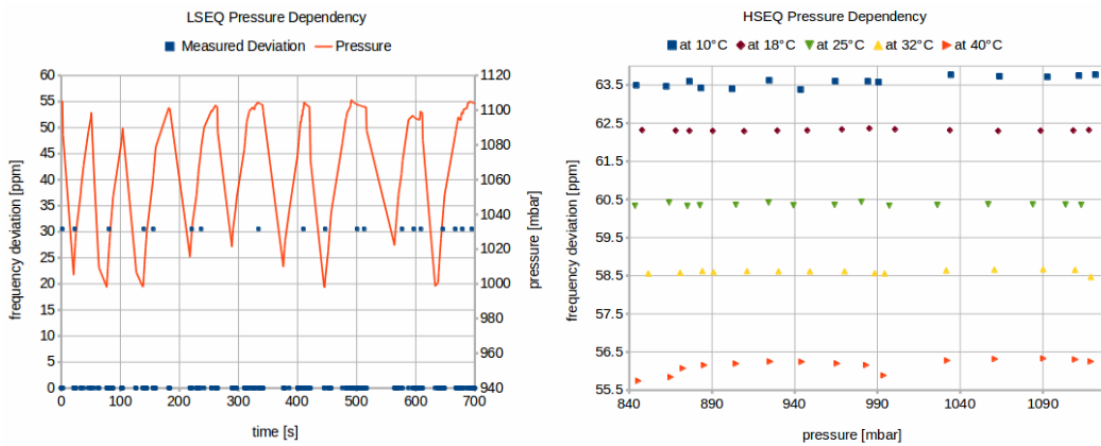
Figure 6.5: LSEQ and HSEQ Pressure Dependency

6.2 The Compensation Model

The aim of this part is to evaluate and prepare the collected data for the model deployment part. The development of the individual compensation models is discussed in Subsection 6.2.1, whereas Subsection 6.2.2 introduces the sampled compensation models, i.e. the compensation functions.

6.2.1 Individual Compensation Models

The first step is to evaluate the results from the temperature and the humidity experiments in order to develop their compensation models. These models are applied on the results of the acceleration and pressure experiments. Afterwards, their experiment results are evaluated. The observed dependencies are modeled using the regression analysis technique. The output of this part is the compensation models of the individual environmental conditions.

6.2.1.1 Temperature Compensation Model

The LSEQ exhibits a temperature dependency, that can be modeled by a quadratic function, i.e. a parabola. Another approach is to perform linear interpolation between the known pairs (*temperature* , *frequency deviation*) to model the dependency. The compensation model hence is given by a function, that is piecewise-defined by linear functions. Both models have been tested with the verification data. The second modeling approach induces less compensation error at extreme temperature values, i.e. at temperatures higher than $40\,°C$ or less than $10\,°C$. The parameters of the LSEQ temperature model is given in Table B.1.

The temperature dependency of the HSEQ can be intuitively modeled by a linear function, but the tests on the verification data revealed that the same approach as for the LSEQ achieves better results. Hence, the compensation model of the HSEQ temperature dependency is given by a piecewise-linear function. The frequency of the HSEQ has a deviation offset from the nominal frequency, cf. Figure 6.1. This deviation can be corrected by achieving a zero-crossing point. For this reason, the data is shifted by the frequency deviation at $25\,°C$, which is $60.4378 ppm$. This value represents a basic correction value, that is characteristic for the HSEQ and can be always applied independent of the correction by the compensation model. The term *Basic Compensation* refers to this correction in the course of this thesis. Table B.1 provides the parameters of the shifted HSEQ temperature model.

The temperature dependency of the LSEQ and HSEQ and the two compensation models of each XO are depicted in Figure 6.6. Mainly the right diagram shows that the piecewise-linear function has less compensation error than the linear function. These models are applied on the output of the other experiments as the first step in their model development in order to compensate the temperature effect.
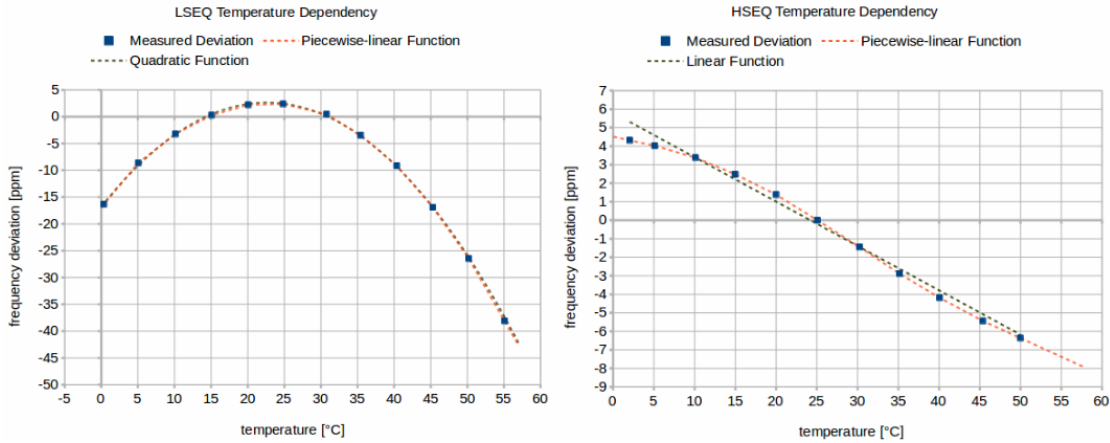
Figure 6.6: LSEQ and HSEQ Temperature Compensation Models

6.2.1.2 Humidity Compensation Model

The hardware setup has some limitations regarding the humidity control loop, see Section 5.1.2.3. For this reason, it is essential to to point out that the humidity compensation model is applied only in the achieved range during the experiments, i.e. no extrapolation is made outside the operation range. The compensation models for the LSEQ and HSEQ are given in Figure 6.7 and Figure 6.8. The left diagrams show the output of the experiments in the achieved humidity range and at the different temperature setpoints. On the right diagrams the same data is depicted after the temperature compensation. Additionally, the developed compensation models are pictured for each temperature range in fine dashed lines. The dependencies are modeled using cubic polynomials, cf. Table B.2 for the parameters of the polynomials.
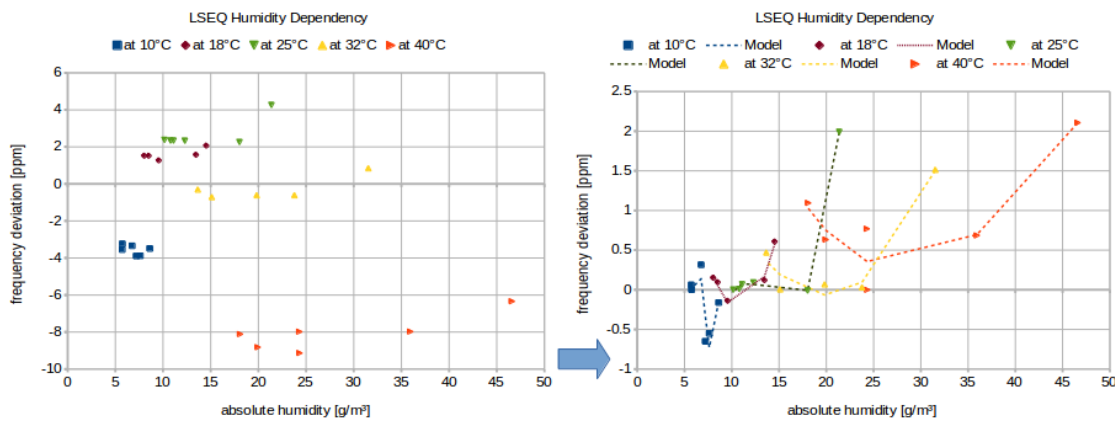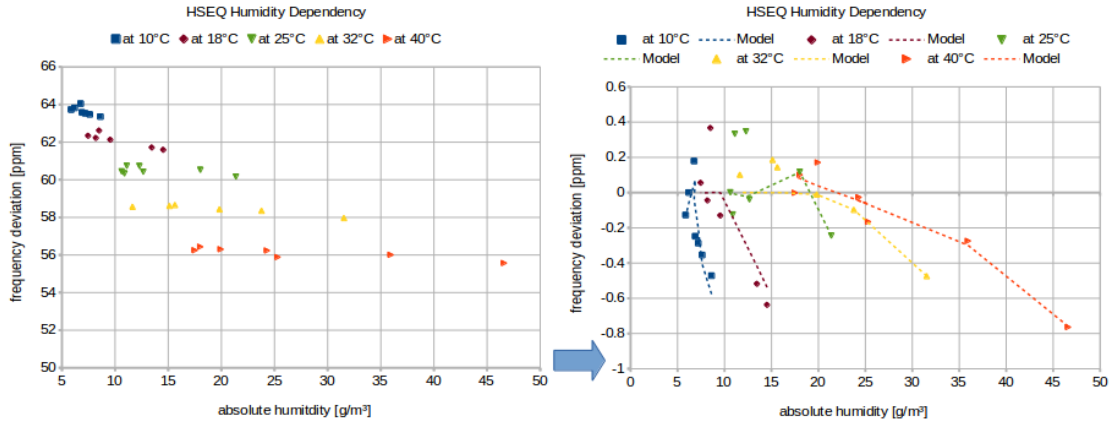

Figure 6.7: LSEQ Humidity Compensation Models

Figure 6.8: HSEQ Humidity Compensation Models

6.2.1.3 Acceleration Compensation Models

The previous compensation models are applied on the result of the acceleration experiments. The first step is the temperature compensation, then the humidity compensation. Due to measurement and compensation errors, the resulting data exhibits a minimal frequency deviation at zero acceleration. To hold to the assumption "*zero deviation at zero acceleration*", the data is shifted horizontally. The shift value is in average $0.03ppm$ for the HSEQ and $0.004ppm$ for the LSEQ. In the following figures the development of the acceleration compensation model is depicted in both directions for the LSEQ, see Figure 6.9 and Figure 6.10, and the HSEQ, see Figure 6.11 and Figure 6.12. The left diagrams show the experiment result and the right ones the compensated and shifted data. The respective compensation models are depicted in fine dashed lines. Tables B.3 and B.4 list the parameters of the modeling functions. Mainly quartic polynomials, i.e. polynomials of degree four, are used to model the dependencies.
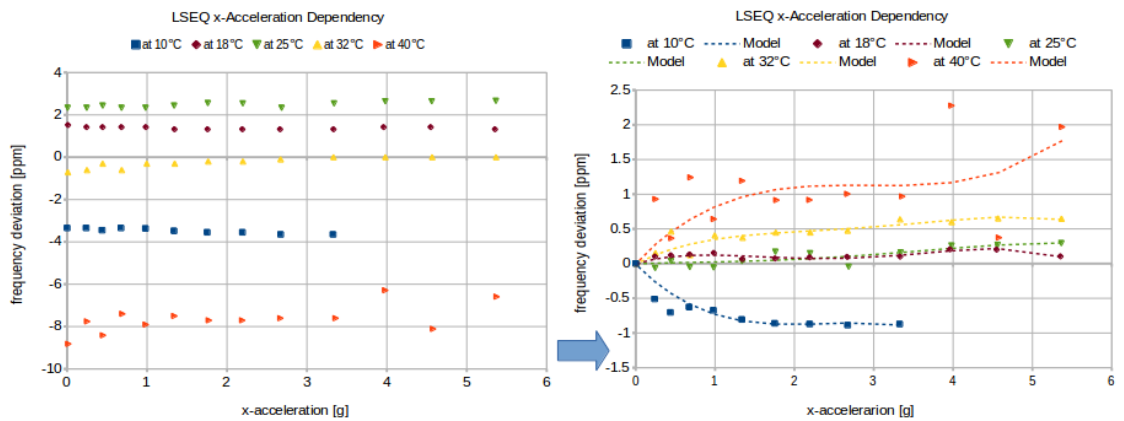

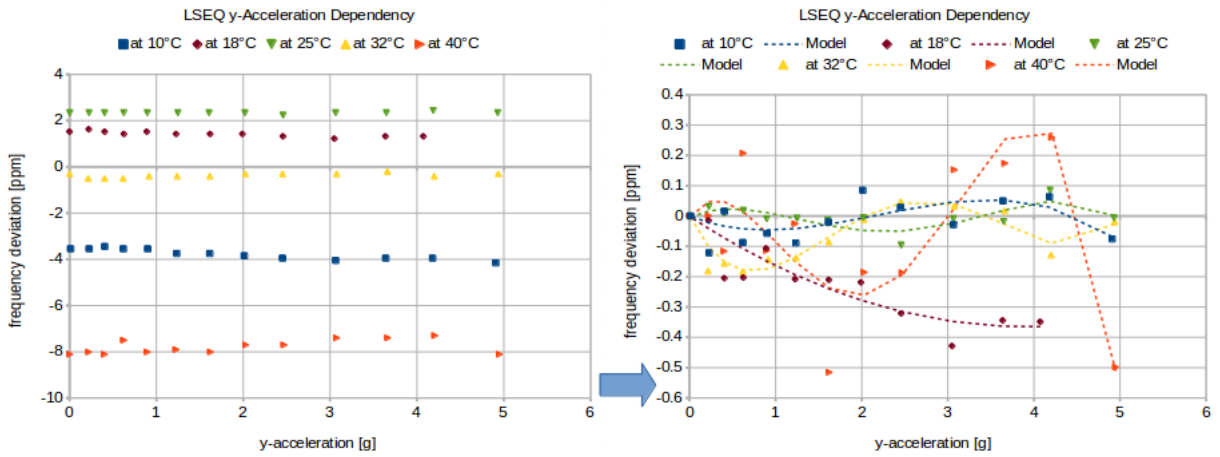Figure 6.9: LSEQ x-Acceleration Compensation Models
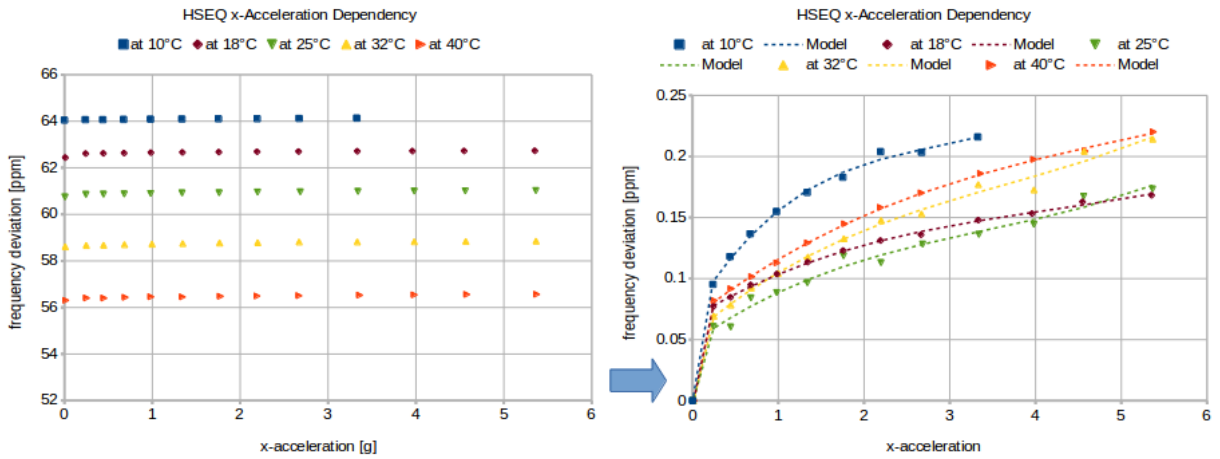
Figure 6.10: LSEQ *y*-Acceleration Compensation Models
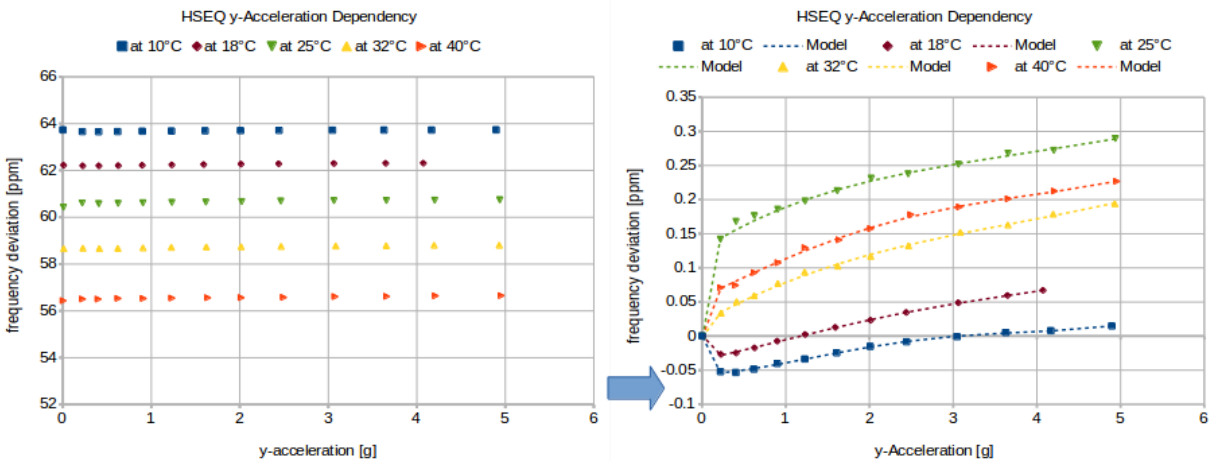

Figure 6.11: HSEQ *x*-Acceleration Compensation Models

Figure 6.12: HSEQ *y*-Acceleration Compensation Models

91

6.2.1.4   Pressure Compensation Model

During the experiments the LSEQ did not expose any observable dependency on the pressure in the achieved operation range. Therefore, no pressure compensation model was developed for the LSEQ.

The joint effect of the temperature and pressure on the HSEQ was discussed in Section 5.3.1. The temperature model hence compensates the major effect, whereas a minimal deviation of a mean of $0.05ppm$ is still measurable after the temperature and humidity compensation, cf. Figure 6.13. Quintic functions, i.e. polynomials of degree five, model the remaining HSEQ dependencies in the various temperature ranges, cf. Table B.5 for the parameters of the polynomials.
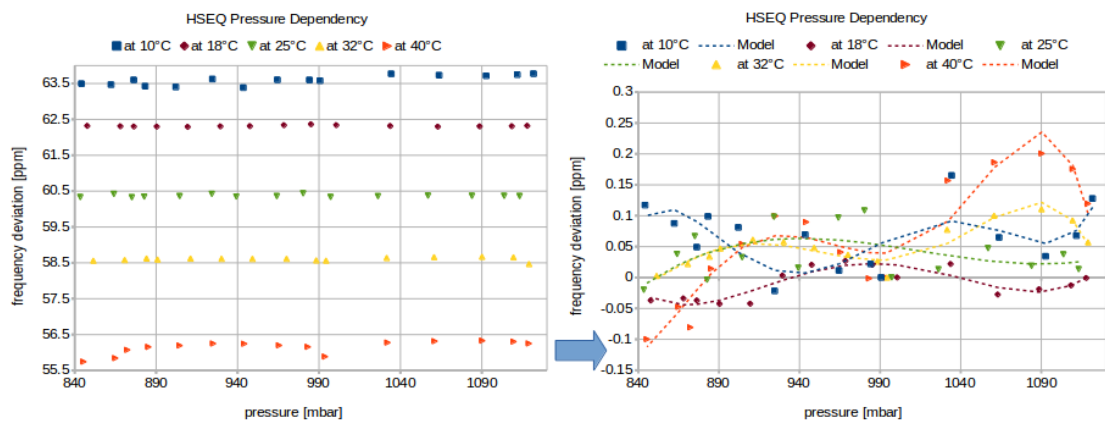

Figure 6.13: HSEQ Pressure Compensation Models

6.2.2   Compensation Functions

This subsection discusses the sampling of the compensation models, which results in the compensation functions. Providing the compensation algorithm on the main controller with the compensation functions and their parameters is the last step in this part.

The sampling step size depends on the modeling function and on the operation range. In this implementation, the number of samples per modeling function was fixed and the sampling step size is calculated out of the number of samples and the width of the respective operation range. The parameters of the compensation functions depend on the experiment design. Table B.6 gives an overview of the characteristics of the sampling procedure.

The result of the sampling procedure is implemented on the main controller afterwards. The compensation functions of the HSEQ for the temperature and the y-acceleration are

depicted in Figure 5.15 and Figure 5.17 as examples for the implementation on the main controller. This comprises the following:

- The sampled values are stored in arrays as correction values in *ppm*.

- The number of rows determines the count of temperature setpoints, whereas the column size determines the number of samples.

- The sampling step size is needed by the compensation algorithm for each compensation function to perform linear interpolation or extrapolation.

6.3   Model Deployment

The compensation algorithm corrects the deviation caused by the studied environmental conditions based on the XO specific compensation model. This is realized by calculating the compensation values out of the individual compensation functions, summing them up and converting them to a correction value for the counter of the Crystal Oscillator based Clock (XOC). To integrate an environmental condition into the model, the compensation algorithm has to be provided with the compensation function and its parameters. Figure 5.15 depicts this for the HSEQ temperature compensation.

In this section the results of the final experiments are introduced. First, initial tests on individual conditions are performed to validate the respective compensation model, see Section 6.3.1. Afterwards, three experiments on the system were performed in the open loop operation mode, see Section 6.3.2. These experiments combine the effects of the four environmental conditions on both XOs. The system operation is triggered by the GPS-receiver. On each GPS_PPS the system outputs the readout of its sensors, the compensation value for each condition and the corrected LSEQ and HSEQ frequencies, cf. Figure 5.19. The last experiment covers the compensation of the temperature effect on the HSEQ in the closed loop operation mode, see Section 6.3.3, where the system operates autonomously and generates its own PPS, cf. Figure 5.20.

6.3.1   Initial Tests

The initial tests in the model deployment part are concerned with individual environmental conditions. The aim is to test the efficiency of the compensation models. This is done by running the compensation algorithm for individual conditions and by comparing the output of the algorithm, i.e. the corrected frequency, with the nominal frequency. In the following, some of the experiments and results are introduced in the course of testing the temperature compensation models.

The temperature has the major effect on the frequency. Therefore, heating and cooling experiments were performed. The temperature inside the chamber was set first to $0\,°C$. The system is triggered by the GPS-receiver and the temperature setpoint is

changed to 55 °C. As the temperature inside the chamber reached the second setpoint and stabilized there, the setpoint is changed back to 0 °C. The output of the system is recorded during the rise and drop time of the temperature. Figure 6.14 and Figure 6.15 show the measured and the compensated HSEQ frequencies in relation to temperature rise and drop during the experiment. Additionally, the basic-compensated frequency is depicted as a shift of the measured frequency. The right diagrams depict the same data on the left ones except the measured frequency to outline the difference between the basic and the temperature compensation.

Figure 6.16 illustrates the result of the experiments on the HSEQ. The non-compensated, the basic-compensated and the temperature-compensated frequencies are shown. The result of the LSEQ is depicted in Figure 6.17. The numerical characteristics of the LSEQ and HSEQ compensation procedure are given in Table C.1. These values are averaged over the duration of the experiments.
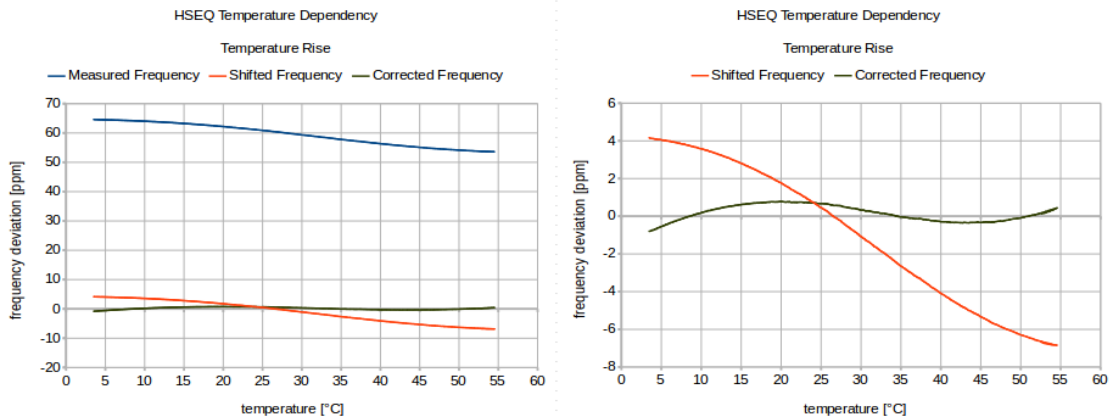

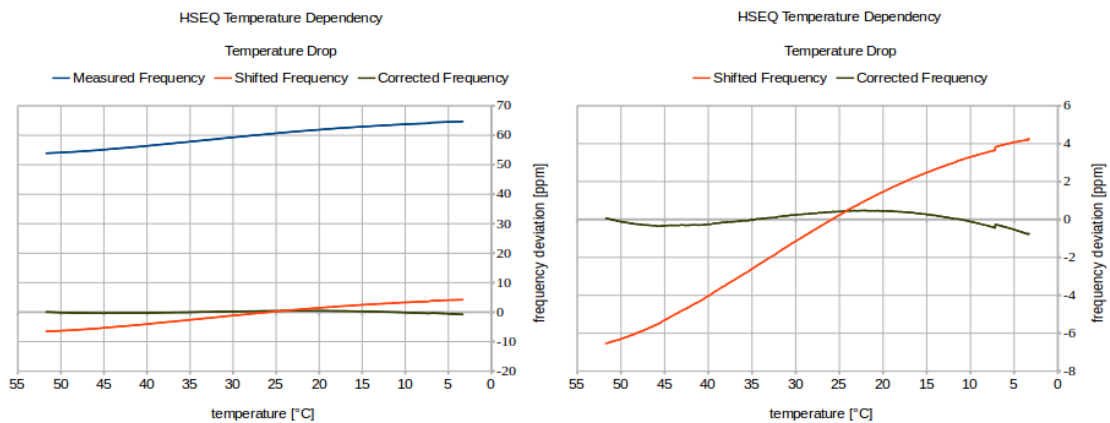Figure 6.14: HSEQ Behavior during the Temperature Rise

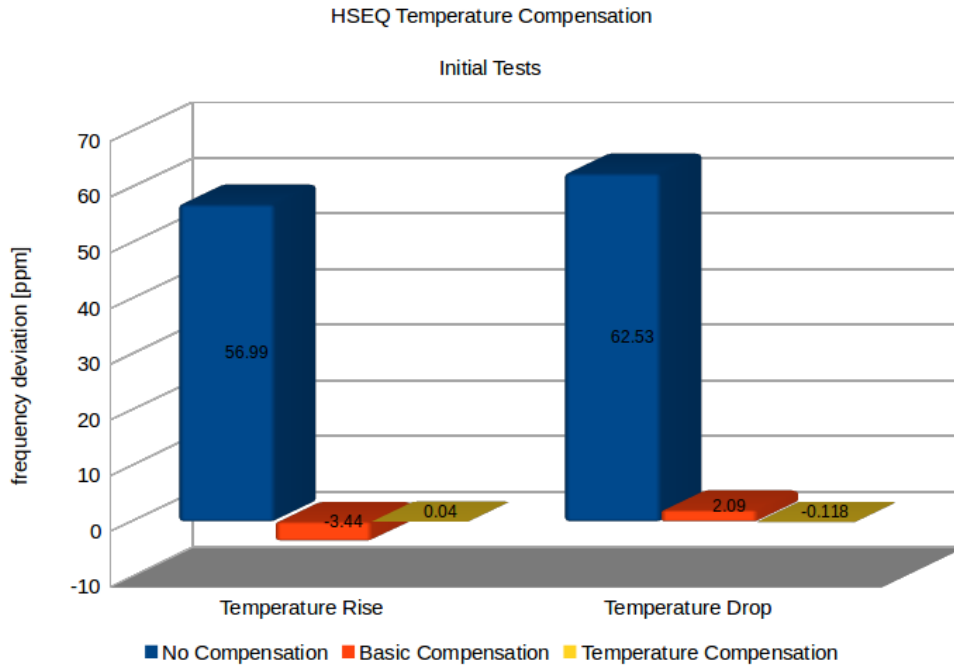Figure 6.15: HSEQ Behavior during the Temperature Drop

94

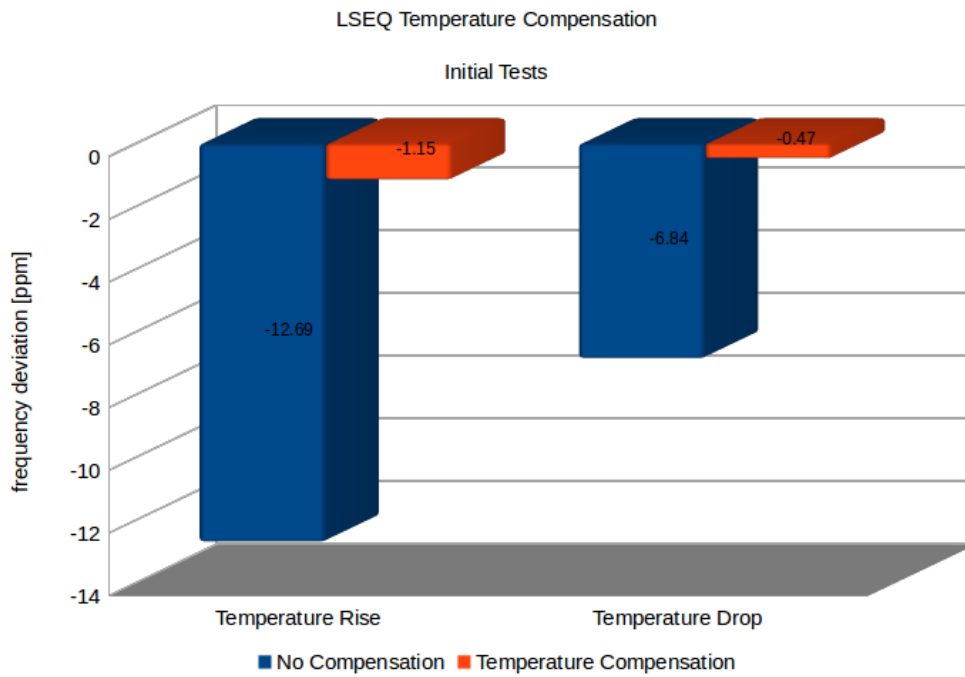Figure 6.16: HSEQ Averaged Deviations in the Initial Tests

Figure 6.17: LSEQ Averaged Deviations in the Initial Tests

The initial tests revealed that, in the temperature rise experiment, the HSEQ and the LSEQ had a deviation over the temperature of $\pm56.99ppm$ and $\pm12.69ppm$, respectively. The basic compensation of the HSEQ reduced this deviation to $\pm3.44ppm$. This is a compensation of 16 to 1. The temperature compensation achieved a reduction to $\pm0.04ppm$ for the HSEQ, which is a compensation of 86 to 1, and $\pm1.15ppm$ for the LSEQ as a compensation of 11 to 1.

In the temperature rise experiment the basic compensation of the HSEQ achieved a compensation of 30 to 1, whereas the temperature compensation achieved a a compensation of 17 to 1 for the HSEQ and of 14 to 1 for the LSEQ.

6.3.2 Open Loop Experiments

After validating the individual compensation models they are combined to form the XO specific compensation model. The compensation algorithm on the main controller corrects the frequency of the LSEQ and the HSEQ based on the environmental conditions in the chamber, that are controlled by the external controller.

Figure C.1 and Figure C.3 illustrate the design of the open loop experiments, i.e. the design from the control loops point of view, where the combinations of the different conditions in relation to the time axis are depicted. Figure C.2 and Figure C.4 depict the comparison between the setpoints of the control loops on the external controller, in continuous lines, and the measured values by the main controller inside the chamber, in dashed lines.

The aim of the open loop experiments is to combine the various environmental conditions in the chamber to reveal their individual and joint effects. For instance, this is equivalent to different weather conditions a mobile system can be exposed to. The averaged measured and compensated frequency deviations are listed in *ppm* and in Hz in Table C.2. These values comprise the measured, the basic-, the temperature- and the full-compensated HSEQ frequencies and the measured and the full-compensated LSEQ frequencies. The term *Full Compensation* reflects the fact that all available compensation models of the studied conditions are applied to correct the measured frequency.

Figure 6.18 illustrates the results of the correction of the HSEQ frequency. For a better illustration of the differences between the compensated values, Figure 6.19 depicts the same data except the non-compensated frequency. The HSEQ had a deviation of $\pm61.78ppm$ in average. The basic compensation reduced the deviation to $\pm1.34ppm$ and the full compensation to $\pm0.128ppm$. This is a compensation of 46 to 1 and then of 10 to 1.

The results of the LSEQ correction are depicted in Figure 6.20. The LSEQ had a deviation of $\pm1.78ppm$ in average. The full compensation reduced the deviation to $\pm0.22ppm$. This is a compensation of 8 to 1.
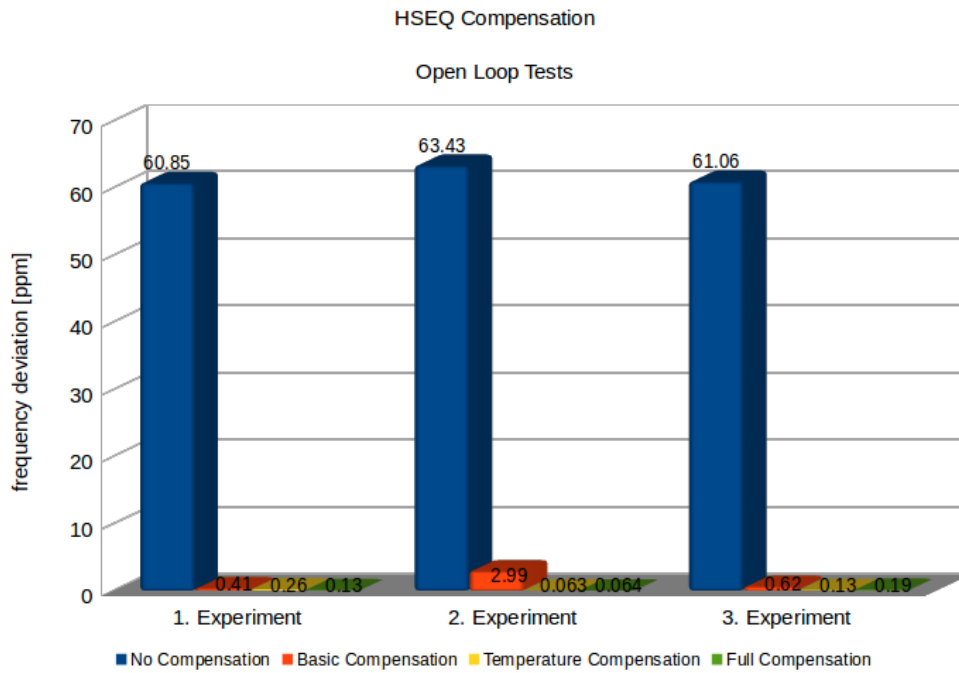
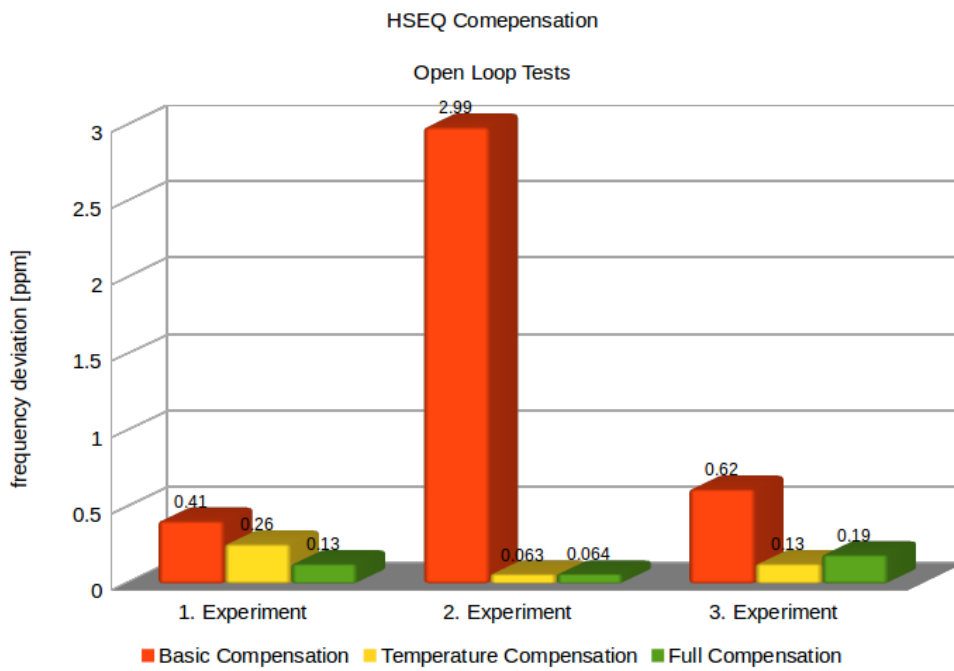Figure 6.18: Open Loop Tests on the HSEQ

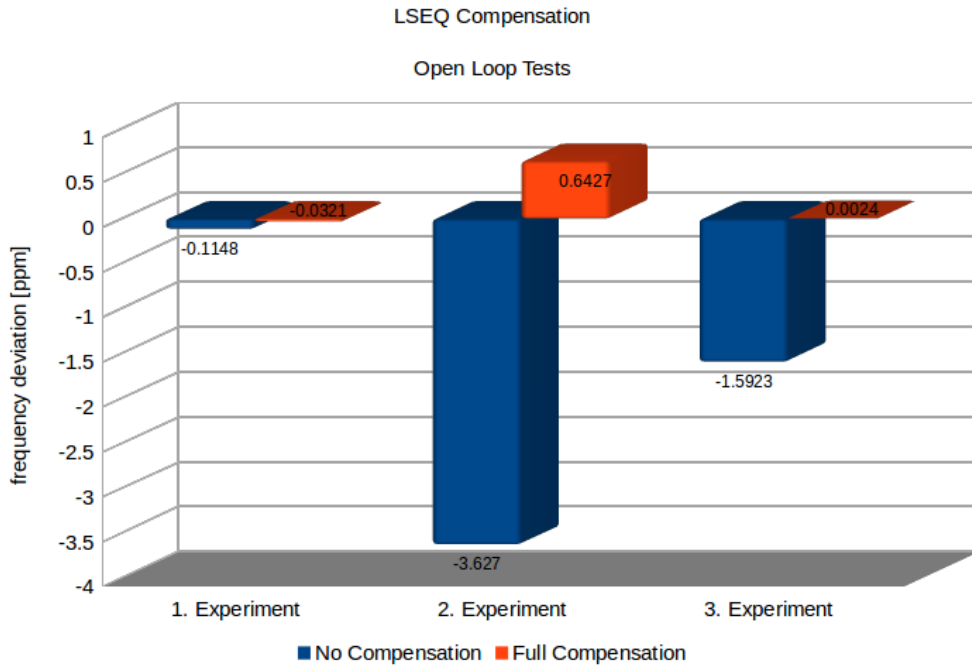Figure 6.19: HSEQ Compensated Frequency

Figure 6.20: Open Loop Tests on the LSEQ

The reduction of the frequency deviation by the compensation model, illustrated in Figure 6.18, Figure 6.19 and Figure 6.20, reflects the achieved improvement in the precision of the XOs since these values are the averaged ones. Additionally, Table C.3 shows the reduction in the variance of the HSEQ compensated frequency, which implies an improvement of the accuracy, Figure 2.1 illustrates the difference between the precision and the accuracy of a clock.

Incidentally, the basic compensation improves the precision of the HSEQ since it performs a shifting of the measured frequency by a fixed value, see Subsection 6.2.1.1, but it does not improve its accuracy.

6.3.3 Closed Loop Experiments

The GPS-receiver provides the system with a GPS_PPS as an initial trigger. Afterwards, the GPS-receiver is disconnected and the system generates its own time signal, the SYS_PPS, based on the HSEQ corrected frequency. The experiment lasted for 10 minutes and is done first without compensation, then with basic compensation and finally with temperature compensation. When the experiment time elapses, the deviation of the SYS_PPS from the GPS_PPS is measured using an oscilloscope. The deviation is measured in ms and converted to ppm. Table C.4 points out the result of the performed experiments at three different temperature values. Figure 6.21 illustrates the results in ppm.
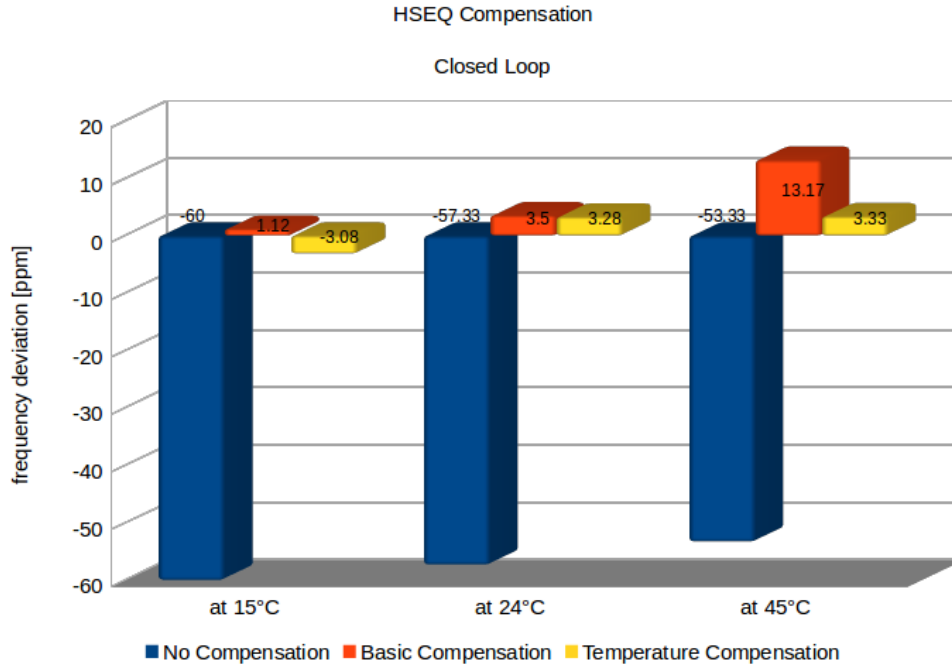
Figure 6.21: Closed Loop Tests on the HSEQ

During the last experiment, i.e. when running the temperature compensation, the system improved its accuracy by considering the time difference t between the GPS_PPS and the SYS_PPS. The GPS-receiver is left connected for 10 minutes before disconnecting it. This is necessary for the system to calculate c_A, the additional correction value. As discussed in Subsection 5.4.2.2, c_A is initially set to zero and updated on each GPS_PPS from the previous correction value c_{Ap} and the current time difference by the following equation:

$$c_A = 0.1 \cdot t + 0.9 \cdot c_{Ap}$$

The timeout T of the waiting timer is set to $0.78ms$. The timeout is set experimentally as a maximum deviation of $\frac{0.78ms}{4} = 0.195ms$ between the two signals, the SYS_PPS and the GPS_PPS, was observed during the experiments.

The closed loop tests revealed that the HSEQ had a deviation over the temperature setpoints $15\,°C$, $24\,°C$ and $45\,°C$ of $\pm60ppm$, $\pm57.33ppm$ and $\pm53.33ppm$, respectively. The basic compensation achieved a reduction to $\pm1.12ppm$, $\pm3.5ppm$ and $\pm13.17ppm$. This is a compensation of 53 to 1, 16 to 1 and 4 to 1.
The temperature compensation and the implemented learning technique achieved a reduction to $\pm3.08ppm$, $\pm3.28ppm$ and $\pm3.33ppm$. This is a compensation of 19 to 1, 17 to 1 and 16 to 1.

6.4 Requirement Fulfillment

This section discusses the presented results while having the defined requirements in Section 3.1 in mind. The following subsections show that, by analysis of the method or by concluding the experimental results, the proposed approach fulfills these requirements.

6.4.1 R1: Extensibility of the Hardware

One of the main concerns of this approach is to develop a compensation model that is XO specific, on one hand, and that is able to fit to the wide range of XOs, on the other hand. The compensation model relies only on the behavior of the XO, that is recorded in the data collection part, see Section 4.2, and modeled in the model development part, see Section 4.3. This means that replacing the XO necessitates redoing both parts, but no XO specific property or configuration plays a role in this approach. For instance, replacing an AT-cut XO with a SC-cut XO is possible even if it will lead to a different behavior and hence to different model parameters. The implementation compensates the frequency deviation of two different XOs with two different behaviors.

This is also applicable for replacing the used sensors. It does not affect the behavior of the XO, but the precision of the collected data and the need to add or remove readout post-processing. Replacing the digital temperature sensor in this implementation by a an analog one necessitates filtering the readout if its noisy, for example.

6.4.2 R2: Extensibility of the Software

The current implementation of the proposed approach considers four environmental conditions, where each condition has its sub-model. Leaving one condition out of consideration is done by removing or not considering its sub-model while calculating the XOC counter correction value out of the individual compensation values. The LSEQ shows no response to the pressure variation and hence no model was developed, whereas the model of the HSEQ consider the compensation models of the four environmental conditions.
To consider a new environmental condition, the behavior of the XO in the presence of this condition has to be recorded and modeled. Afterwards, the corresponding sub-model has to be considered while calculating the XOC counter correction value. The existing sub-models remain untouched. This has to be done also if the operation range of some condition needs to be expanded or shifted.

The XO behavior is modeled using an offline learning technique. Additionally, the system is able to improve its compensation by implementing an online learning technique, see Section 4.3.2. A simple technique is implemented, that is based on observing the timeliness of the SYS_PPS in comparison with the GPS_PPS over time and considering any noticeable differences in addition to the calculated XOC counter correction values.

6.4.3 R3: Manageable System Complexity

The main sources of complexity in a compensation system are the following:

- The number of the considered environmental conditions: This source of complexity is managed by developing a sub-model for each condition and by combining the output of each sub-model by the offline learning technique to calculate the final XOC counter correction value, see Figure 4.4.

- The possible interdependencies between several environmental conditions: The previous solution structures the effects of each condition in its sub-model, but it does not reduce the complexity of interdependencies between them. Hence, this complexity is managed as follows:

    - While studying the effect of some environmental condition on the XO, the other conditions are kept constant.

    - The temperature has the highest impact on the frequency of the XO and on the used sensors among the considered environmental conditions. To achieve a well-defined temperature dependency, the data collection of other conditions is repeated at the different temperature setpoints, which cover the achievable temperature operation range.

    - The environmental conditions are ranked by the level of their impact on the XO frequency in their operation ranges. The experiments yields the following ranking: Temperature and humidity as permanent disturbing factors, then the acceleration when its present. The effect of the pressure is hardly noticeable.

    - The development of the sub-models in the model development part is performed by considering the before mentioned ranking, i.e. the temperature sub-model is developed first and applied on the remaining data, then the humidity is modeled and so on.

6.4.4 R4: Accuracy Improvement at Low Cost

The open loop experiments show that the full compensation is able to achieve an improvement of one order of magnitude for both XOs, whereas the temperature compensation and the online learning achieved an improvement of two orders of magnitude for the HSEQ. For instance, if the requirement on the system is not to have a deviation of more than $1ms$ in the absence of the external time reference, the uncompensated HSEQ provides a holdover of $17s$ whereas the compensated HSEQ provides a holdover of $309s$.

These results are achieved with the regression analysis as an offline learning technique and a simple averaging filter as on online learning technique. The current offline sampling of the models needs $4KBytes$ of Read-Only Memory (ROM). The CPU has a workload of 40% in the open loop mode when compensating the effects on both XOs and of 30% in the closed loop mode while the HSEQ temperature compensation and the online

learning technique are running. Better results can be achieved by reducing the sampling size to have less sampling and interpolation errors or by using online calculation of the compensation values. Possible improvements will be the scope of the next chapter, see Section 7.2.

CHAPTER 7

Conclusion and Future Work

This chapter concludes the thesis by summarizing the main contributions and results, as well as giving an overview concerning the possible improvements on the implementation and future system extensions.

7.1 Summary

In the previous chapters a model-driven approach to compensate the effects of the environmental conditions on a Crystal Oscillator based Clock (XOC) with the results of its implementation are presented. This approach relies on a Quartz Crystal Oscillator (XO) specific compensation model in the sense that it depends on the observed behavior of the XO in the presence of the environmental conditions to correct the clock counter. The model does not depend on any specific feature of the XO, such as the cut type. Furthermore, the approach relies also on commonly used sensors.

The proposed approach does not require an explicit model of the quartz. To define an explicit physical model, all relevant physical properties of the XO including their interdependencies, the dependency of the XO and the measuring equipment on the environmental conditions have to be precisely known. In order to model the quartz behavior, an implicit model using a machine learning technique is developed, which represents a more convenient practice.

The deployed hardware provides two XOs, the High Speed External Quartz (HSEQ) with a nominal frequency of 8MHz and the Low Speed External Quartz (LSEQ) with a nominal frequency of 32.768kHz. Two models are developed to compensate the frequency deviation of the available XOs. The system clock is based on the HSEQ because of its high nominal frequency, whereas the LSEQ can be used as a base for a Real-Time Clock (RTC) because its nominal frequency is a power of two (2^{15}), which allows to

simply generate a precise Pulse Per Second (PPS) when the 15-bit counter of the RTC overflows.

The direct dependencies, that were observed in the data collection part, support the decision to apply the regression analysis as a modeling technique. The implementation deploys sub-models, one for each environmental condition, instead of one enormous model with higher complexity. Hence, the system complexity is managed by structuring the complexity in the sub-models and by the experiment design, which guarantees that the individual and the joint effects of the environmental conditions are differentiable in the collected data, such that an accurate and efficient modeling of the XO behavior is possible. This architecture makes it possible to extend the existing approach to consider additional conditions by developing additional sub-models.

Apart from the offline modeling technique, an online learning technique is implemented to improve the correction carried out by the compensation model. The timeliness of the generated time signal is compared to the external reference time when it is available. Any significant differences over time are considered in addition to the calculated correction value.

Furthermore, the proposed approach fits to different application fields. The requirements on the system holdover and on its implementation costs determine the applicable implementation of this approach including the used modeling technique and hence the achievable improvement in the frequency deviation. An improvement of one order of magnitude for both XOs is achieved, not considering the basic compensation of the HSEQ, that eliminates the observed deviation of $60.4378 ppm$ at $25\,^{\circ}\mathrm{C}$ to $0 ppm$, see Subsection 6.2.1.1. The temperature compensation combined with the online learning technique achieves a further improvement of one order of magnitude in the precision of the HSEQ. Additionally, the variance, i.e. the accuracy, of the HSEQ frequency is improved by 178 to 1, in average.

Compared to the related work, see Section 3.2, the selection of the XO and the environmental conditions of importance do not constrain the application of this approach. A reasonable improvement in the XO accuracy and precision are achieved with a manageable system complexity. Further improvements are the scope of the next section.

7.2 Outlook

This section introduces possible extensions for the developed approach as well as further improvements on the current implementation.

7.2.1 Data Collection

Since the temperature has a major effect on the XO frequency, the temperature sensor should be mounted as close as possible to the deployed XO. In combination with the implemented temperature filter, this will provide the compensation model with more accurate temperature values.

The experiments revealed that the humidity effect can not be ignored, especially in combination with extreme temperature values, i.e. below $5\,°\mathrm{C}$ and above $45\,°\mathrm{C}$. The hardware setup allows to control the humidity in the increasing direction from the current room relative humidity up to approximately 100% only, see Subsection 5.1.2.3. As a result, a less accurate humidity model and a narrow operation range are obtained. Deploying a humidity controller, that can be interfaced by the external controller, achieves subtler humidity control in both directions and hence a more accurate humidity model.

The effect of the acceleration is studied under the assumption, that the system is mainly exposed to accelerations in one direction at the same time, such as in passenger cars. This is done by applying the acceleration condition once in the x- and then in the y-direction of the XOs by changing the placement of the Printed Circuit Board (PCB) on the plastic plate, see Subsection 6.1.3. The acceleration compensation model is acceptable when this assumption is true. On the contrary, there are applications where this assumption is not true, e.g. in helicopters and military track vehicles the acceleration in three dimensions has to be considered. Hence, the hardware setup should provide the ability to realize such scenarios, .i.e. to apply various acceleration values in the range $[min; max]$ of each direction, especially considering that the XO behaves differently when applying the acceleration in the x- and in the y-direction, see Subsection 6.2.1.3.

The external controller allows the automation of the data collection part depending on the system application. The number of environmental conditions, their coverage sets and the duration and combination of the experiments are application-specific parameters. They can be designed once and provided in a configuration file to the external controller to perform the data collection part automatically while the behavior of the XO is recorded.

7.2.2 Model Development

The regression analysis as an offline learning technique achieved an improvement of one order of magnitude in the frequency deviation of both XOs. This result can be improved by decreasing the sampling step size of the modeling functions, which reduces the sampling errors. Furthermore, implementing the calculation of the compensation values on the main controller will eliminate the sampling errors and decrease the memory consumption of the compensation algorithm.

Considering the coefficients of the compensation functions as calibration parameters allows to update the compensation model during runtime without the need to recompile

and download the C-program to the microcontroller.

The simple averaging filter as an online learning technique provides an additional improvement of one order of magnitude in the HSEQ frequency deviation. Improving the online learning technique to particularly consider the aging phenomenon can be done after collecting and modeling aging drift data, which requires long term observation of the XO behavior. A possible approach is presented in Section 4.3.2.

7.2.3 Model Deployment

The main controller is equipped with a sliding contact to obtain the time signal from the external reference time. In order to be able to perform experiments with the other environmental conditions in the closed loop mode, a second sliding contact is necessary to deliver the generated time signal to the measuring equipment, e.g. to the oscilloscope. The experiments with the environmental temperature in the closed loop mode are performed by connecting a wire between the main controller and the oscilloscope. The chamber in this case does not provide less temperature tightness, but it does not support any acceleration or pressure experiments.

A further extension to the existing approach is to detect the manipulation of the signal of the external reference time. The *Seconds Generator*, see Subsection 5.4.2.2, can be updated to estimate an expectation interval, where the reference signal has to be received. Any deviation from that interval will be considered as a manipulation of the reference signal and it will not be considered in the time signal generation or in the implemented online learning technique.

Hardware Setup
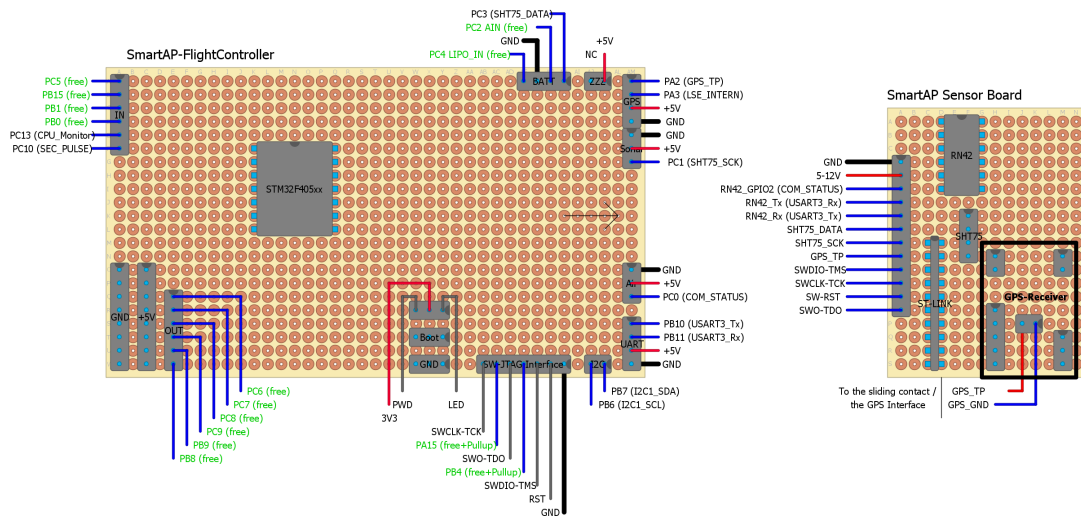
Figure A.1: Pinout of the Main Controller and its Extension Board
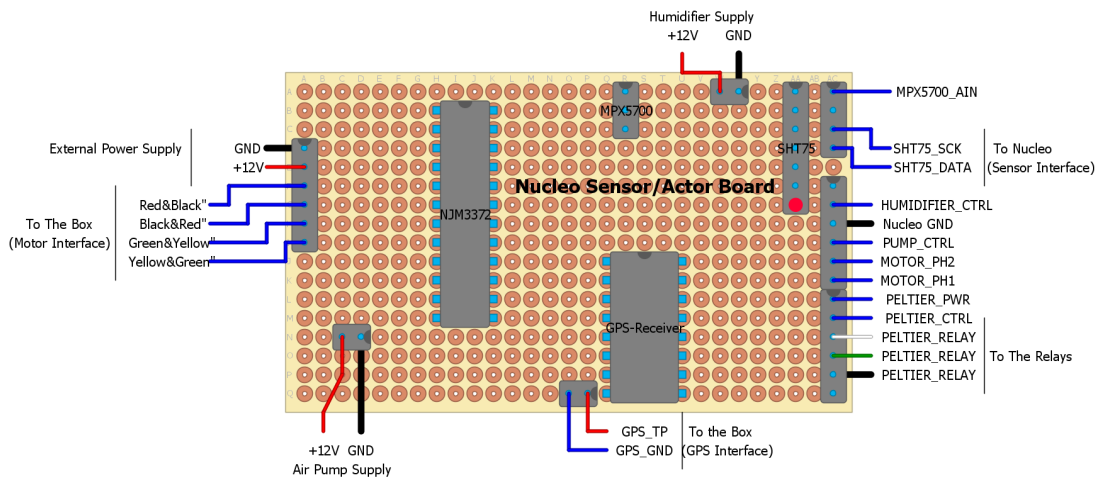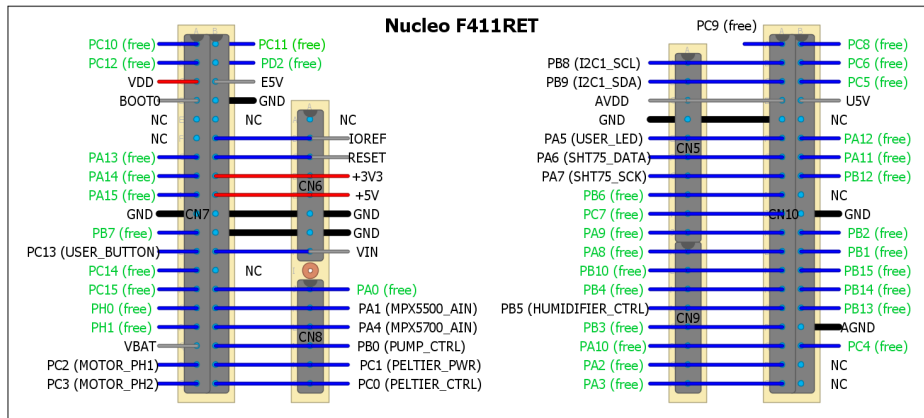
Figure A.2: Pinout of the External Controller and its Extension Board

Compensation Models and Functions

This appendix lists the parameters of the developed compensation functions. The parameters are the coefficients of polynomials, which are calculated via curve-fitting techniques in order to model the dependency of the quartz frequency on the various environmental conditions.

	LSEQ		HSEQ	
$f(x) = m * x + d$	m	d	m	d
$x \leq 0$	+1.72E+000	-1.70E+001	-9.60E-002	+4.51E+000
$x \in (0; 5]$	+1.64E+000	-1.69E+001	-9.60E-002	+4.51E+000
$x \in (5; 10]$	+1.06E+000	-1.40E+001	-1.28E-001	+4.68E+000
$x \in (10; 15]$	+7.11E-001	-1.04E+001	-2.20E-001	+5.79E+000
$x \in (15; 20]$	+3.84E-001	-5.51E+000	-2.20E-001	+5.79E+000
$x \in (20; 25]$	+3.52E-002	+1.50E+000	-2.72E-001	+6.83E+000
$x \in (25; 30]$	-3.23E-001	+1.04E+001	-2.80E-001	+7.01E+000
$x \in (30; 35]$	-8.45E-001	+2.65E+001	-2.94E-001	+7.45E+000
$x \in (35; 40]$	-1.15E+000	+3.72E+001	-2.64E-001	+6.41E+000
$x \in (40; 45]$	-1.58E+000	+5.46E+001	-2.35E-001	+5.25E+000
$x \in (45; 50]$	-1.95E+000	+7.13E+001	-2.01E-001	+3.68E+000
$x > 50$	-2.38E+000	+9.29E+001	-2.01E-001	+3.68E+000

Table B.1: Parameters of the HSEQ and LSEQ Temperature Modeling Functions

	$10\,^{\circ}\mathrm{C}$	$18\,^{\circ}\mathrm{C}$	$25\,^{\circ}\mathrm{C}$	$32\,^{\circ}\mathrm{C}$	$40\,^{\circ}\mathrm{C}$
HSEQ: $f(x) = a * x^3 + b * x^2 + c * x + d$					
a	+5.03E-001	+0.00E+000	+6.65E-003	+6.83E-005	-1.08E-004
b	-1.07E+001	+5.88E-002	-2.77E-001	+6.91E-003	+1.61E-002
c	+7.50E+001	-1.27E+000	+3.74E+000	-3.58E-001	-6.46E-001
d	-1.72E+002	+6.60E+000	-1.64E+001	+3.79E+000	+8.07E+000
LSEQ: $f(x) = a * x^3 + b * x^2 + c * x + d$					
a	+5.03E-001	+0.00E+000	+6.65E-003	+6.83E-005	-1.08E-004
b	-1.07E+001	+5.88E-002	-2.77E-001	+6.91E-003	+1.61E-002
c	+7.50E+001	-1.27E+000	+3.74E+000	-3.58E-001	-6.46E-001
d	-1.72E+002	+6.60E+000	-1.64E+001	+3.79E+000	+8.07E+000

Table B.2: Parameters of the HSEQ and LSEQ Humidity Modeling Functions

	10 °C	18 °C	25 °C	32 °C	40 °C
x-Acceleration: $f(x) = a*x^3 + b*x^2 + c*x + d$					
a	+4.22E-03	+6.02E-04	+9.98E-04	+9.86E-04	+4.96E-04
b	-3.57E-02	-7.64E-03	-1.03E-02	-1.09E-02	-7.75E-03
c	+1.15E-01	+4.26E-02	+5.04E-02	+6.04E-02	+5.55E-02
d	+7.19E-02	+6.79E-02	+4.75E-02	+5.44E-02	+6.74E-02
y-Acceleration: $f(x) = a*x^4 + b*x^3 + c*x^2 + d*x + e$					
a	+5.37E-04	+2.89E-04	-1.22E-04	+0.00E+00	+3.01E-04
b	-5.57E-03	-2.74E-03	+2.57E-03	+1.10E-03	-2.31E-03
c	+1.62E-02	+6.39E-03	-1.90E-02	-1.25E-02	-1.04E-03
d	+5.41E-03	+2.47E-02	+7.88E-02	+7.02E-02	+5.97E-02
e	-5.59E-02	-3.41E-02	+1.27E-01	+1.97E-02	+5.67E-02

Table B.3: Parameters of the HSEQ Acceleration Modeling Functions

	10 °C	18 °C	25 °C	32 °C	40 °C
x-Acceleration: $f(x) = a*x^4 + b*x^3 + c*x^2 + d*x + e$					
a	+0.00E+00	-8.25E-03	-1.36E-03	-5.93E-03	+7.89E-05
b	-6.91E-02	+8.64E-02	+1.18E-02	+6.99E-02	+4.49E-02
c	+4.96E-01	-2.84E-01	-2.05E-02	-2.90E-01	-3.99E-01
d	-1.15E+00	+3.27E-01	+3.54E-02	+5.76E-01	+1.16E+00
e	-9.61E-03	+1.08E-03	-1.68E-03	-5.06E-04	+1.28E-02
y-Acceleration: $f(x) = a*x^4 + b*x^3 + c*x^2 + d*x + e$					
a	+0.00E+00	+0.00E+00	-6.40E-03	+1.63E-02	-3.76E-02
b	-1.15E-02	+0.00E+00	+6.06E-02	-1.72E-01	+3.13E-01
c	+7.57E-02	+2.38E-02	-1.68E-01	+5.65E-01	-7.24E-01
d	-1.09E-01	-1.86E-01	+1.23E-01	-5.78E-01	+3.65E-01
e	-8.79E-04	-8.48E-04	-3.20E-03	+1.14E-03	-2.03E-03

Table B.4: Parameters of the LSEQ Acceleration Modeling Functions

	10 °C	18 °C	25 °C	32 °C	40 °C
$f(x) = a*x^5 + b*x^4 + c*x^3 + d*x^2 + e*x + g$					
a	+8.36E-12	+0.00E+00	+0.00E+00	-4.16E-12	-1.03E-11
b	-4.10E-08	+4.06E-10	+4.64E-12	+1.98E-08	+4.95E-08
c	+8.02E-05	-1.59E-06	+6.73E-09	-3.76E-05	-9.49E-05
d	-7.82E-02	+2.33E-03	-4.92E-05	+3.55E-02	+9.06E-02
e	+3.80E+01	-1.51E+00	+5.93E-02	-1.67E+01	-4.31E+01
g	-7.37E+03	+3.66E+02	-2.14E+01	+3.13E+03	+8.17E+03

Table B.5: Parameters of the HSEQ Pressure Modeling Functions

		10 °C	18 °C	25 °C	32 °C	40 °C
HSEQ						
Temperature	Step Size	1.00E+000	1.00E+000	1.00E+000	1.00E+000	1.00E+000
	#Samples	51	51	51	51	51
Humidity	Step Size	5.51E-002	1.41E-001	2.15E-001	3.98E-001	5.82E-001
	#Samples	51	51	51	51	51
x-Acceleration	Step Size	6.66E-002	1.07E-001	1.07E-001	1.07E-001	1.08E-001
	#Samples	51	51	51	51	51
y-Acceleration	Step Size	9.79E-002	8.15E-002	9.88E-002	9.87E-002	9.91E-002
	#Samples	51	51	51	51	51
Pressure	Step Size	5.55E+000	5.40E+000	5.40E+000	5.35E+000	5.47E+000
	#Samples	51	51	51	51	51
LSEQ						
Temperature	Step Size	1.00E+000	1.00E+000	1.00E+000	1.00E+000	1.00E+000
	#Samples	56	56	56	56	56
Humidity	Step Size	7.37E-002	1.67E-001	2.87E-001	4.58E-001	7.31E-001
	#Samples	40	40	40	40	40
x-Acceleration	Step Size	8.53E-002	1.37E-001	1.38E-001	1.38E-001	1.38E-001
	#Samples	40	40	40	40	40
y-Acceleration	Step Size	1.26E-001	1.04E-001	1.26E-001	1.27E-001	1.27E-001
	#Samples	40	40	40	40	40

Table B.6: Characteristics of the Compensation Functions

APPENDIX C

Experiments Result

The numerical results of the model deployment part, see section 6.3 are listed in this appendix.

C.1 Initial Tests

	Temperature Rise		Temperature Drop	
	HSEQ			
	Deviation [Hz]	Deviation [ppm]	Deviation [Hz]	Deviation [ppm]
Non-Compensated	4787.41	+56.99	5252.15	+62.53
Basic-Compensated	-289.59	-3.44	175.15	+2.09
T-Compensated	3.39	+0.04	-9.94	-0.118
	LSEQ			
Non-Compensated	-0.4159	-12.69	0.2242	-6.84
T-Compensated	-0.0376	-1.15	0.0156	-0.47

Table C.1: Characteristics of the HSEQ and LSEQ Initial Temperature Tests

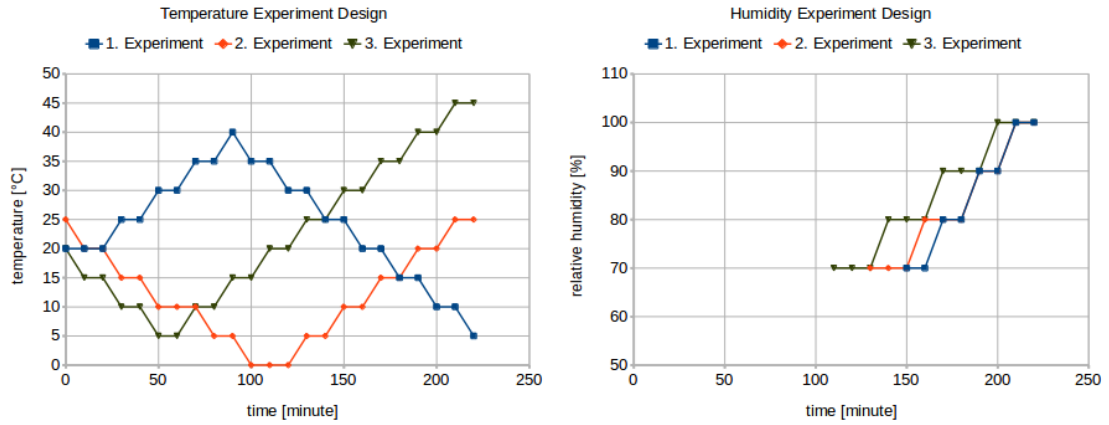## C.2 Open Loop Tests

C.2.1 Experiment Design

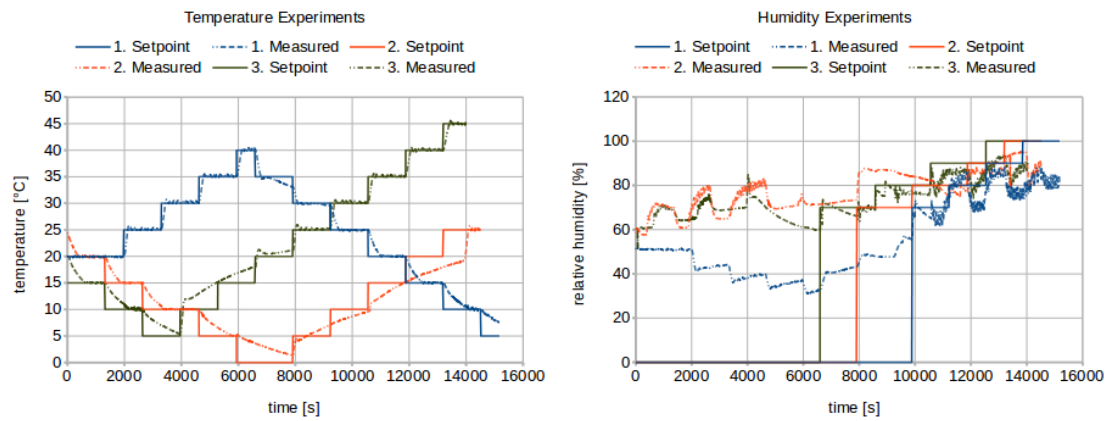Figure C.1: Temperature and Humidity Experiment Design

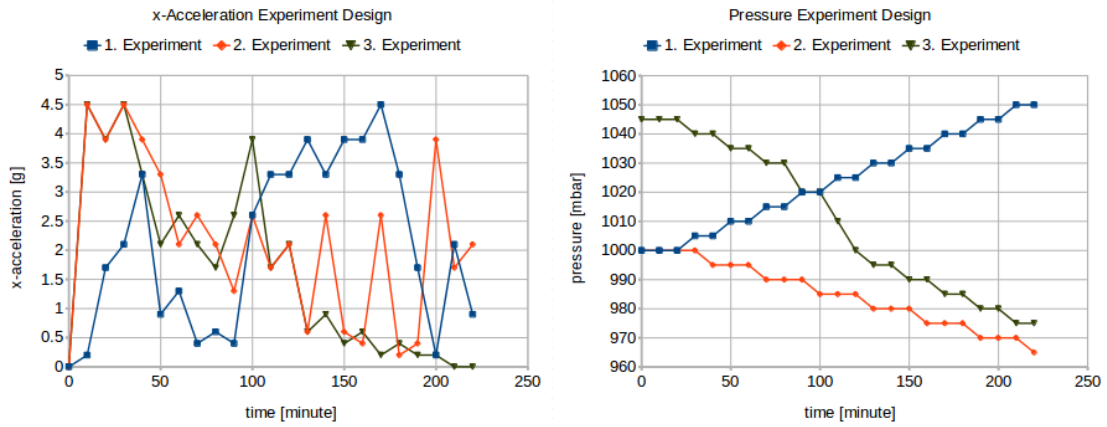Figure C.2: Temperature and Humidity Experiments

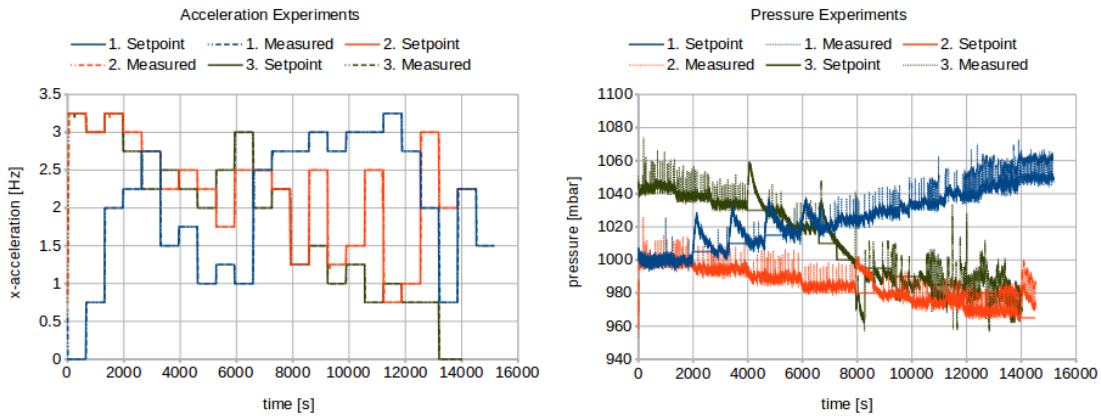Figure C.3: *x*-Acceleration and Pressure Experiment Design

Figure C.4: *x*-Acceleration and Pressure Experiments

C.2.2 Experiment Results

HSEQ			
		Deviation[Hz]	Deviation[ppm]
1. Experiment	No Compensation	5111.42	60.85
	Basic Compensation	34.42	0.41
	Temperature Compensation	22.02	0.26
	Full Compensation	11.09	0.13
2. Experiment	No Compensation	5328.50	63.43
	Basic Compensation	251.50	2.99
	Temperature Compensation	5.29	0.063
	Full Compensation	5.37	0.064
3. Experiment	No Compensation	5129.26	61.06
	Basic Compensation	52.26	0.62
	Temperature Compensation	10.76	0.13
	Full Compensation	16.36	0.19
LSEQ			
1. Experiment	No Compensation	-0.9962	-0.1148
	Full Compensation	-0.0011	-0.0321
2. Experiment	No Compensation	-0.8812	-3.6270
	Full Compensation	+0.0211	+0.6427
3. Experiment	No Compensation	-0.9478	-1.5923
	Full Compensation	+0.0001	+0.0024

Table C.2: Results of the HSEQ and LSEQ Open Loop Experiments

		Variance[ppm^2]
1. Experiment	No Compensation	4.41
	Basic Compensation	4.41
	Temperature Compensation	0.03
	Full Compensation	0.02
2. Experiment	No Compensation	1.3
	Basic Compensation	1.3
	Temperature Compensation	0.01
	Full Compensation	0.03
3. Experiment	No Compensation	8.13
	Basic Compensation	8.13
	Temperature Compensation	0.04
	Full Compensation	0.03

Table C.3: Improvements of the HSEQ Accuracy

C.3 Closed Loop Tests

	Deviation [ms]	Deviation [ppm]
at 15 °C		
No Compensation	-36	60
Basic Compensation	+0.76	1.12
Temperature Compensation	-1.85	3.08
at 24 °C		
No Compensation	-34.4	57.33
Basic Compensation	+2.1	3.5
Temperature Compensation	+1.97	3.28
at 45 °C		
No Compensation	-32	53.33
Basic Compensation	+7.9	13.17
Temperature Compensation	+2	3.33

Table C.4: The deviation between the GPS_PPS and the SYS_PPS

Acronyms

XO	Quartz Crystal Oscillator
XOC	Crystal Oscillator based Clock
GPS	Global Positioning System
OCXO	Oven Controlled Crystal Oscillator
GPSDO	Global Positioning System Disciplined Oscillator
PPS	Pulse Per Second
UTC	Coordinated Universal Time
NIST	National Institute of Standards and Technology
ADC	Analog to Digital Converter
AI	Artificial Intelligence
OCXO	Oven Controlled Crystal Oscillator
ANN	Artificial Neural Network
SCXO	Stress Compensated Crystal Oscillator
TCXO	Temperature Compensated Crystal Oscillator
GLONASS	Global Navigation Satellite System
RTC	Real-Time Clock
PCB	Printed Circuit Board

LSEQ	Low Speed External Quartz
HSEQ	High Speed External Quartz
SmartAP	Smart Autopilot
IMU	Inertial Measurement Unit
PLL	Phase Lock Loop
TEC	Thermoelectric Cooler
PWM	Pulse Width Modulated
ROM	Read-Only Memory

Bibliography

[1] A. Burns and A. J. Wellings, *Real-Time Systems and Programming Languages.* Boston, MA, USA: Addison-Wesley Longman Publishing Co., Inc., 3rd ed., 2001.

[2] M. Joseph, ed., *Real-Time Systems: Specification, Verification and Analysis.* Prentice Hall International, 2 ed., 2001.

[3] M. A. Weiss, D. W. Allan, D. D. Davis, and J. Levine, "Smart clock: a new time," in *1992 Conference Record IEEE Instrumentation and Measurement Technology Conference*, (Metropolitan, NY, USA), IEEE, IEEE, 1992.

[4] H. Kopetz, *Real-Time Systems: Design Principles for Distributed Embedded Applications.* Norwell, MA, USA: Kluwer Academic Publishers, 1st ed., 1997.

[5] F. Cristian, "Probabilistic clock synchronization," vol. 3, pp. 146–158, 1989.

[6] J. R. Vig and F. L. Walls, "Fundamental limits on the frequency instabilities of quartz crystal oscillators," in *Frequency Control Symposium, 1994. 48th., Proceedings of the 1994 IEEE International*, pp. 506–523, Jun 1994.

[7] M. Bloch, O. Mancini, T. McClelland, and L. Terracciano, "Acceleration "G" compensated quartz crystal oscillators," in *2009 IEEE International Frequency Control Symposium Joint with the 22nd European Frequency and Time forum*, pp. 175–180, April 2009.

[8] S. Yamamoto and O. Ozeki, "Rf conducted noise measurements of automotive electrical and electronic devices using artificial network," *IEEE Transactions on Vehicular Technology*, vol. 32, pp. 247–253, Nov 1983.

[9] R. N. Dean, A. Anderson, S. J. Reeves, G. T. Flowers, and A. S. Hodel, "Electrical noise in mems capacitive elements resulting from environmental mechanical vibrations in harsh environments," *IEEE Transactions on Industrial Electronics*, vol. 58, pp. 2697–2705, July 2011.

[10] M. Lombardi, A. Novick, V. Zhang, N. I. O. STANDARDS, T. B. C. TIME, and F. DIV., *Characterizing the Performance of GPS Disciplined Oscillators with Respect to UTC(NIST).* Defense Technical Information Center, 2005.

[11] D. W. Allan, Chairman, J. A. Barnes, F. Cordara, M. Garvey, W. Hanson, J. Kusters, R. Smythe, and F. L. Walls, "Precision oscillators: dependence of frequency on temperature, humidity and pressure," in *Frequency Control Symposium, 1992. 46th., Proceedings of the 1992 IEEE*, pp. 782–793, May 1992.

[12] The General Conference on Weights and Measures (CGPM), "The 13th Conference Generale des Poids et Mesures CGPM," 1967. `http://www.bipm.org/en/CGPM/db/13/1/`. Accessed 29.11.2016.

[13] "Basic SoS Concepts, Glossary and Preliminary Conceptual Model." `http://amadeos-project.eu/wp-content/uploads/2015/07/AMADEOS_D2.2_v2.6-final.pdf`. Accessed 29.11.2016.

[14] O. P. Layden, W. L. Smith, A. E. Anderson, M. B. Bloch, D. E. Newell, and P. C. Sulzer, "Crystal-controlled oscillators," *IEEE Transactions on Instrumentation and Measurement*, vol. 21, pp. 277–286, Aug 1972.

[15] J. R. Vig, "Introduction to Quartz Frequency Standards," Tech. Rep. SLCET-TR-92-1, Army Research Laboratory, Electronics and Power Sources Directorate, 1992.

[16] Leica Geosystems AG, Heerbrugg, Switzerland, *Introduction to GPS (Global Positioning System)*, 1999. Version 1.0. Available at `http://www.utdallas.edu/~aiken/GPSCLASS/GPSBasics.pdf`. Accessed 29.11.2016.

[17] M. A. Lombardi, "The Use of GPS Disciplined Oscillators as Primary Frequency Standards for Calibration and Metrology Laboratories." `http://tf.nist.gov/general/pdf/2297.pdf`, 2008. Accessed 29.11.2016.

[18] R. F. Graf, ed., *Modern Dictionary of Electronics (Seventh Edition)*. Boston: Newnes, 1999.

[19] R. Bishop, *The Mechatronics Handbook, Second Edition - 2 Volume Set*. Mechatronics Handbook 2e, CRC Press, 2002.

[20] S. Gerhard-Helge and W. Kastner, *Prozessautomatisierung*. Springer, 1998.

[21] R. Bellman, *An Introduction to Artificial Intelligence: Can Computers Think?* Boyd & Fraser, 1978.

[22] S. J. Russell and P. Norvig, *Artificial Intelligence: A Modern Approach*. Pearson Education, 2 ed., 2003.

[23] H. Motulsky and A. Christopoulos, *Fitting Models to Biological Data Using Linear and Nonlinear Regression: A Practical Guide to Curve Fitting*. Oxford University Press, 2004.

[24] R. L. Filler and J. R. Vig, "Long-term aging of oscillators," *IEEE Transactions on Ultrasonics, Ferroelectrics, and Frequency Control*, vol. 40, pp. 387–394, July 1993.

[25] M. I. of Technology. Engineering Systems Division, "Engineering systems research and practice." `https://esd.mit.edu/WPS/internal-symposium/esd-wp-2003-01.20.pdf`, 2002. Accessed 29.11.2016.

[26] J. Esterline, "Trim effect compensation using an artificial neural network," 2014. US Patent App. 14/336,951.

[27] W. Zhou, L. Li, B. Feng, W. Zhang, S. Qin, and W. Wang, "A study of temperature compensated crystal oscillator based on stress processing," in *Frequency Control Symposium, 2007 Joint with the 21st European Frequency and Time Forum. IEEE International*, pp. 272–274, May 2007.

[28] R. Filler, "The acceleration sensitivity of quartz crystal oscillators: a review," *Ultrasonics, Ferroelectrics, and Frequency Control, IEEE Transactions on*, vol. 35, pp. 297–305, May 1988.

[29] R. Brendel, C. El Hassani, M. Brunet, and E. Robert, "Influence of magnetic field on quartz crystal oscillators," in *Frequency Control, 1989., Proceedings of the 43rd Annual Symposium on*, pp. 268–274, May 1989.

[30] F. Walls and J.-J. Gagnepain, "Environmental sensitivities of quartz oscillators," *Ultrasonics, Ferroelectrics and Frequency Control, IEEE Transactions on*, vol. 39, pp. 241–249, March 1992.

[31] H. Hellwig, "Environmental sensitivities of precision frequency sources," *Instrumentation and Measurement, IEEE Transactions on*, vol. 39, pp. 301–306, Apr 1990.

[32] J.-J. Gagnepain, "Sensitivity of quartz oscillators to the environment: characterization methods and pitfalls," *Ultrasonics, Ferroelectrics, and Frequency Control, IEEE Transactions on*, vol. 37, pp. 347–354, Sept 1990.

[33] S. Galliou, M. Mourey, F. Marionnet, R. J. Besson, and P. Guillemot, "An oscillator for space," in *Frequency Control Symposium and PDA Exhibition Jointly with the 17th European Frequency and Time Forum, 2003. Proceedings of the 2003 IEEE International*, pp. 430–434, May 2003.

[34] J. Esterline, "Temperature compensation of crystal oscillators using an artificial neural network," in *Frequency Control Symposium (FCS), 2012 IEEE International*, pp. 1–7, May 2012.

[35] S. Haykin, *Neural Networks: A Comprehensive Foundation*. Upper Saddle River, NJ, USA: Prentice Hall PTR, 2nd ed., 1998.

[36] J. C. Esterline, "Trim effect compensation using an artificial neural network," in *European Frequency and Time Forum International Frequency Control Symposium (EFTF/IFC), 2013 Joint*, pp. 963–966, July 2013.

[37] G. D. Swann and S. Kamalasadan, "An approach for temperature and frequency control of a crystal oscillator," in *Industrial Electronics, 2008. IECON 2008. 34th Annual Conference of IEEE*, pp. 2976–2981, Nov 2008.

[38] A. Bowman and A. Azzalini, *Applied Smoothing Techniques for Data Analysis: The Kernel Approach with S-Plus Illustrations.* Oxford Statistical Science Series, OUP Oxford, 1997.

[39] M. Tanaka, "Fuzzy data processing method and data smoothing filter," 4 1995. US Patent 5,398,303.

[40] G. A. Wood and L. S. Jennings, "On the use of spline functions for data smoothing," *Journal of Biomechanics*, vol. 12, no. 6, pp. 477 – 479, 1979.

[41] H. Dudaicevs, Y. Manoli, W. Mokwa, M. Schmidt, and E. Spiegel, "A fully integrated surface micromachined pressure sensor with low temperature dependence," in *Solid-State Sensors and Actuators, 1995 and Eurosensors IX.. Transducers '95. The 8th International Conference on*, vol. 1, pp. 616–619, Jun 1995.

[42] L. Ljung, ed., *System Identification (2Nd Ed.): Theory for the User.* Upper Saddle River, NJ, USA: Prentice Hall PTR, 1999.

[43] S. y. Wang, B. Neubig, K. Sato, T. Hosoda, E. Seydel, J. h. Wu, T. f. Ma, and J. Wang, "Aging models and parameters of quartz crystal resonators and oscillators," in *Piezoelectricity, Acoustic Waves, and Device Applications (SPAWDA), 2015 Symposium on*, pp. 382–385, Oct 2015.

[44] Sky-Drones, "Smartap autopilot flight control system," 2014. Version 2.0. Available at `http://sky-drones.com/`. Accessed 29.11.2016.

[45] GEYER ELECTRONIC, *12.80104, Quartz Crystal KX-38*, 1 2007.

[46] GEYER ELECTRONIC, *12.87800 to 12.87899, Quartz Crystal KX-K*, 1 2010.

[47] STMicroelectronics, *STM32F405xx ARM Cortex-M4 32b MCU+FPU*, 6 2013. Rev 4.

[48] InvenSense Inc., *PS-MPU-6000A-00, Integrated Silicon Pressure Sensor On-Chip Signal Conditioned, Temperature Compensated and Calibrated*, 8 2013. Revision: 3.4.

[49] Measurement Specialties, Inc., *MS5611-01BA03, Barometric Pressure Sensor, with stainless steel cap*, 10 2012.

124

[50] u-blox, *LEA-6S u-blox 6 GPS Module*, 4 2013. Revision E2.

[51] Roving Networks, Inc., *RN42, Bluetooth Module*, 11 2013. Version 2.32.

[52] Bluegiga Technologies, *BLED112, Bluetooth Smart Dongle*, 4 2014. Version 1.1.

[53] STMicroelectronics, "Nucleo-f411re stm32 nucleo-64 development board with stm32f411ret6 mcu," 2014. Version 2.0. Available at `http://www.st.com/web/catalog/tools/FM116/SC959/SS1532/LN1847/PF260320`. Accessed 29.11.2016.

[54] STMicroelectronics, *STM32F411RET6 ARM Cortex-M4 32b MCU+FPU*, 11 2014. Rev 3.

[55] Sensirion, *SHT75, Humitidy and Temperature Sensor*, 4 2009. Version 4.2.

[56] Freescale Semiconductor, *MPX5700, Integrated Silicon Pressure Sensor On-Chip Signal Conditioned, Temperature Compensated and Calibrated*, 10 2012. Rev 10.

[57] Laird Technologies, Inc., *AA-070-24-22, Thermoelectric Assembly TEA*. Revision E2.

[58] New Japan Radio Co., Ltd., *NJM3772, Dual Stepper Motor Driver*.

[59] Sensirion, "Introduction to humidity. basic principles on physics of water vapor," 2009. Version 2.0. Available at `https://www.sensirion.com/fileadmin/user_upload/customers/sensirion/Dokumente/Humidity_Sensors/Sensirion_Humidity_Sensors_Introduction_to_Relative_Humidity_V2.pdf`. Accessed 29.11.2016.